

Egypt: Assessing the Effects of Farm-Level Irrigation Modernization on Water Availability and Crop Yields

Final Report (Summer 2011 and Winter 2011/2012)

Gijs Simons, Wilco Terink, Hazem Badawy, Gé van den Eertwegh, Wim Bastiaanssen (2012)



Index

Index	3
1 Introduction	15
1.1 Project background	15
1.2 Overview of irrigation modernization efforts in the Nile delta	15
1.3 Project scope and objectives	16
1.4 Selected study areas	17
1.5 Report outline	18
2 Data availability and modeling approach	19
2.1 Collection of field data	19
2.1.1 Summer fieldwork	19
2.1.2 Winter fieldwork	21
2.1.3 Additional data from Egyptian sources	23
2.2 Remote Sensing	25
2.2.1 Available and selected satellite data	25
2.2.2 Crop classification	27
2.2.3 The SEBAL approach - theory and model setup	29
2.2.4 Analysis of equity and reliability of water distribution	32
2.2.5 Comparison with historical data	33
2.3 Simulation modeling	34
2.3.1 Water and solute balance modeling using SWAP	34
2.3.2 Data, model schematization and parameterization	37
2.3.3 Calibration and model runs	48
2.4 Capacity building	56
3 Results summer 2011	57
3.1 Cropping pattern	57
3.2 Water consumption	58
3.2.1 Rice	58
3.2.2 Cotton	61
3.2.3 Maize	64
3.3 Crop yield	65
3.3.1 Rice	65
3.3.2 Cotton	69
3.3.3 Maize	72
3.4 Crop water productivity	73
3.4.1 Rice	73
3.4.2 Cotton	74
3.4.3 Maize	76
3.5 Gross return	76
3.6 Reliability of irrigation water availability	77
3.7 Canal seepage losses	78
3.8 Drainage water recycling	79
3.8.1 Rice	80
3.8.2 Cotton	81
3.8.3 Maize	82

3.9	Salinity	83
3.9.1	Rice	83
3.9.2	Cotton	84
3.9.3	Maize	85
4	Results winter 2011-2012	88
4.1	Cropping pattern	88
4.2	Water consumption	89
4.2.1	Wheat	89
4.2.2	Berseem	92
4.3	Crop yield	95
4.3.1	Wheat	95
4.3.2	Berseem	97
4.4	Crop water productivity	97
4.4.1	Wheat	97
4.4.2	Berseem	99
4.5	Gross return	99
4.6	Reliability of irrigation water availability	100
4.7	Canal seepage losses	100
4.8	Drainage water recycling	101
4.8.1	Wheat	101
4.8.2	Berseem	102
4.9	Salinity	103
4.9.1	Wheat	104
4.9.2	Berseem	104
5	Discussion	108
5.1	Overall effects of modernization	108
5.1.1	Rice	108
5.1.2	Cotton	108
5.1.3	Maize	109
5.1.4	Wheat	110
5.1.5	Berseem	111
5.2	Usefulness and limitations of the integrated approach	111
5.2.1	Input data availability	112
5.2.2	Interpretation and availability of satellite data	113
5.2.3	Congruency between methodologies	113
5.2.4	Other factors influencing crop health	114
6	Conclusions and recommendations	116
	References	118
	Appendix	121
	Appendix A: Fieldwork sheet	121
	Appendix B: Daily meteorological data	122
	Appendix C: Uncertainty assessment in SWAP	124
	Appendix D: Attendance list kickoff workshop	125
	Appendix E: SEBAL Validation	126

Tables

Table 1: Crop yield values obtained from farmer surveys. Applied conversion factors are as follows: 1 feddan = 0.42 ha, 1 ardebb of rice “shaeer kebeer” = 300 kg, 1 ardebb of seed cotton = 150 kg, 1 ardebb of maize = 140 kg).....	20
Table 2: Acquired data of relevant parameters in the study areas.	23
Table 3: Total acreage of main crops in El Sefsaf, Daqalt and El Gemeza in summer 2011 (source: PMU IIIMP).	24
Table 4: List of available high resolution satellite images during summer 2011 with cloud-free conditions over the study areas.	26
Table 5: Overview of pixel sizes per satellite (a) and sizes of individual fields b)	27
Table 6: Total rainfall and reference evapotranspiration (ET_{ref}) for the summer (May 1 st - October 31 st , 184 days) for each branch canal.....	38
Table 7: Total rainfall and reference evapotranspiration (ET_{ref}) for the winter for each branch canal.	39
Table 8: Derived SWAP soil-physical parameters.	41
Table 9: Schematization of the SWAP soil profile.	41
Table 10: Rice crop parameters (Allen et al., 1998).....	43
Table 11: Maize crop parameters (Allen et al., 1998).	43
Table 12: Cotton crop parameters (Allen et al., 1998).....	43
Table 13: Wheat crop parameters (Allen et al., 1998).	44
Table 14: Berseem crop parameters (Allen et al., 1998).....	44
Table 15: Salinity levels used for the SWAP model (Amer and de Ridder, 1989).	48
Table 16: Ratio between SEBAL ET_a and ET_p per branch canal and per crop.	52
Table 17: Calibration parameters for each branch canal and crop for the summer season.	52
Table 18: Calibration parameters for each branch canal and crop for the winter season.	52
Table 19: Summarized calibration results for each branch canal and crop for the summer season. The error term shows the % difference between the average SEBAL ET_a and SWAP ET_a , thus the error introduced in the analysis by the calibration procedure.....	53
Table 20: Summarized calibration results for each branch canal and crop for the winter season. The error shows the % difference between the average SEBAL ET_a and SWAP ET_a	53
Table 21: Final SWAP calibration parameters for each branch canal and crop. No value indicates that this parameter is not used during the calibration process.....	54

Table 22: Defined SWAP simulations (30 model runs).	55
Table 23: Average rice water consumption during the 2011, 2002 and 1995 growing seasons.....	60
Table 24: Applied irrigation volumes, transpiration (T_a) and water losses through evaporation (E_a) for rice per branch canal and upstream/downstream location.	61
Table 25: Average cotton water consumption during summer seasons 2011, 2002 and 1995.	63
Table 26: Water consumption (T_a) and water losses through evaporation (E_a) for Cotton per branch canal and upstream/downstream location.....	64
Table 27: Maize evapotranspiration during summer 2011.....	65
Table 28: Water consumption (T_a) and water losses through evaporation (E_a) for maize per branch canal and upstream/downstream location.	65
Table 29: Rice yield statistics for summer seasons 2011, 2002 and 1995. Harvest indices are based on a moisture content of 0.14.	69
Table 30: Average seed cotton yield during summer seasons 2011, 2002 and 1995. Harvest indices are based on a seed cotton moisture content of 0.08 (Baskin et al.).....	71
Table 31: Maize yields during summer 2011. Harvest indices are based on a moisture content of 0.15 (Willcutt, 2010).....	72
Table 32: Average rice crop water productivity during summer seasons 2011, 2002 and 1995.	74
Table 33: Average seed cotton water productivity during summer seasons 2011, 2002 and 1995.	75
Table 34: Average maize water productivity during summer season 2011.....	76
Table 35: Total irrigation, number of irrigation applications, and irrigation depth per irrigation application for Cotton per branch canal and upstream/downstream location.	78
Table 36: Total irrigation, number of irrigation applications, and irrigation depth per irrigation application for Maize per branch canal and upstream/downstream location.	79
Table 37: Total irrigation, number of irrigation applications, and irrigation depth per irrigation application for Rice per branch canal and upstream/downstream location.	79
Table 38: Drainage flux for each branch canal and upstream/downstream location where Rice is grown. Drainage is expressed in mm as well as percentage of the total outflow flux ($Q_{out} = T_a + E_a +$ Drainage).	80
Table 39: Drainage flux for each branch canal and upstream/downstream location where Cotton is grown. Drainage is expressed in mm as well as percentage of the total outflow flux ($Q_{out} = T_a + E_a +$ Drainage).	81
Table 40: Drainage flux for each branch canal and upstream/downstream location where maize is grown. Drainage is expressed in mm as well as percentage of the total outflow flux ($Q_{out} = T_a + E_a +$ Drainage).	82

Table 41: Solute balance for rice for each branch canal and upstream/downstream location. Solutes enter the field by irrigation and a bottom flux, and leave the field by drainage. Solutes are shown in kg/ha.	83
Table 42: Solute balance for cotton for each branch canal and upstream/downstream location. Solutes enter the field by irrigation and a bottom flux, and leave the field by drainage. Solutes are shown in kg/ha.	84
Table 43: Solute balance for Maize for each branch canal and upstream/downstream location. Solutes enter the field by irrigation and a bottom flux, and leave the field by drainage. Solutes are shown in kg/ha.	85
Table 44: Average wheat water consumption for winter seasons 1997/1998, 2002/2003 and 2011/2012.	90
Table 45: Applied irrigation volumes, transpiration (T_a) and water losses through evaporation (E_a) for wheat per branch canal and upstream/downstream location.	91
Table 46: Average berseem water consumption in W-10, Daqalt and El Gemeza in winter 2011/2012.	93
Table 47: Applied irrigation volumes, transpiration (T_a) and water losses through evaporation (E_a) for berseem per branch canal and upstream/downstream location.	94
Table 48: Average wheat yield in W-10, Daqalt and El Gemeza in winter seasons 2011/2012, 2002/2003 and 1997/1998. Harvest indices are based on a moisture content of 0.14 (Van Gastel et al., 2002)	96
Table 49: Average wheat water productivity for W-10, Daqalt and El Gemeza in winter periods 2011/2012, 2002/2003 and 1997/1998.	98
Table 50: Total irrigation, number of irrigation applications, and irrigation depth per irrigation application for wheat per branch canal and upstream/downstream location.	101
Table 51: Total irrigation, number of irrigation applications, and irrigation depth per irrigation application for berseem per branch canal and upstream/downstream location.	101
Table 52: Drainage flux for wheat fields, per branch canal and upstream/downstream location. Drainage is expressed in mm as well as percentage of the total outflow flux ($Q_{out} = T_a + E_a +$ Drainage).	102
Table 53: Drainage flux for berseem fields, per branch canal and upstream/downstream location. Drainage is expressed in mm as well as percentage of the total outflow flux ($Q_{out} = T_a + E_a +$ Drainage).	103
Table 54: Solute balance for Wheat for each branch canal and upstream/downstream location. Solutes enter the field by irrigation and a bottom flux, and leave the field by drainage. Solutes are shown in kg/ha.	104
Table 55: Solute balance for berseem for each branch canal and upstream/downstream location. Solutes enter the field by irrigation and a bottom flux, and leave the field by drainage. Solutes are shown in kg/ha.	105

Figures

Figure 1: Location of the study areas (in yellow) within the Mit Yazid canal command area (blue). The background image is a Landsat TM5 image acquired on September 13, 2008.....	17
Figure 2: Distribution of sampled fields in the Daqalt (l) and W-10 (r) areas. Colors indicate the three main summer crops.	19
Figure 3: Field picture of a traditional marwa in Daqalt (l) and a lined marwa in W-10 (r).	21
Figure 4: Distribution of sampled fields in the Daqalt (l), W-10 (m), and El Gemeza (r) areas. Colors indicate the two main winter crops.....	21
Figure 5: Top: Traditional irrigation practices with water being locally pumped from the canals and used for surface irrigation on the fields. Bottom: new, centralized irrigation pumping stations in El Gemeza are not yet operational.	22
Figure 6: Measured flow rate in mm/day at the inlet of the Daqalt and El Gemeza canal command areas (source: PMU IIIMP).....	24
Figure 7: Distributions of salinity levels in the irrigation canals for each of the three branch canal areas. Salinity levels were obtained at upstream, middle, and downstream locations (source: PMU IIIMP). El Sefsaf is part of the W-10 branch canal area.	25
Figure 8: Excerpt of false-color RapidEye images for agricultural fields in the W-10 command area. The left image was captured on 2011/08/22, the right image on 2011/09/07. As the images show, a lot of the fields are harvested within this period of 16 days, making these images an important source of information in the supervised classification.	28
Figure 9: Schematic view of the SEBAL algorithm.....	30
Figure 10: Example of a slicing of distances from the main inlet for the W-10 (l) and Daqalt (r) branch canal command area. The areas have been sliced so that each area occupies 10% of the total area. The red dot indicates the inlet point of the branch canal.....	33
Figure 11: Rice water productivity in summer 1995 (top) and 2002 (bottom) in W-10 and Daqalt.....	34
Figure 12: SWAP model domain and transport processes (van Dam, 2000).	35
Figure 13: Schematization of the SWAP model (van Dam, 2000).....	36
Figure 14: Method used in SWAP to derive actual transpiration and soil evaporation of partly covered soil from basic input data (Kroes et al., 2008).	37
Figure 15: Rainfall and ET_{ref} of summer season for the three branch canal areas.....	39
Figure 16: Rainfall and ET_{ref} of winter season for the three branch canal areas.	39
Figure 17: Observed pF curve for Zenkalon derived according to laboratory measurements and model calibration (Bastiaanssen et al., 1996) and simulated pF curve using Mualem-Van Genuchten function (van Genuchten, 1980).....	40

Figure 18: Observed unsaturated hydraulic conductivity curve for Zenkalon derived according to estimations, laboratory measurements, and model calibration (Bastiaanssen et al., 1996) and simulated unsaturated hydraulic conductivity curve using Mualem (1976).....	41
Figure 19: Typical partitioning of assimilated dry matter among leaves, stem, roots and storage organs as function of development stage (Van Dam, 2000).	43
Figure 20: Illustration of a traditional drainage system in Egypt (Amer and de Ridder, 1989).	45
Figure 21: Groundwater level for the summer growing season (2011 through 31 October 2011) for Maize in Daqalt.	46
Figure 22: Calculated SEBAL ET distributions for cotton for each of the branch canal areas.	49
Figure 23: Calculated SEBAL ET distributions for maize for Daqalt and W-10.....	50
Figure 24: Calculated SEBAL ET distributions for rice for each of the branch canal areas.	50
Figure 25: Calculated SEBAL ET distributions for wheat for each of the branch canal areas.	51
Figure 26: Calculated SEBAL ET distributions for berseem for each of the branch canal areas.	51
Figure 27: Kickoff workshop at the EALIP office, October 26-27 2011.	56
Figure 28: Summer 2011 land use map of the study areas.	57
Figure 29: Temporal evolution of the vegetation index (NDVI) for the summer agricultural classes based on the available high-resolution satellite data (combined with MODIS data for June).	58
Figure 30: Spatial distribution of seasonal water consumption (Eta) of rice in W-10, Daqalt and El Gemeza (clockwise) during summer 2011.....	59
Figure 31: Head-tail analysis of water consumption from rice fields in W-10 and Daqalt. Dashed lines indicate a variability range (mean plus and minus standard deviation per 10% section)	60
Figure 32: Rice water stress for each branch canal and upstream/downstream location. Rice water stress is expressed as percentage water of potential transpiration.	61
Figure 33: Spatially distributed water consumption of cotton in W-10, Daqalt and El Gemeza (clockwise).	62
Figure 34: Head-tail analysis of water consumption from cotton fields in W-10 and Daqalt. Dashed lines indicate a variability range (mean plus and minus standard deviation per 10% section)	63
Figure 35: Cotton water stress for each branch canal and upstream/downstream location. Cotton water stress is expressed as percentage water of potential transpiration.	64
Figure 36: Spatially distributed rice yield for summer 2011 in W-10, Daqalt and El Gemeza (clockwise).	68
Figure 37: Head-tail analysis of rice yields in W-10 and Daqalt. Dashed lines indicate a variability range (mean plus and minus standard deviation per 10% section)	69

Figure 38: Literature values of cotton ETa plotted against the achieved cotton lint and seed cotton yield (adopted from Zwart, 2010). The green dot indicates the combination of Daqalt average ETa and yield, which falls outside the range of seed cotton observed globally.	70
Figure 39: Spatially distributed seed cotton yield in W-10, Daqalt and El Gemeza (clockwise).	71
Figure 40: Head-tail analysis of seed cotton yield in W-10 and Daqalt. Dashed lines indicate a variability range (mean plus and minus standard deviation per 10% section)	72
Figure 41: Spatially distributed rice crop water productivity in W-10, Daqalt and El Gemeza (clockwise).	73
Figure 42: Head-tail analysis of rice water productivity in W-10 and Daqalt. Dashed lines indicate a variability range (mean plus and minus standard deviation per 10% section).....	74
Figure 43: Spatially distributed seed cotton water productivity for summer 2011 in W-10, Daqalt and El Gemeza (clockwise).	75
Figure 44: Head-tail analysis of seed cotton water productivity in W-10 and Daqalt. Dashed lines indicate a variability range (mean plus and minus standard deviation per 10% section)	76
Figure 47: Reliability of irrigation water delivery, expressed in the absolute average deviation from the mean (AVEDEV) per branch canal command area.	78
Figure 48: Drainage flux of Rice for each branch canal and upstream/downstream location.	80
Figure 49: Drainage flux of cotton for each branch canal and upstream/downstream location.	81
Figure 50: Drainage flux of maize for each branch canal and upstream/downstream location.	82
Figure 51: Rice salinity stress expressed as percentage of potential transpiration.	84
Figure 52: Maize salinity stress expressed as percentage water of potential transpiration.	85
Figure 53: Maize solute concentrations [dS/m] throughout the soil profile for the downstream El Gemeza field (top left), the downstream Daqalt field (top right), and the downstream W-10 field (bottom). The x-axis represents the day of the growing season, while the y-axis represents the soil depth. It should be noted that the discretization of soil depth is smaller in the top soil.	87
Figure 54: Land use in W-10, Daqalt and El Gemeza (in clockwise order) during winter 2011/2012.	88
Figure 55: Temporal evolution of the average vegetation index (NDVI) for wheat and berseem based on the available high-resolution satellite data.	89
Figure 56: Spatially distributed seasonal water consumption of wheat fields in W-10, Daqalt and El Gemeza (clockwise).	90
Figure 57: Head-tail analysis of wheat water consumption in W-10 and Daqalt during winter 2011/2012. Dashed lines indicate a variability range (mean plus and minus standard deviation per 10% section)	91
Figure 58: Wheat water stress for each branch canal and upstream/downstream location. Wheat water stress is expressed as percentage water of potential transpiration.	92

Figure 59: Spatially distributed seasonat water consumption of berseem fields in W-10, Daqalt and El Gemeza (clockwise) in winter 2011/2012.	93
Figure 60: Head-tail analysis of berseem water consumption in W-10 and Daqalt during winter 2011/2012. Dashed lines indicate a variability range (mean plus and minus standard deviation per 10% section)	94
Figure 61: Berseem water stress for each branch canal and upstream/downstream location. Berseem water stress is expressed as percentage water of potential transpiration.	95
Figure 62: Spatially distributed wheat yield in W-10, Daqalt and El Gemeza (clockwise) in 2011/2012. 96	
Figure 63: Head-tail analysis of wheat yield in W-10 and Daqalt for winter 2011/2012. Dashed lines indicate a variability range (mean plus and minus standard deviation per 10% section)	97
Figure 64: Spatially distributed wheat water productivity in W-10, Daqalt and El Gemeza (clockwise) for winter 2011/2012,.....	98
Figure 65: Head-tail analysis of wheat water productivity in W-10 and Daqalt for winter 2011/2012. Dashed lines indicate a variability range (mean plus and minus standard deviation per 10% section)	99
Figure 67: Reliability of irrigation water delivery per branch canal command area, expressed in the average absolute deviation from the mean (AVEDEV) of the evaporative fraction.	100
Figure 68: Drainage flux of wheat for each branch canal and upstream/downstream location.	102
Figure 69: Drainage flux of Berseem for each branch canal and upstream/downstream location.	103
<i>Figure 70: Berseem solute concentrations [dS/m] in the soil profile for the downstream El Gemeza field (top left), the downstream Daqalt field (top right), and the downstream W-10 field (bottom). The x-axis represents the day of the growing season, while the y-axis represents the soil depth. It should be noted that the discretization of soil depth is smaller in the top soil. ...</i>	<i>106</i>

List of Definitions

Crop factor (Kc)

Kc is defined as the ratio of the crop potential evapotranspiration over the reference crop evapotranspiration, usually alfalfa or grass.

Crop water productivity

The amount of fresh crop yield (kg) that is obtained per unit of consumed water (ET_a , in m^3).

Evaporation

The process in which a liquid is converted into a gaseous state. It is the loss of water from the soil or open water to the atmosphere.

Evapotranspiration (ET)

Evapotranspiration is the sum of surface evaporation and plant transpiration in mm of water per time unit.

- **Actual (ET_a)**
Actual evapotranspiration is defined as the evapotranspiration with measured crop and environmental conditions.
- **Potential (ET_p)**
Potential evapotranspiration is defined as the evapotranspiration achievable with observed crop NDVI and weather conditions, but without any moisture stress.
- **Reference (ET_{ref})**
The role of weather variation on ET can be studied using the reference evapotranspiration, which depends solely on meteorological conditions. The reference evapotranspiration is based on a fictional crop that has physical properties being comparable to well watered and short clipped grass (FAO: Allen et al., 1998).

Transpiration (T)

Process by which water that is absorbed by plants, usually through the roots, is evaporated into the atmosphere from the plant surface, such as leaf pores.

- **Actual (T_a)**
Transpiration under current environmental and crop conditions.
- **Potential (T_p)**
Transpiration under the current environmental and crop conditions, but without any moisture stress.

Water consumption

The removal of water from the hydrological cycle. In practice this is synonymous to evapotranspiration. These terms are used interchangeably in this report.

Water use

Any deliberate application of water to a specified purpose. The term does not distinguish between uses that remove the water from further use (evaporation, transpiration, flows to sinks) and uses that have little quantitative impact on water availability (navigation, hydropower, most domestic uses). (Perry, 2007)

1 Introduction

1.1 Project background

In August 2010, the World Bank published a call for proposals in the framework of a simulation modeling and remote sensing study to assess the effects of farm-level irrigation modernizations on water availability and crop yields in the Nile Delta. The proposal of a team consisting of WaterWatch, FutureWater and GeoMAP was selected for execution of the study, with WaterWatch taking the lead in this joint effort. FutureWater, a hydrological scientific consultancy company from The Netherlands, was included in the team for their expertise in hydrological modeling. GeoMAP was selected as a local partner because of their experienced field team and expertise in the local agricultural conditions.

Originally, the project was planned to focus on the winter season 2010/2011 and summer season 2011. A delay in the start of the study, due to revision of the Terms of Reference, altered the project timeline and resulted in the choice of new seasons of interest, being summer 2011 and winter 2011/2012. The effective start of the project was shifted to September 2011. A kick-off workshop in Egypt was organized in October 2011, coinciding with a World Bank mission to Cairo. The final workshop, disseminating the preliminary results, was held in September 2012.

This final report presents and discusses the methodology and results of the analyses for the summer season 2011 and winter season 2011/2012. The report incorporates two rounds of detailed comments from the project steering committee assembled by the World Bank:

- Theodore Hsiao, Department of Land, Air and Water Resources, University of California, Davis
- Donald Slack, Department of Agricultural and Biosystem Engineering, University of Arizona, Tucson
- Muluneh Yitayew, Department of Agricultural and Biosystem Engineering, University of Arizona, Tucson
- Peter Waller, Department of Agricultural and Biosystem Engineering, University of Arizona, Tucson
- Albert Clemmens, Arid Land Agricultural Research Center, Maricopa, Arizona
- Richard Allen, Department of Civil Engineering and Department of Biological and Agricultural Engineering, University of Idaho, Kimberly

1.2 Overview of irrigation modernization efforts in the Nile delta

Historical irrigation management in the Nile Delta is characterized by a seasonally adjusted rotational schedule of water supply, with water being available to the farmer only for a limited number of days before the supply is turned “off”. Together with the lack of effective control at the secondary and tertiary level of the system and the basic infrastructure, this rotational system has resulted in inefficient application of irrigation water, water losses, and an inequitable water distribution.

Under the World Bank funded Irrigation Improvement Project (IIP, 1996 - 2006) and Integrated Irrigation Improvement and Management Project (IIIMP, ongoing), attempts have been made to improve the management of irrigation and drainage in the two command areas of the Mit Yazid and Mahmoudia canals in the Nile delta, located in the Governorates of Alexandria, Beheira, Kafr El Sheikh and Gharbia. Specific objectives of the irrigation modernization include the improvement of equitable water distribution, water use efficiency, water quality, and ultimately to increase agricultural production and alleviate poverty.

Irrigation improvements under the IIP and IIIMP have taken place at different levels of the irrigation system in the aforementioned canal command areas. In this report, the term *marwa* is used for the infrastructure at quaternary (farm) level, *mesqa* for the tertiary level and the secondary canals are termed branch canals. At present, branch canal and *mesqa* improvements have been carried out or are currently ongoing, and water user associations have been formed for sustainable operation and maintenance and irrigation management. Modernization of the *marwas* under IIIMP is currently ongoing at selected locations.

The application of continuous flow, as a replacement of the typical system of rotational flow, is one of the main measures that have been taken to solve problems related to the distribution of water in the irrigation network. Water delivery services to the farmers are improved and the flexibility of the water management system is increased. The flow in the branch canal is determined by regulation of the discharge at the head of the canal, while taking into account the area served by the canal and its cropping pattern (i.e. crop water demands).

Lifting of the water from the branch canal into the *mesqa* network has been centralized through an electric pump set at a single control point, with the purpose of increasing the equity of water distribution and reducing operational cost. Water losses through seepage from the *mesqas* are reduced by piping of the tertiary canals, also allowing for pressurized water delivery. Similar improvements have recently been made to selected *marwas* under IIIMP, either by lining of the canals with brick and mortar or piping by low-pressure pipes up to the on-farm gate.

1.3 Project scope and objectives

The objective of the current project, as formulated by the World Bank, is to assess the effects of farm-level irrigation modernization of quaternary canals on water availability (in terms of quantity, quality, reliability, and equity in distribution) and yields of smallholder farmers in two command areas in the Nile Delta. By including a third command area without modernization, the effects of *mesqa* and branch canal improvements are also assessed. A related objective of the study is to facilitate close collaboration with staff of the relevant Egyptian authorities in order to build capacity in the use of the proposed integrated approach for possible subsequent application in other areas where such modernization interventions are being planned.

The methodological approach for the assessment is based on an innovative combination of fieldwork observations and measurements of water quantity and quality; satellite-based spatial quantification of cropping pattern, crop evapotranspiration and crop yields; and physically based modeling of water and solute transport. An assessment is performed for the 2011 summer period and the 2011/2012 winter period. Historical data on crop water parameters are also included for the assessment of modernization effects.

The current study is one of the first attempts to assess the effects of farm-level irrigation modernization in a more integrated and quantitative way, covering not only changes in irrigation water supply but also in consumptive use and crop yields (implicitly also water productivity in terms of crop yield per unit of water consumed), water quality and water reuse from the drains, and equity in farm-level irrigation water distribution. The insights gained will feed into the proposed World Bank supported Farm-level Irrigation Modernization Project (FIMP) which aims to modernize farm-level quaternary canals and improve irrigation and cropping practices on 80,000 ha farmed by about 140,000 households in the Nile Delta.

1.4 Selected study areas

All selected study areas are part of the command area of the Mit Yazid main canal (see Figure 1). The W-10 and Daqalt branch canals were selected for assessment of the irrigation improvements on the marwa and mesqa levels respectively. Both command areas comprise about 4,500 farmer households and 2,600 ha of irrigated land. Crops are grown in a winter and a summer season. Typical winter crops are wheat and berseem (Egyptian clover), and summer crops are mainly rice, cotton and maize. The general winter and summer growing seasons extend from November to April, and May to October respectively. W-10 has served as a pilot area for marwa improvements under IIIMP, and therefore is one of the first locations where extensive modernization of the farm-level irrigation system has taken place. At present, Daqalt has only been modernized up to the level of the mesqas.

On recommendation by Dr. Mohamed Nour El-Din, advisor to the IIIMP office of the Ministry of Water Resources and Irrigation (MWRI), the command area of the El Gemeza branch canal was selected as a reference area without irrigation improvements. The irrigation system in this area has not yet been modified in the framework of IIIMP, and is scheduled for modernization at the end of 2012 (Dr. M. Nour El-Din, pers. comm.).

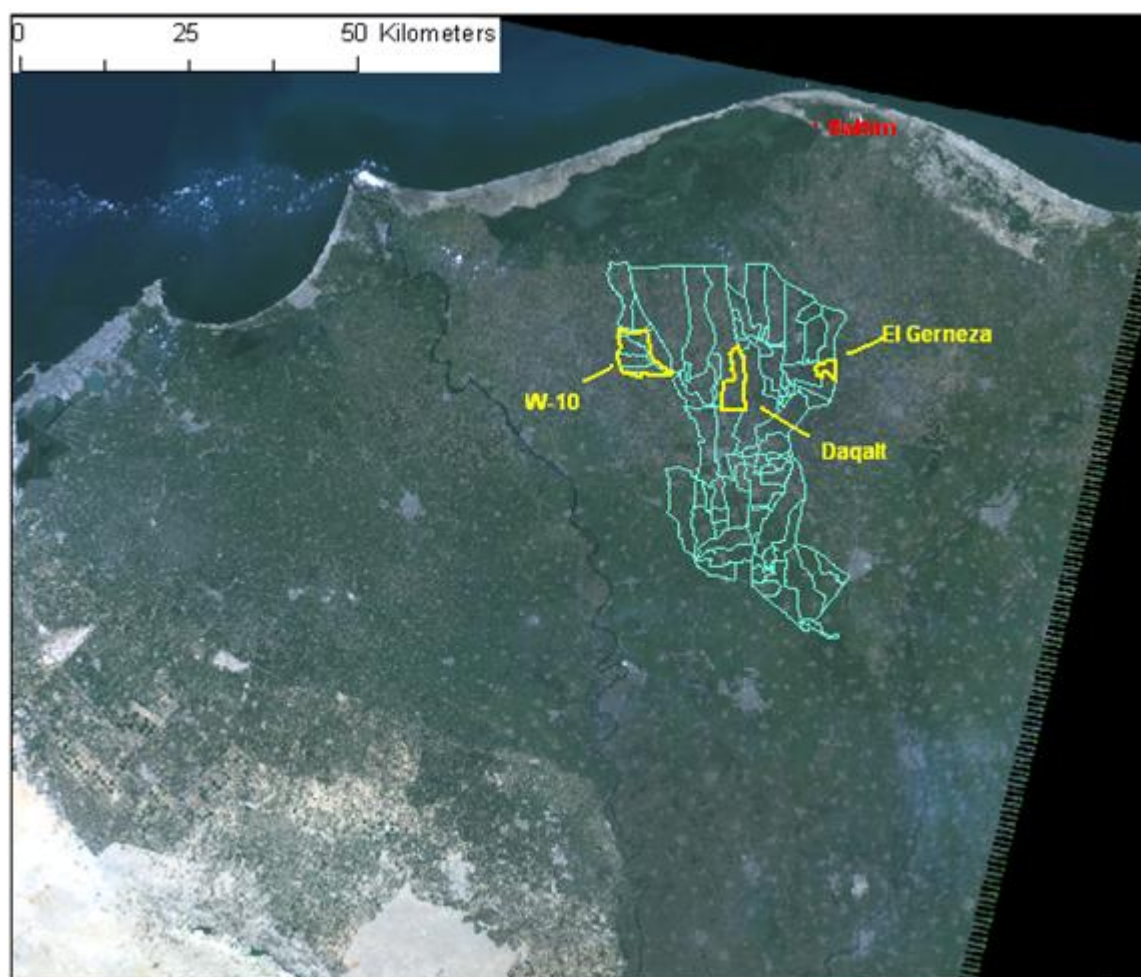


Figure 1: Location of the study areas (in yellow) within the Mit Yazid canal command area (blue). The background image is a Landsat TM5 image acquired on September 13, 2008.

1.5 Report outline

This interim report presents and discusses the integrated methodology and obtained results for the summer season 2011 and winter season 2011/2012. Chapter 2 provides an overview of all information that is collected on the field situation in the study areas (Section 2.1), with Section 2.2 and 2.3 giving a detailed description of the approach that was adopted in the project and the tools that were used in the remote sensing interpretation and simulation modeling. Chapter 3 presents and discusses the results that were found for summer 2011 for each crop and area, including a comparison with outcomes of a previous study in the same area. Similar information on the winter 2011/2012 analysis is presented in Chapter 4. Overall effects of irrigation modernization, as well as the opportunities and limitations of the methodology, are discussed in Chapter 5. Finally, Chapter 6 presents the conclusions on the effects of farm-level irrigation modernization and the use of an integrated approach to quantify this, also giving some recommendations on how a similar study could be improved in the future.

2 Data availability and modeling approach

2.1 Collection of field data

2.1.1 Summer fieldwork

The summer fieldwork was performed by GeoMAP in October 2011, at the end of the summer growing season. One of the main components of this fieldwork consisted of the identification of crop types on sampled fields, with a focus on rice, cotton and maize. In Daqalt 152 fields were sampled, with 156 fields being sampled in W-10 (see Figure 2 for their spatial distribution). Every field was photographed and documented in a field sheet, as included in Appendix A. In El Gemeza, fieldwork was not performed during summer, as the selection of El Gemeza as a reference area was decided some time after the start of the project, which was too late in the season (after harvest time) to perform any crop identification. However, the number of field observations in the other two areas provides enough basis for a supervised land use classification of El Gemeza (see Paragraph 2.2.2), with the exception of maize (see Section 3.1).

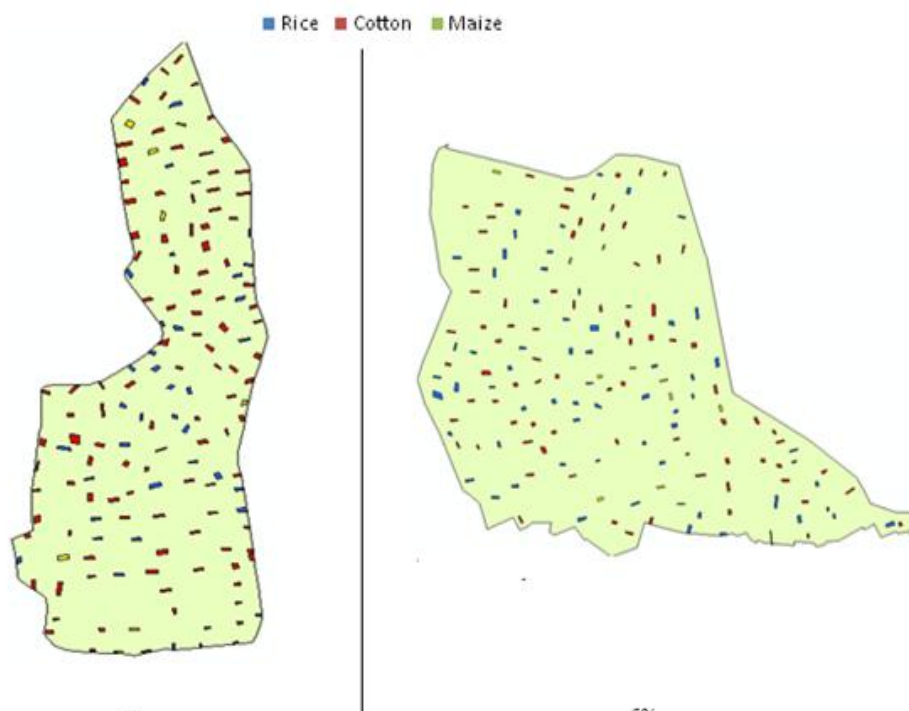


Figure 2: Distribution of sampled fields in the Daqalt (l) and W-10 (r) areas. Colors indicate the three main summer crops.

A second important component of the fieldwork was the conducting of farmer surveys to acquire information on field-level conditions and practices. Questions that were asked concerned irrigation practices, irrigation frequencies and actual crop yields. Table 1 summarizes the yields per crop that were obtained from the farmer surveys. It shows that cotton and maize yields were typically lower in Daqalt, while the maximum reported rice yield in Daqalt exceeded that in W-10. For rice in W-10 it should be noted that the cultivated breed of rice is of the “shaeer kebeer” type, which is accounted for in the utilized conversion factor from Egyptian volumetric units (ardebbs) to kilograms. For cotton, the yield is reported including the cotton seed, causing higher numbers if compared to values exclusively for cotton lint production.

Table 1: Crop yield values obtained from farmer surveys. Applied conversion factors are as follows: 1 feddan = 0.42 ha, 1 ardebb of rice “shaeer kebeer” = 300 kg, 1 ardebb of seed cotton = 150 kg, 1 ardebb of maize = 140 kg).

Branch Canal	Crop	Range of crop yields (in reported units per feddan)	Range of crop yields (in kg/ha)
W-10	Rice	10 - 12 ardebb	7143 - 8571
	Cotton	8 - 9 quintals	2857 - 3214
	Maize	18 - 22 ardebb	6000 - 7333
Daqalt	Rice	3 - 4 tons	7143 - 9524
	Cotton	5 - 6 quintals	1786 - 2143
	Maize	11 - 12 ardebb	3667 - 4000

Regular irrigation is necessary for all crops as rainfall is almost absent during the summer season. Commonly practiced irrigation methods in all three areas are reported to include basin irrigation for rice, and border or furrow irrigation for the other crops. Efforts were made by the field team to acquire data on the irrigation behavior of the farmers per branch canal command area and per crop. It turned out that information on applied amounts of irrigation water were difficult to obtain during the field surveys. The target group of uneducated farmers was unable to answer these questions, even when discussing the length of time they leave their pumps on. However, frequencies of irrigation applications were obtained, and the irrigated amount was selected as calibration parameter in the hydrological model (see Section 2.3.3).

In addition to the aforementioned field-specific information, general observations regarding the state of the irrigation systems in the study areas were noted and reported. Figure 3 illustrates the difference between the state of *marwas* in Daqalt, where channels are still traditional and earthen, and the modernized *marwas* in W-10. These observations are in line with the modernizations as described in Section 1.2.



Figure 3: Field picture of a traditional marwa in Daqalt (l) and a lined marwa in W-10 (r).

2.1.2 Winter fieldwork

The winter fieldwork was performed by GeoMAP in March 2012, in all three selected branch canal command areas. A total of 175 fields were visited in Daqalt, with 175 and 75 fields being sampled in W-10 and El Gemeza respectively. Their spatial distribution is depicted in Figure 3. A procedure similar to that described in Section 2.1.1 was followed, with crop type identification being focused on wheat and berseem as the two main winter crops.

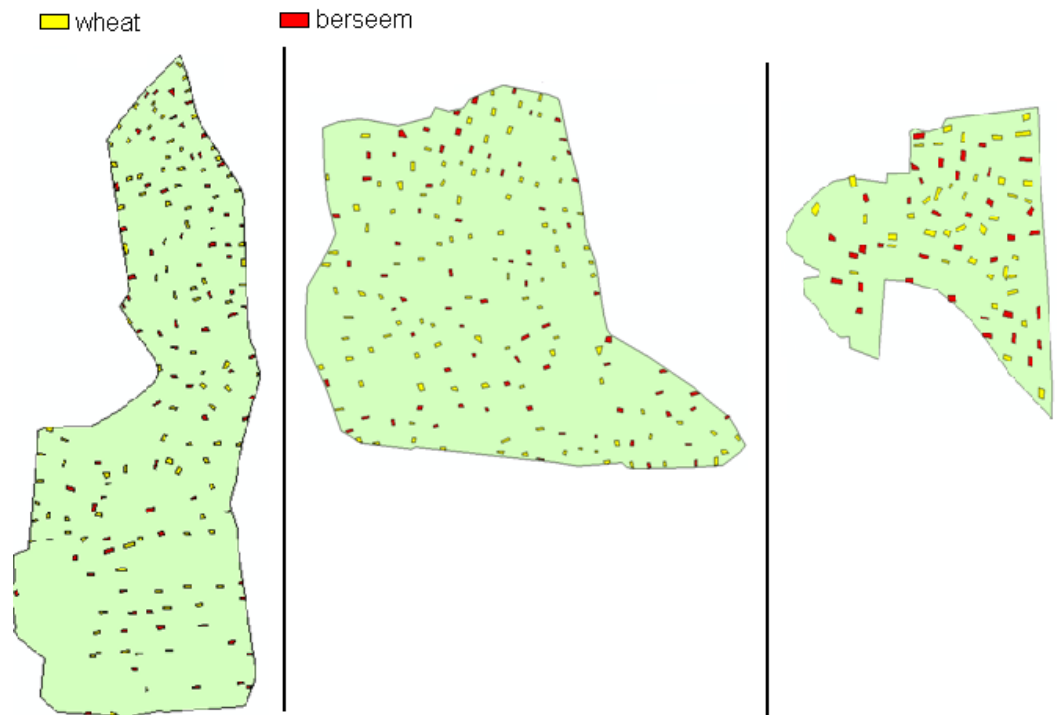


Figure 4: Distribution of sampled fields in the Daqalt (l), W-10 (m), and El Gemeza (r) areas. Colors indicate the two main winter crops.

For wheat, farmer surveys indicated that applied amounts of irrigation and frequencies are very much dependent on rainfall. It was reported that farmers could suffice with two to three irrigation applications during the entire wheat growing cycle. Basin or border irrigation were the commonly observed irrigation types for wheat. On average, a wheat yield of 15 ardebb per feddan (5357 kg/ha) was reported for the winter season 2011/2012.

For berseem, a more regular irrigation schedule was reported, with intervals between irrigation applications being 10 days on average. Farmer survey results indicate that berseem stands apart from the other winter (and summer) crops, in terms of multiple cultivation cycles and the purpose of growing it. Berseem is mainly grown as fodder, either in dried form or directly from the land. It is cultivated in a number of growing cycles, varying from 1 to 3, during a single winter season. It was reported that berseem is often harvested after the first cultivation cycle, leaving it to dry on the field to be able to store it and use it as fodder during summer. The berseem that is grown afterwards is mostly left on the field for cattle to graze on. At the end of the season, the berseem seed is harvested. An additional reason for leaving berseem on the field is for enrichment of the soil, for the benefit of the subsequent summer crop. As farmers indicated that they rarely sell berseem to the government, they do not calculate yields. Instead, they mainly regard berseem fields per unit of surface area, renting it to cattle owners with a standard price of LE 125 per kirat (1/24 feddan). For this reason, and the variety of cultivation practices associated with growing berseem, it was not feasible (nor relevant) to analyze “yield” from berseem fields in the current study. Therefore, the analysis for berseem is limited to conditions related to water availability and solute transport.

General observations during the winter fieldwork, regarding conditions of irrigation infrastructure and water availability, confirmed the extent of irrigation improvements reported in Section 1.4. As illustrated by Figure 5, modernization efforts in El Gemeza are currently underway under IIIMP, but none of the newly installed equipment was seen operational at the time of the fieldwork.



Figure 5: Top: Traditional irrigation practices with water being locally pumped from the canals and used for surface irrigation on the fields. Bottom: new, centralized irrigation pumping stations in El Gemeza are not yet operational.

2.1.3 Additional data from Egyptian sources

As it is outside the scope of the current project to organize an extensive field campaign to measure farm-level canal flow, groundwater levels and salinity content, the study relies on data that is collected in existing measurement campaigns. Contact has been established with the Water Management Research Institute (WMRI) of the MWRI, the IIIMP office of the MWRI, the Soil Water and Environment Research Institute (SWERI) of the Ministry of Agriculture and Land Reclamation (MALR), and several foreign consultants involved in IIIMP, to assess the availability of data on water flow, water application, and water quality (salinity) measurements. Based on this communication, an overview of all recorded measurements of relevant parameters was compiled. It was concluded that none of the relevant parameters are currently monitored on the *mesqa* or *marwa* scale in W-10, Daqalt and El Gemeza, and therefore the branch canal level is the highest degree of spatial detail that can be obtained. Ultrasonic flow measurement devices are reportedly purchased as part of the IIIMP program, but not operationally available for the study areas during the year under consideration.

With the help of Dr. Mohamed Nour El-Din, advisor to the IIIMP PMU of the MWRI, the data listed in Table 2 were acquired for the summer 2011 period. Unfortunately, as mentioned before, none of these measurements are performed at the *mesqa* or *marwa* level, which means that no conclusions on spatial variation of these parameters can be drawn beyond the branch canal level. Still, the branch canal measurements provide useful information on the actual conditions in the study areas during summer 2011, which is valuable input to the SWAP model (see Section 2.3). The apparent lack of measurements in the W-10 area is striking, since this area is otherwise well documented in technical reports and most interventions have taken place here. Data that are available for W-10 are recorded for the command area of the El Sefsaf canal, which is part of the total W-10 command area. Given the lack of any further information, the El Sefsaf data are used as an indication of the general conditions in all of W-10, in terms of cropping pattern, water supply and salinity levels. It should be noted that the on/off water delivery schedule is logically not available for W-10, since the water supply to this area operates on a continuous flow schedule.

Table 2: Acquired data of relevant parameters in the study areas.

<i>Parameter</i>	<i>W-10</i>	<i>Daqalt</i>	<i>El Gemeza</i>
Daily water delivery schedules (on/off)	-	available	available
Water supply (m ³ /feddan/day)	-	at inlet	at inlet
Branch canal water levels (m)	-	upstream and downstream	upstream and downstream
Electrical Conductivity (dS/m)	head, middle and tail (El Sefsaf)	head, middle and tail	head, middle and tail
Cropping patterns (seasonal)	available(El Sefsaf)	available	available

Table 3 presents the reported acreages of the main summer crops for each of the areas. Relative areas are comparable, with rice being the dominant crop in all three areas. Of the three selected crops, maize cultivation is the least abundant. The very small acreage of maize causes limitations for several analyses described in Chapter 3, particularly those associated with evaluating spatial variability.

Table 3: Total acreage of main crops in El Sefsaf, Daqalt and El Gemeza in summer 2011 (source: PMU IIIIMP).

	El Sefsaf (W-10)		Daqalt		El Gemeza	
	Area (ha)	Area (%)	Area (ha)	Area (%)	Area (ha)	Area (%)
Rice	458	60.6	1263	59.2	352	58.2
Cotton	216	28.6	419	19.7	168	27.8
Maize	32	4.2	209	9.8	59	9.8
Other crops	50	6.6	242	11.3	26	4.2
Total area	756	100	2133	100	605	100

Water supply at the branch canal level is given in Figure 6, converted from m³/feddan/day to mm/day. El Gemeza flow rates display the variability to be expected due to the rotational flow schedule, with high peaks but also reaching 0 mm/day on several occasions. The El Gemeza rotational water delivery schedule, also delivered by the IIIMP PMU, indicates typical periods of 4 days on and 6 days off. Flow in the Daqalt canal is more constant. Although there is still some variability to be seen in Figure 4, at least some irrigation water is available during the entire period. As stressed earlier, it is not possible to draw conclusions from these data for specific farmers at the *marwa* level, as field-scale flow measurements (eg. head vs. tail end) are not being conducted.

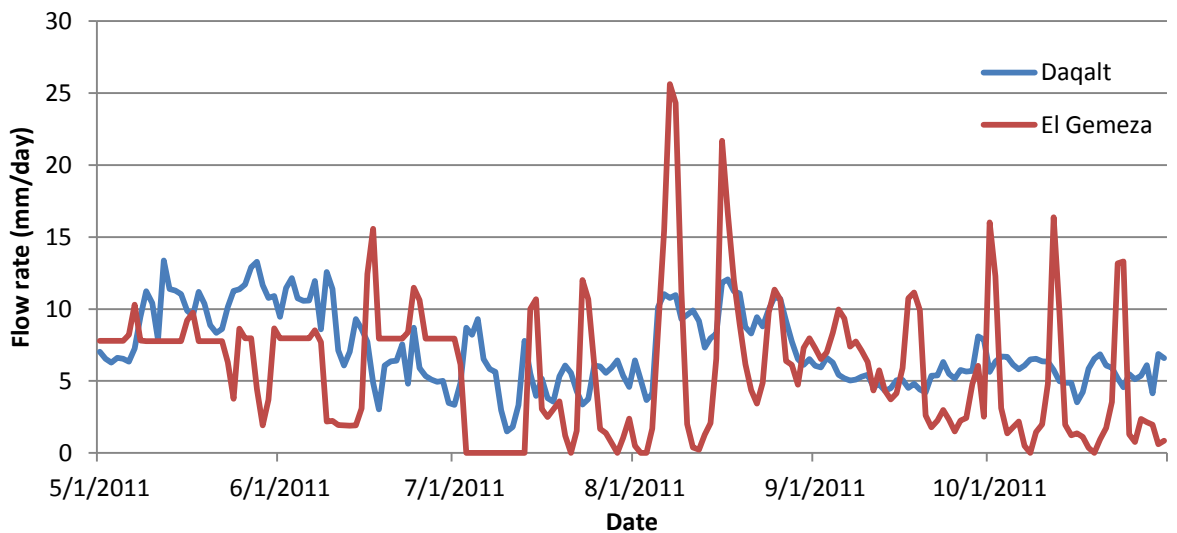


Figure 6: Measured flow rate in mm/day at the inlet of the Daqalt and El Gemeza canal command areas (source: PMU IIIIMP).

Salinity levels in the irrigation water were obtained from electrical conductivity measurements. These measurements were available for three locations (upstream, middle, and downstream) along the different branch canals. These irrigation water salinity levels are used as a direct input to the hydrological model,

as explained in more detail in Section 2.3.2.8. There is no obvious temporal pattern in the recorded salinity levels of the irrigation water during the summer season. However, there are consistent differences between the three locations (head, middle, tail) for each of the canal command areas. Figure 7 presents the distribution of measured salinity levels for each of the measurement sites. As indicated by the figure, downstream salinity levels are higher than those recorded upstream.

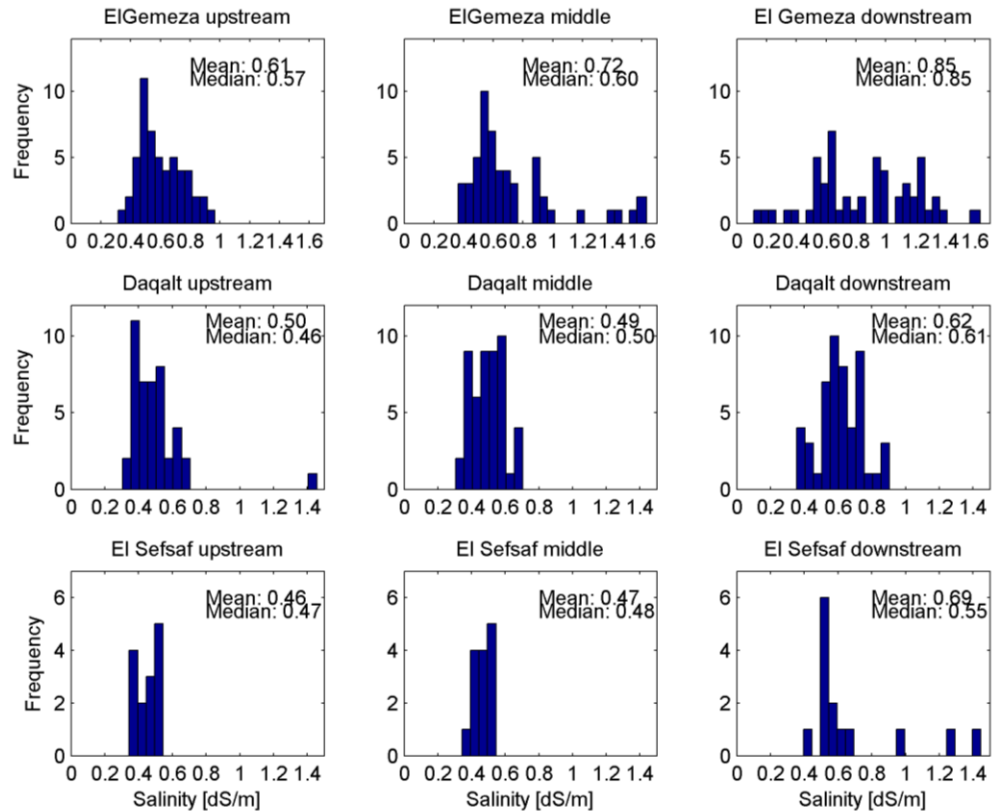


Figure 7: Distributions of salinity levels in the irrigation canals for each of the three branch canal areas. Salinity levels were obtained at upstream, middle, and downstream locations (source: PMU IIIMP). El Sefsaf is part of the W-10 branch canal area.

2.2 Remote Sensing

2.2.1 Available and selected satellite data

As the study commenced during the harvest phase of the summer season 2011, no satellites could be programmed for the summer season and the summer remote sensing analysis relies on archived images. A variety of different archives was searched including Landsat, ASTER, SPOT, RapidEye, Worldview, ALOS and IRS Resourcesat, in order to ensure the optimal high-resolution coverage within the available budget. This is especially important in the Nile Delta because of the very small size of agricultural fields, caused by land division over time.

Following the discontinuity of the Landsat 5 satellite in November 2011, an important source of high-resolution satellite data was no longer available during the winter season. In combination with the

Landsat 7 scanline error, resulting in data gaps in the images, regular coverage of the complete study could not be relied upon. Additional budget was made available to program the ASTER satellite, and a time series of 15 meter ASTER images was achieved from December 2011 onwards, of which 10 images were sufficiently cloud-free to include in the analysis.

Table 4 lists all useful images that were acquired for performing the remote sensing analysis of the summer and winter season 2011/2012. All Landsat 5 data used in this study is provided by the European Space Agency (ESA). Some Landsat 7 images were available for the winter season, but ASTER data was preferred due to the higher spatial resolution and the absence of data gaps in the images.

Table 4: List of available high resolution satellite images during summer 2011 with cloud-free conditions over the study areas.

Date (2011/2012)	Sensor	Spatial resolution (m)
May 17	Landsat 5 TM	30
July 4	Landsat 5 TM	30
July 12	ASTER	15
July 28	Landsat 7 ETM+	30
August 21	Landsat 5 TM	30
August 22	RapidEye	5
September 7	RapidEye	5
September 22	Landsat 5 TM	30
September 26	Worldview 2	2
October 8	Landsat 5 TM	30
December 3	Landsat 7 ETM+	30
December 19	ASTER	15
December 28	ASTER	15
January 29	ASTER	15
February 5	ASTER	15
February 27	SPOT 5	10
March 17	ASTER	15
March 24	ASTER	15
April 9	ASTER	15
April 25	ASTER	15
May 4	ASTER	15
May 11	ASTER	15

The images listed in Table 4 are the basis for 27 two-weekly products of required inputs for the SEBAL analysis (see Section 2.2.3), ranging from May 1st, 2011, to May 14th, 2012. For the data gap in June, the temporal variation of land surface characteristics is determined from MODIS satellite imagery (June 6th and June 22nd were selected). These images have a significantly lower spatial resolution of 250 meters, with thermal pixels being 1000m, but the high overpass frequency (daily) allows for the construction of a temporal curve per crop for the required variables. This function was used, in combination with the spatial variability obtained from the high resolution image that is most representative in terms of surface conditions, to produce two-weekly high resolution products. The same procedure was followed to

compensate for the lack of high-resolution images in November 2011, to bridge the gap between the end of Landsat 5 data provision and the start of the ASTER programming.

Table 5 presents an overview of all images used and their corresponding pixel sizes, as well as the area of individual fields as sampled during the fieldwork. The table shows that the optical bands of the different satellites are smaller than the minimum field sizes in the region for all but one sensor, with MODIS having significantly larger pixel sizes that are insufficient to make field level observations. The thermal pixels of ASTER and Landsat, which also play an important role in the interpretation of remote sensing information (Section 2.2.3), are larger than the average field sizes. This is unfortunate but cannot be avoided, as no currently operational satellite with a regular overpass offers thermal data at a sufficient spatial resolution to distinguish the individual fields. Sections 2.2.2 and 2.2.3 describe how the listed images have been put to use in this study

Table 5: Overview of pixel sizes per satellite (a) and sizes of individual fields b)

a)

	<i>pixel area (ha)</i>		<i>no. of images</i>	
	<i>optical</i>	<i>thermal</i>	<i>summer</i>	<i>winter</i>
<i>Worldview 2</i>	0.0004	-	1	0
<i>RapidEye</i>	0.0025	-	2	0
<i>SPOT 5</i>	0.01	-	0	1
<i>ASTER</i>	0.0225	0.81	1	10
<i>Landsat 7</i>	0.09	0.36	1	1
<i>Landsat 5</i>	0.09	1.44	5	0
<i>MODIS</i>	6.25	100	2	1

b)

	<i>field size (ha)</i>	
	<i>summer</i>	<i>winter</i>
<i>mean</i>	0.48	0.39
<i>minimum</i>	0.13	0.13
<i>maximum</i>	1.76	1.10
<i>st. dev.</i>	0.23	0.17

2.2.2 Crop classification

In order to produce spatial outputs of water consumption and yield for each individual crop, it is necessary to perform a spatial classification of crop types in the study areas. The main crops were distinguished based on the available satellite imagery and the summer and winter fieldwork expeditions.

For the summer 2011 classification, the ASTER, Worldview 2 and RapidEye images were selected for use in the crop classification because of their high resolution, and the date of their overpass. The first step was an unsupervised classification to distinguish general classes of agricultural, natural and artificial types of

land cover. Minimum and maximum Normalized Difference Vegetation Index (NDVI) threshold values were afterwards used to eliminate pixels wrongfully classified from each class.

Subsequently, a supervised maximum likelihood classification was performed on the basis of spectral signatures to distinguish the main crop types within the agricultural class. Training sets of spectral signatures were based on the spectral reflectances of the fields sampled in the fieldwork (Section 2.1.1), using the ESRI ArcGIS software package. Of particular interest are the Rapideye images which have 16 days between them, a period which appears to cover the time of harvest for most of the rice fields (Figure 8). These images also contribute an additional red-edge band (located between the optical and near-infrared part of the spectrum), which is especially useful in distinguishing different crop types. To cover both the start and end of the summer season, and thus account for the difference in growing season length between the crops, the Landsat images of May 17th and October 8th were also included in the classification procedure. An added advantage of these images is the presence of a short wave infrared band, which is absent (RapidEye, Worldview 2), or no longer operational (ASTER), on the higher resolution satellites. Actual acreages per crop as reported by the PMU of IIIMP (Table 3) were accounted for in the classification procedure.

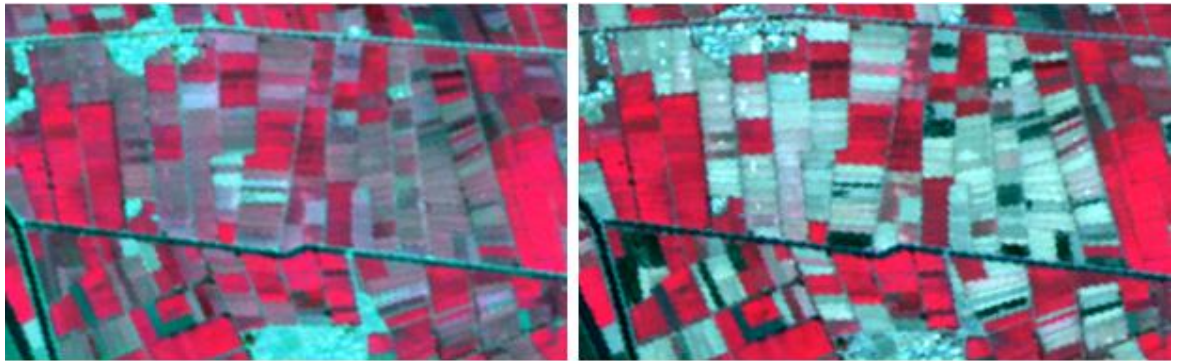


Figure 8: Excerpt of false-color RapidEye images for agricultural fields in the W-10 command area. The left image was captured on 2011/08/22, the right image on 2011/09/07. As the images show, a lot of the fields are harvested within this period of 16 days, making these images an important source of information in the supervised classification.

A similar procedure was followed to distinguish between wheat, berseem and other crops for the winter 2011/2012 season, using the available ASTER and SPOT images for the unsupervised classification and the winter fieldwork results for the supervised classification. As no IIIMP data on total cropping acreages for the winter season, fieldwork observations (with in general a ratio of 60% wheat fields against 40% berseem fields) were used for reference in the crop classification.

Table 5 indicates that the satellite images used in the summer and winter crop classification all have significantly smaller pixel sizes than the average, and even the minimum, field size in the area. This fact, in combination with the large amount of fields sampled in each of the branch canal command areas, leads to the belief that the classification could be performed at a sufficient level of accuracy for extracting crop specific information later on. Still, mixed pixels will occur in the images, and these pollute the spectral signature of the individual crop classes. The use of different sensors with different pixel sizes, particularly for the summer season, introduces an additional error due to the need for georeferencing/orthorectification. For these reasons, it was decided to include all sampled fields in the training set of the supervised classification, to make optimal use of the fieldwork observation and reduce

this error as much as possible. The downside of this is the lack of a reference set with a sufficient population to quantify the accuracy of the classification.

2.2.3 The SEBAL approach - theory and model setup

A satellite does not measure parameters like evapotranspiration or crop growth directly. It measures spectral radiance, which can be converted into surface energy balances, including evapotranspiration, through remote sensing algorithms. In the current study, the WaterWatch in-house algorithm SEBAL (Surface Energy Balance Algorithm for Land) is used to quantify the heat and water vapor exchange rates at the land-atmosphere interface. The theoretical and computational approach of SEBAL is well documented in Bastiaanssen et al. (1998), Bastiaanssen (2000), Bastiaanssen et al. (2005) and Teixeira et al. (2009). METRIC is a US derivative of the original SEBAL model and is extensively described in Allen et al. (2007; 2011).

Figure 9 provides a schematic overview of the SEBAL algorithm. In this study, SEBAL is applied biweekly for the period from May 1st until October 31st, 2011, defined as the main summer cropping season in the Nile Delta, with biweekly conditions represented by the available satellite imagery (Table 4). The spatial resolution of the model runs is chosen in accordance with the input satellite data. Satellite radiances are converted first into land surface characteristics such as surface albedo, NDVI and surface temperature. No data on soil type, crop type, or hydrological conditions are required to apply SEBAL. Inputs additional to satellite images consist of a digital elevation model (obtained from the NASA SRTM mission) and a basic satellite-derived land use map, discriminating between water, vegetated areas, bare soil and built-up area. Also, the SEBAL model requires routine weather data: wind speed, relative humidity, and air temperature. These are available three-hourly from Baltim, the nearest meteorological station that is operational during the studied period, located at approximately 35 km from the study areas (Figure 1). Daily air temperature, relative humidity and wind speed are included in Appendix B. Following the guidelines of FAO (Allen et al., 1998), reference evapotranspiration (ET_{ref}) is inferred from the Baltim weather data and atmospheric transmissivity (based on MSG shortwave radiation, <http://landsaf.meteo.pt>).

The primary basis for the SEBAL model is the surface energy balance. The instantaneous actual evapotranspiration (E_t) flux is calculated for each cell of the remote sensing image as a 'residual' of the surface energy budget equation:

$$ET = R_n - G - H \quad (1)$$

where ET is the latent heat flux (W/m^2), R_n is the net radiation flux at the surface (W/m^2), G is the soil heat flux (W/m^2), and H is the sensible heat flux to the air (W/m^2). The terms of the surface energy balance are different for different types of surfaces. For vegetation the ET value is larger than the H flux, whereas for bare soil the situation is vice versa. SEBAL uses these differences in energy balance behavior of the different surfaces to get a first estimate on the surface energy balance for all pixels.

In Equation (1), the soil heat flux (G) and sensible heat flux (H) are subtracted from the net radiation flux at the surface (R_n) to compute the "residual" energy available for evapotranspiration (λE). Soil heat flux is empirically calculated as a G/R_n fraction using vegetation indices, surface temperature, and surface albedo. Sensible heat flux is computed using wind speed observations, estimated surface roughness, and surface to air temperature differences that are obtained through a sophisticated self-calibration between dry ($\lambda E=0$) and wet ($H=0$) pixels. SEBAL uses an iterative process to correct for atmospheric instability caused by buoyancy effects of surface heating.

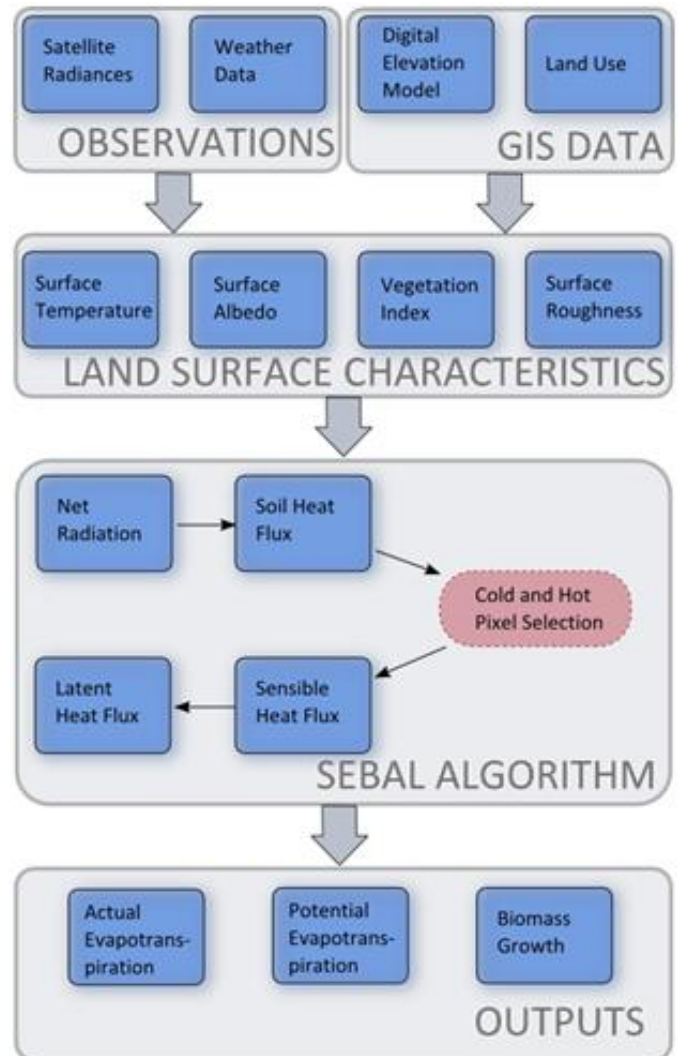


Figure 9: Schematic view of the SEBAL algorithm.

The λE time integration in SEBAL is split into three steps. The first step is to compute the instantaneous evaporative fraction. The second step is the conversion from the instantaneous evaporative fraction into 24 hour values by making the evaporative fraction variable according to advection conditions. The evaporative fraction EF is:

$$EF = \lambda E / (R_n - G) \quad (-) \quad (2)$$

The 24 hour latent heat flux can be determined as:

$$\lambda E_{24} = \psi EF R_{n,24} \quad (W/m^2) \quad (3)$$

where ψ is a correction term that accounts for the EF variability during the day due to advection. For simplicity, the 24 hour value of G is ignored in Equation (3).

The second step is the conversion from a daily latent heat flux into monthly values, which has been achieved by application of the Penman - Monteith equation:

$$\lambda E_{PM} = (s_a R_{n,24} + \rho_a c_p \Delta e / r_a) / (s_a + \gamma (1 + r_s / r_a)) \quad (W/m^2) \quad (4)$$

where s_a (mbar/K) is the slope of the saturated vapor pressure curve, $\rho_a c_p$ (J/m³ K) is the air heat capacity, Δe (mbar) is the vapor pressure deficit, γ (mbar/K) is the psychrometric constant and r_a (s/m) is the aerodynamic resistance. The parameters s_a , Δe and r_a are controlled by meteorological conditions, and R_n and r_s by the hydrological conditions.

The SEBAL computations can only be executed for cloudless days. The result of λE_{24} from Eq. (3) has been explored to convert the Penman - Monteith equation (Eq. 4) and to quantify r_s inversely using $\lambda E_{24} = \lambda E_{PM}$. The spatial distribution of r_s so achieved, will consequently be used to compute λE_{24} by means of Equation (4) for all days without satellite images available (Bastiaanssen and Bandara, 2001). The total ET_a for a given period can be derived from the longer term average λE flux by correcting for the latent heat of vaporization and the density of water.

The resulting actual evapotranspiration (ET_a), which is the sum of evaporation from bare soil or open water bodies and the transpiration of crops, is in this study also referred to as consumptive use. It is important to understand that the consumptive use is the amount of water lost into the atmosphere and thus it cannot be reused but is lost from the hydrological basin. The ET_a from the SEBAL algorithm is crop type independent, which makes SEBAL applicable in areas where a detailed description of the land use is lacking.

Potential evapotranspiration (ET_p) is computed in SEBAL by taking the Penman-Monteith equation using a bulk surface resistance that has no stress factors. Following FAO56, the minimum stomatal resistance of 100 s/m for crop evapotranspiration is used. The remotely sensed Leaf Area Index (LAI) is inserted into the expression of bulk surface resistance, and an empirical relationship for effectiveness of double-sided green leaves has been applied. The result is a map of spatially distributed minimum bulk surface resistance values. In case that the actual value of surface resistance is lower due to specific locally prevailing conditions, the value of minimum bulk surface resistance is adjusted. The net radiation and soil heat flux values are kept identical for ET_a and ET_p prevailing climatic conditions. The accuracy of the net radiation is determined by the solar radiation and the value of the empirical coefficients for net longwave radiation. The modification of ET_a to ET_p does not change these coefficients, and modified air temperatures due to adjusted soil moisture and Bowen ratio values will be marginally different. The value for soil heat flux is mainly controlled by light extinction, and modifying G creates more uncertainty than keeping it as it is. By computing ET_p in this manner, the crop factor (Kc) as described in FAO56 is another output of SEBAL.

Biomass production is calculated according to the principles of the ecological production model of Monteith (1972). This model is based on total Active Photosynthetically Absorbed Radiation (APAR) and a light use efficiency (ϵ) that converts the radiation absorbed into a dry matter production value. Sunshine duration is used to compute global radiation on a day-to-day basis. The interception of this radiation by biological active canopies is derived from the vegetation index. The light use efficiency is approximated as a maximum value for c_3 crops (2.5 gr MJ⁻¹) and a reduction factor depending on the opening of the stomata (Bastiaanssen and Ali, 2003). The opening of the stomata is inversely proportional to the canopy resistance r_s . Hence, the energy balance is also used for the derivation of crop yield.

Actual crop yield (eg. rice grain) is a fraction of the total dry matter biomass produced. This fraction is described by the Harvest Index:

$$Y = Bio * HI / (1 - \theta) \quad (5)$$

in which Y is the fresh crop yield, Bio is the seasonal dry matter production from SEBAL, HI is the Harvest Index and is θ the moisture content.

The distribution of assimilates of a cultivar determines the final physical yield. Since field data on crop yield are collected (Table 1), the Harvest Index can be calculated from the seasonal biomass production calculated by SEBAL, in combination with a crop-specific moisture content taken from literature. Doorenbos and Kassam (1979) - under the aegis of FAO - published a list of common harvest indices, i.e. the ratio of grain to total above ground dry matter production. For rice, Badawi (1995) determined an average Harvest Index from agronomical experiments in the Nile Delta.

To determine the efficiency of water use, the crop water productivity (kg/m^3) is calculated by dividing the physical crop yield by the consumptive use (ET_a). Also, the gross return ($\$/\text{ha}$) is calculated following the methodology of Hellegers *et al.* (2009), using locally prevailing market prices. These parameters are thus related to the amount of water that actually is lost to the hydrological system, rather than the amount of water applied to the crop.

2.2.4 Analysis of equity and reliability of water distribution

As the improvement of equitable distribution of water is a specific goal of the IIIMP, the spatial variation of consumptive use, crop yield and crop water productivity within the branch canal command areas is investigated.

In order to quantify the head-tail differences in water consumption, crop yield and water productivity, the inlet of the areas is fixed and the distance of every pixel from the inlet point is computed. Then, these distances are sliced and normalized for the maximum distance. A histogram equalization procedure is applied to create zones of equal sizes (Figure 10). For each of these zones, the average consumptive use, crop yield and crop water productivity is evaluated, as well as the standard deviation to evaluate the variability of the values occurring in each slice. Subsequently, the slope of the data plotted from the head to the tail end and the percentage difference between head and tail can be analyzed. For El Gemeza, the head-tail analysis was not performed due to its very small size, with only approximately 35 individual fields being counted along the branch canal.

In the absence of *marwa* flow measurements, the temporal reliability of the supply of irrigation water at the farm level is assessed from the SEBAL results. To this end, the evaporative fraction (EF) is taken as a measure of adequacy; i.e. the sufficiency of water use in the irrigation system (IWMI, 1999). Following IWMI research, reliability of irrigation water availability can be described by the temporal variability of soil moisture or a surrogate such as the evaporative fraction. A low average deviation from the mean (AVEDEV) value then reflects temporal stable water supply conditions. It does not provide information on the adequacy of the irrigation application, but provides information on whether the time since last irrigation is too long (high AVEDEV) or is acceptable (low AVEDEV).

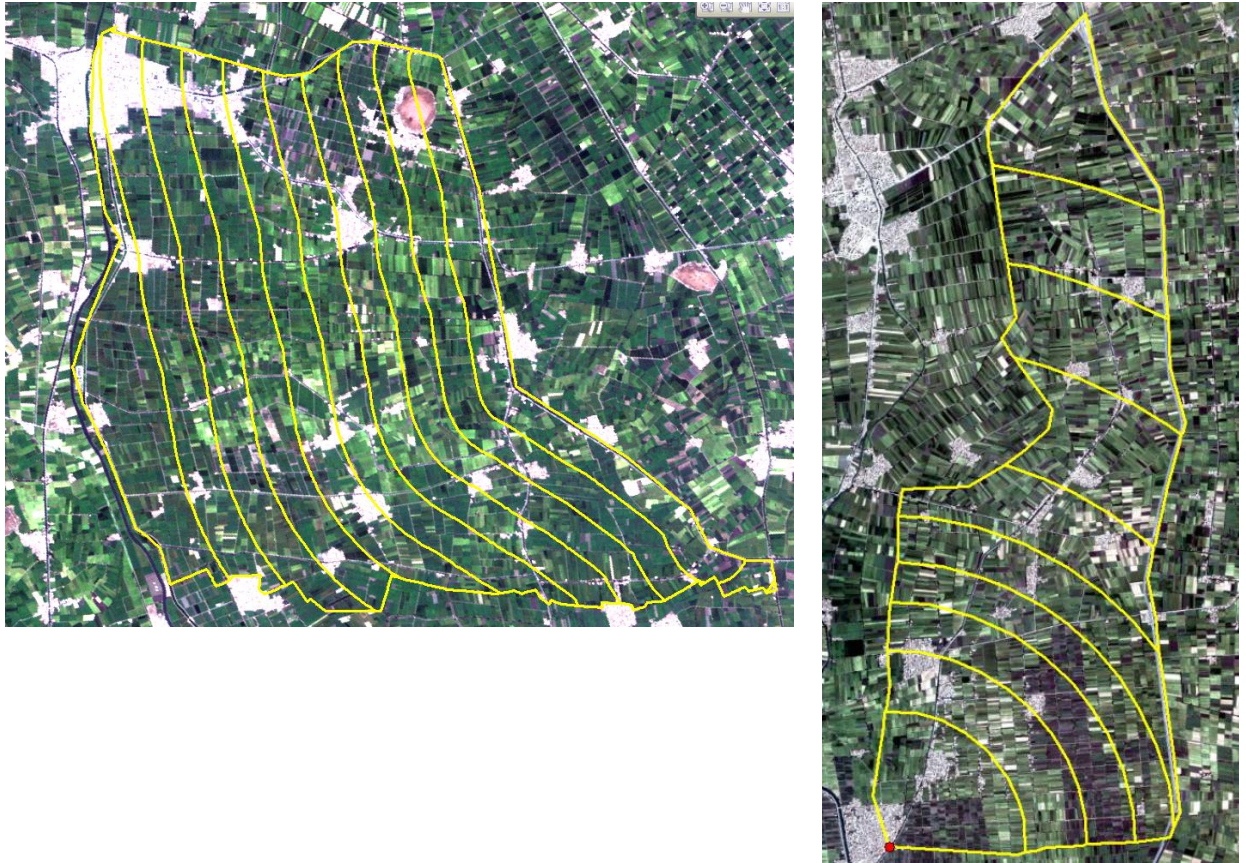


Figure 10: Example of a slicing of distances from the main inlet for the W-10 (l) and Daqalt (r) branch canal command area. The areas have been sliced so that each area occupies 10% of the total area. The red dot indicates the inlet point of the branch canal.

2.2.5 Comparison with historical data

Previously, WaterWatch performed a remote sensing study to assess the effects of the implementation of the Irrigation Improvement Project (IIP), by comparing the years 1995 and 2002. This study was performed at a larger, main canal scale, but does include spatially discrete outputs of water consumption, crop yield, and crop water productivity in the W-10 and Daqalt areas. These historical data are used in a comparison of past conditions and summer 2011 results.

Figure 11 depicts the improved crop water productivity for rice, computed in the previous study. The overall increase in crop water productivity is attributed to the introduction of a high-yielding rice variety at the time of the IIP. Maize was not distinguished in this study, and therefore cannot be included in the comparison. As 1995 is prior to the start of the IIP in W-10 and Daqalt, it is assumed that these results reflect the traditional irrigation conditions. As the historical study was partly based on lower resolution satellite imagery (NOAA, 1km), spatial variations at the field level observed in this study were far smaller than in the current project, making it unfeasible to compare the equity of the parameters under consideration. Therefore, only area-averaged values of water consumption, crop yield and water productivity were compared.

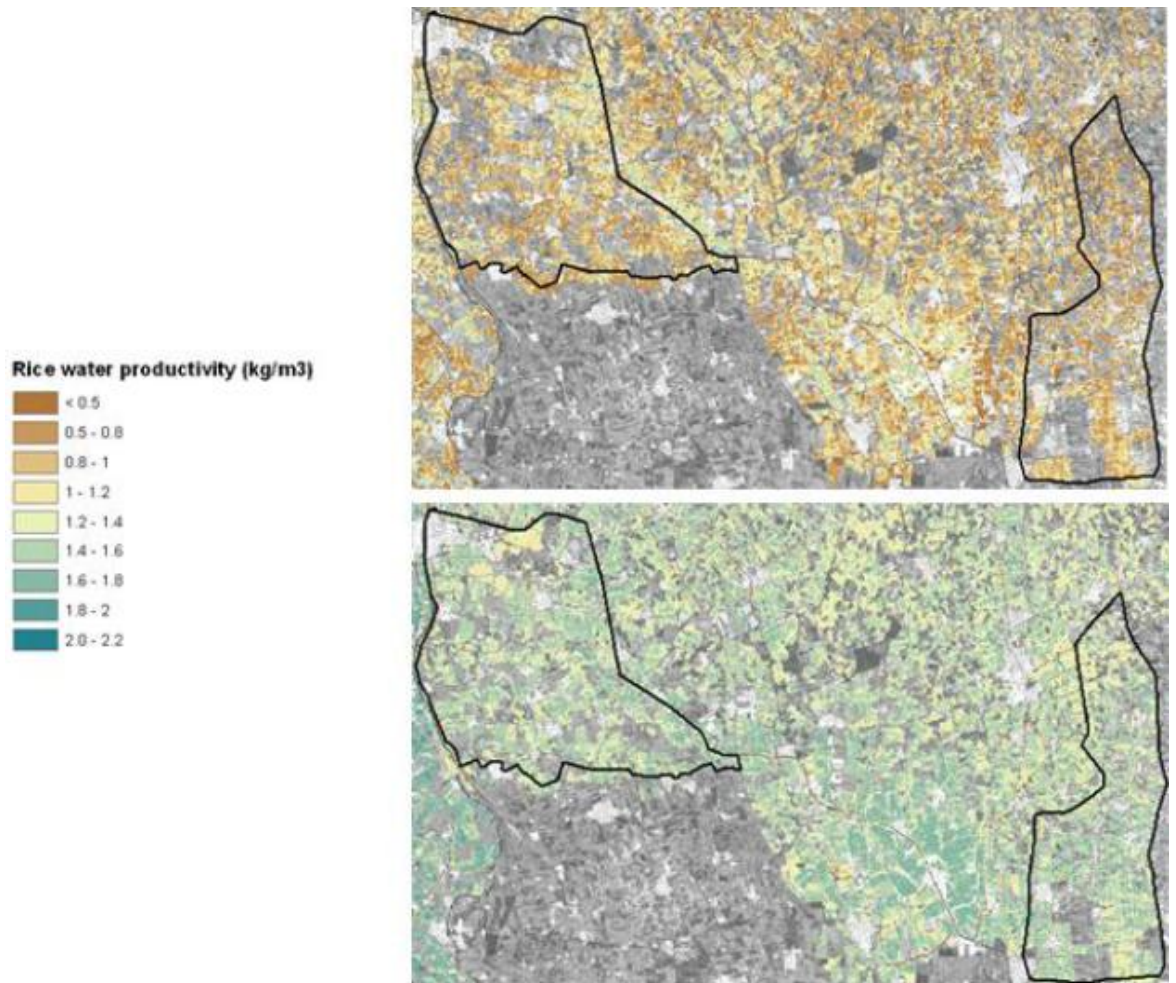


Figure 11: Rice water productivity in summer 1995 (top) and 2002 (bottom) in W-10 and Daqalt.

2.3 Simulation modeling

2.3.1 Water and solute balance modeling using SWAP

The Soil-Water-Atmosphere-Plant (SWAP) (van Dam, 2000; Kroes et al., 2008) was selected as the tool for performing the simulation modeling component of the project. SWAP is developed at Wageningen University and is the successor of the agro-hydrological model SWATR(E) (Feddes et al., 1978). SWAP was selected for several reasons:

- It has been widely tested for environments similar to the current study area (e.g. Bastiaanssen et al., 1996; Salem et al., 1996);
- It is capable of modeling irrigation, drainage and salinity processes under conditions of shallow water tables;
- It is capable of modeling hydrological processes in the entire domain (Figure 12) from the plane just above the canopy to a plane in the shallow groundwater;
- It is world-wide known, used, and appreciated.

SWAP simulates transport of water, solutes and energy in the vadose zone in interaction with vegetation development. In this zone water and solute transport processes are predominantly vertical, and therefore

SWAP is a one-dimensional, vertically directed model. The water transport module in SWAP is based on the Richards' equation, which is a combination of Darcy's law and the continuity equation.

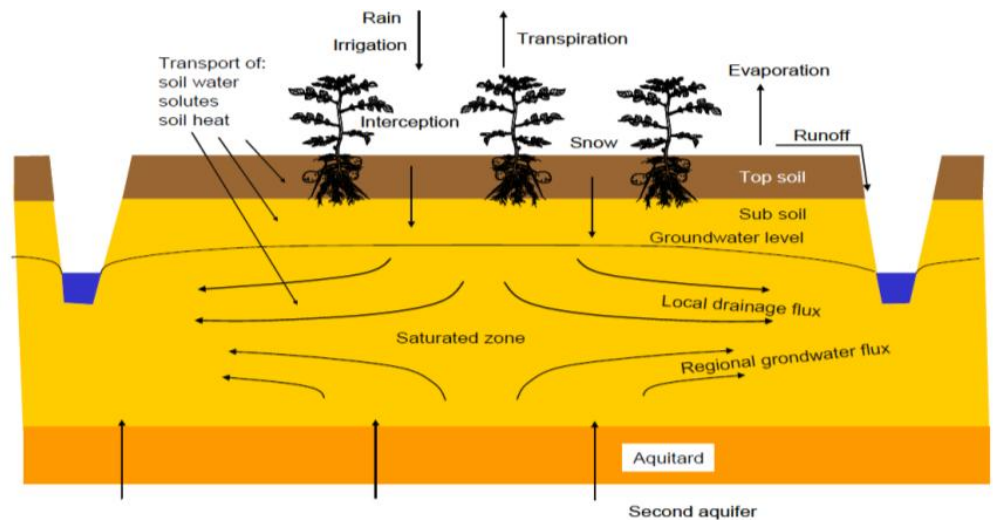


Figure 12: SWAP model domain and transport processes (van Dam, 2000).

Figure 13 shows the schematization of the SWAP model. The vertical flow of water through a 1-D column with defined soil layer characteristics is simulated, with the upper boundary condition consisting of meteorological data (including rain and evapotranspiration) and irrigation inputs, corrected by an interception component dependent on the LAI. The bottom boundary is controlled by soil water pressure head, flux, or the relation between head and flux. Actual transpiration depends on the moisture and salinity conditions in the root zone, weighted by the root density. Actual evaporation depends on the capacity of the soil matrix to transport water to the soil surface. This capacity is determined by the soil water retention and hydraulic functions. Surface runoff is calculated when the height of water ponding on the soil surface exceeds a critical depth. SWAP also simulates drainage, which is incorporated as a sink term in the numerical solution of the Richards' equation. For field-scale applications, often the drainage equations of Hooghoudt (Hooghoudt, 1940) and Ernst (Ernst, 1956) are used.

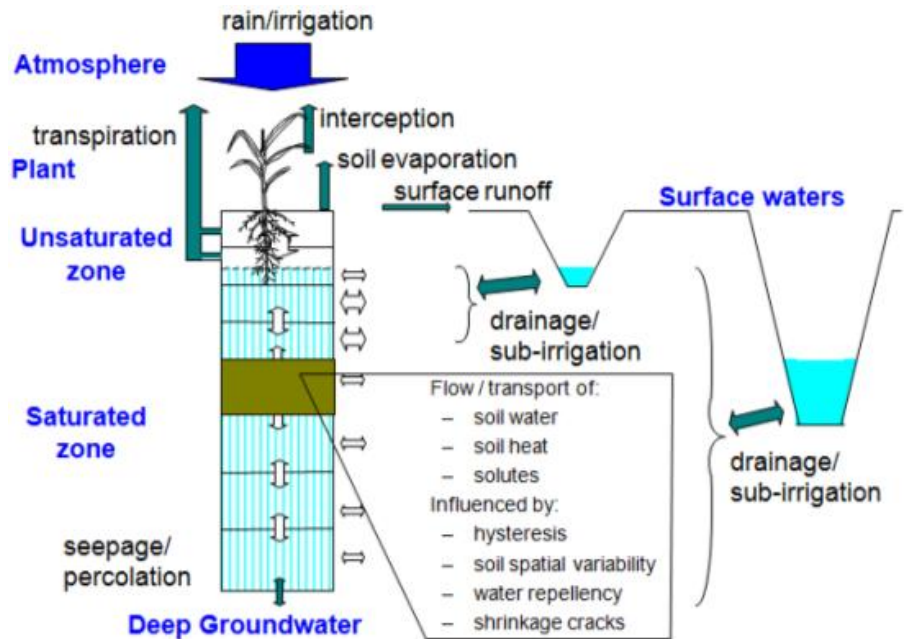


Figure 13: Schematization of the SWAP model (van Dam, 2000).

The calculation of actual transpiration and evaporation in SWAP is illustrated in Figure 14. Starting point in the calculations is the determination of the potential evapotranspiration of different uniform surfaces. The model offers two methods to calculate this potential evapotranspiration: the Penman Monteith method and the reference evapotranspiration method. The latter is used in the current study. It uses a crop factor (K_c , output from SEBAL per fortnight) in order to calculate the potential evapotranspiration of dry and wet uniform canopy and of wet soil. In order to partition the potential evapotranspiration into a potential transpiration rate and potential evaporation rate, SWAP uses the remotely sensed LAI per fortnight and a light extinction factor according to Beer's law. Actual transpiration (T_a) is based on potential transpiration (T_p) using the layered soil moisture and solute concentrations in relation to the distribution of roots. Open water evaporation in SWAP is calculated as the potential evaporation rate of wet soils. More details regarding this can be found in Van Dam (2000) and Kroes et al. (2008).

Irrigation inputs to the model can be prescribed at fixed times, scheduled according to different criteria, or by using a combination of both. In this way, SWAP provides the option of simulating irrigation conditions under a rotational schedule, where water availability is fixed at certain days; being the traditional situation in the Egyptian Nile Delta, and a continuous flow system where the timing of irrigation application will be determined by the farmers' interpretation of crop water stress. Daily crop water stress is expressed as the fraction of actual and potential transpiration (T_a/T_p). This stress is used in combination with a threshold in SWAP (denoted as T_{stress} hereafter), which triggers irrigation in SWAP if the stress (T_a/T_p) on a certain day drops below T_{stress} (e.g. 0.90).

The T_{stress} option is very useful for the current project; it enables the model to distinguish between the traditional rotational flow system (El Gemeza and Daqalt), in which irrigation is set as fixed, and the continuous flow system (W-10, demand driven), in which T_{stress} can be translated into a certain amount of crop stress that is allowed before irrigation is applied. By taking a relative high T_{stress} value, it is assumed that irrigation water is available almost anytime at anyplace, which is assumed to be the reality in the W-10 branch canal area. Therefore, this option will be used in the current study to distinguish between the

rotational flow and continuous flow system. More details regarding irrigation scheduling can be found in Section 2.3.2.5.

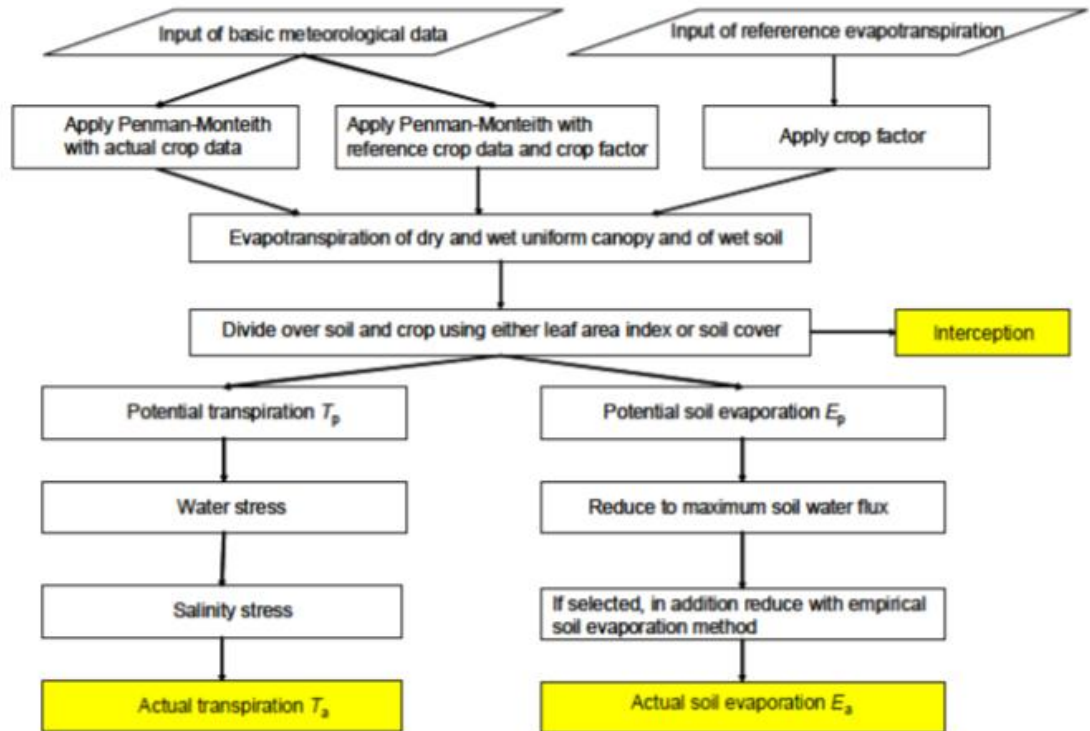


Figure 14: Method used in SWAP to derive actual transpiration and soil evaporation of partly covered soil from basic input data (Kroes et al., 2008).

2.3.2 Data, model schematization and parameterization

The SWAP model input consists of files for main input, meteorological data, crop growth, and drainage. To evaluate the impact of irrigation modernizations on crop yields, water productivity, reuse, drainage and seepage flows, the following data is required:

- Meteorology (rain and reference evapotranspiration)
- Soil hydraulic parameters
- Crop information
- Drainage information
- Initial soil water condition
- Bottom boundary condition
- Irrigation scheduling (fixed, demand driven, irrigation depth)
- Salinity levels (irrigation water, soil water, soil)
- Historical crop yields from Egypt

The current study uses data obtained from a mix of field observations, field surveys, and remote sensing interpretation. Not all the required data, however, was locally available or could be retrieved from remote sensing. Fortunately, many studies have already been piloted in this study area (Bastiaanssen et al., 1996; Amer and de Ridder, 1989). Therefore, data from other studies, which were conducted in the proximity of the study areas, are used in the current study if no local field data was available. The

remainder of this section describes the sources of data that are used, and the assumptions that were made, for a hydrological assessment of the farm-level irrigation modernization.

2.3.2.1 Meteorology - upper model boundary

Rainfall plus irrigation, minus the sum of transpiration, evaporation and interception determines the amount of infiltration in the soil and groundwater fluxes. In general, the sums of rainfall plus irrigation and transpiration plus evaporation plus interception are large compared to their difference, which equals infiltration. This means that relative errors in these sums will increase relative errors in infiltration and groundwater fluxes. Therefore, it is very important to have accurate data on rainfall and evapotranspiration. These meteorological fluxes form, together with irrigation, the upper model boundary.

The meteorological station nearest to the three studied branch canals is Baltim. Rainfall data from this station is used for all three areas. Besides rainfall, the reference evapotranspiration (ET_{ref}) is of major importance. The reference evapotranspiration, in combination with the crop factor (K_c), determines the potential transpiration in SWAP (see Section 2.3.1). In SWAP there is an option to let the model calculate the ET_{ref} using the Penman-Monteith equation (Monteith, 1965), or to provide SWAP with ET_{ref} values. In the current study, the ET_{ref} was derived from meteorological records (see Appendix B) and remotely sensed atmospheric transmissivity to ensure consistency with the ET_{ref} computed by SEBAL.

The time-series of rainfall and ET_{ref} for the general summer season (May 1st - October 31st) are shown in Figure 15 for the three branch canal areas. It is clear that rainfall is very low during summer season. The ET_{ref} is on average 5 mm/day throughout the season and is comparable for all three locations. As only one meteorological station is used in determining ET_{ref} , spatial variations are caused mainly by atmospheric transmissivity. As differences between the three areas are minuscule, only one line for ET_{ref} is depicted. The computed ET_{ref} ranges from a minimum of 3 mm/day to a maximum of 8 mm/day.

The time-series of rainfall and ET_{ref} for the general winter season (November 1st - May 14th) are shown in Figure 16 for the three branch canal areas. The total amount of rainfall during the winter season is 163 mm (Table 6), and is therefore much higher than during the summer season. The ET_{ref} is on average 3 mm/day throughout the winter season, and varies between 1 and 7 mm/day. The total amounts of rainfall and ET_{ref} for all three branch canal areas are shown in Table 7.

Table 6: Total rainfall and reference evapotranspiration (ET_{ref}) for the summer (May 1st - October 31st, 184 days) for each branch canal.

Branch canal	Rainfall [mm]	ET_{ref} [mm]
El Gemeza	1	1008
Daqalt	1	1008
W-10	1	1006

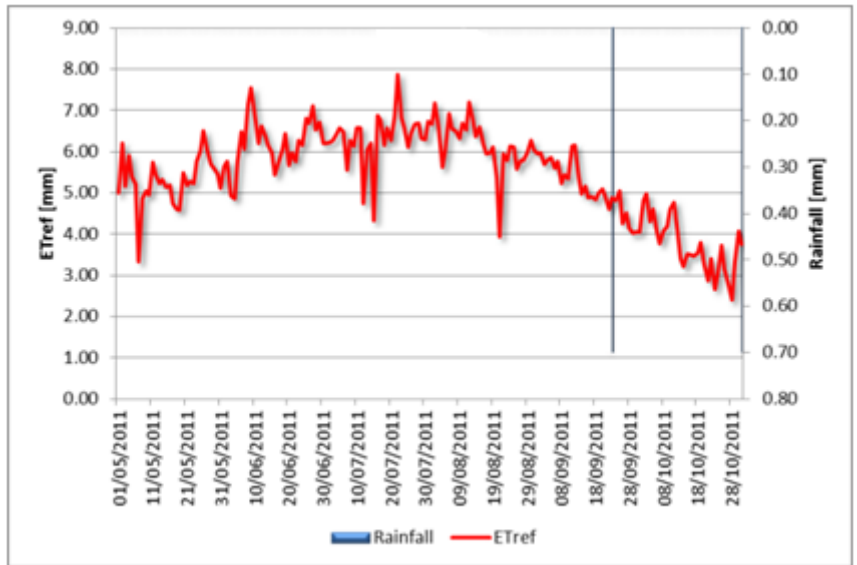


Figure 15: Rainfall and ET_{ref} of summer season for the three branch canal areas.

Table 7: Total rainfall and reference evapotranspiration (ET_{ref}) for the winter for each branch canal.

Branch canal	Rainfall [mm]	ET_{ref} [mm]
El Gemeza	163	564
Daqalt	163	564
W-10	163	564

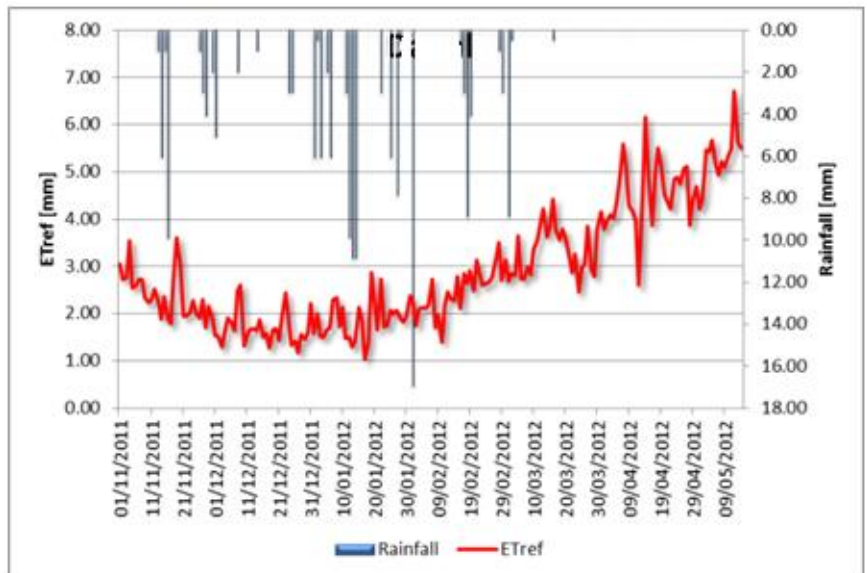


Figure 16: Rainfall and ET_{ref} of winter season for the three branch canal areas.

2.3.2.2 Soil hydraulic parameters

Soil-water flow in SWAP is calculated using the Richards' equation:

$$\frac{\partial \theta}{\partial t} = \frac{\partial \left[K(h) \left(\frac{\partial h}{\partial z} + 1 \right) \right]}{\partial z} - S_a(h) - S_d(h) - S_m(h) \quad (6)$$

where θ is the volumetric water content ($\text{cm}^3 \text{cm}^{-3}$), t is time (d), $K(h)$ is hydraulic conductivity (cm d^{-1}), h is soil water pressure head (cm), z is the vertical coordinate (cm), $S_a(h)$ is soil water extraction rate by plant roots ($\text{cm}^3 \text{cm}^{-3} \text{d}^{-1}$), $S_d(h)$ is the extraction rate by drain discharge in the saturated zone (d^{-1}) and $S_m(h)$ is the exchange rate with macro pores (d^{-1}). SWAP solves this equation numerically, using known relations between θ , h , and K . These relations are expressed in the water retention curve and the unsaturated hydraulic conductivity curve. These curves are often derived from laboratory measurements. If these curves are known, then the Mualem-Van Genuchten (Van Genuchten, 1980) function can be used to fit a curve to the measured curves. The resulting soil hydraulic parameters are then subsequently used to parameterize the soil layers in the SWAP model.

Parameterization

Bastiaanssen et al. (1996) performed a study towards the transportability and inter-comparison of crop-water-environment-models in the Nile Delta in Egypt. They derived a pF-curve (Figure 17) and unsaturated hydraulic conductivity curve (Figure 18) for the Zenkalon area in the Nile Delta. pF is defined as the log to the base 10 of the soil moisture tension expressed in cm of water column height. These soils were taken as representative for the three branch canal areas, because they belong to the same black to brown clay loam soil types as the soils in the study area (Amer and de Ridder, 1989). Using the Mualem-Van Genuchten function (Van Genuchten, 1980) the curves were fitted, and are shown as simulated curves in Figure 17 and Figure 18. The soil parameters corresponding with these curves are shown in Table 8.

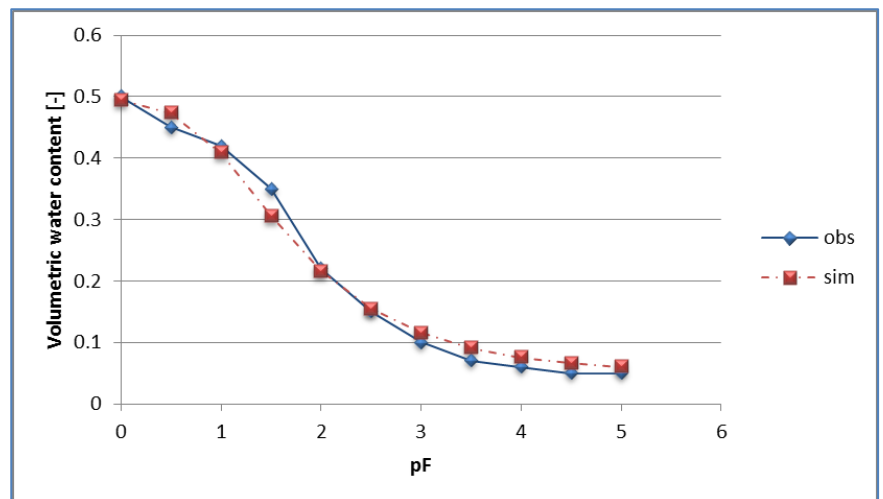


Figure 17: Observed pF curve for Zenkalon derived according to laboratory measurements and model calibration (Bastiaanssen et al., 1996) and simulated pF curve using Mualem-Van Genuchten function (van Genuchten, 1980).

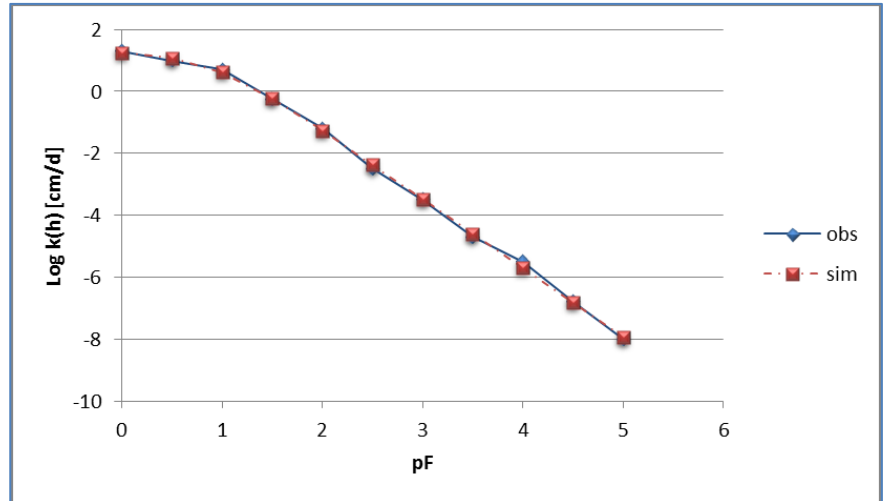


Figure 18: Observed unsaturated hydraulic conductivity curve for Zenkalon derived according to estimations, laboratory measurements, and model calibration (Bastiaanssen et al., 1996) and simulated unsaturated hydraulic conductivity curve using Mualem (1976).

Table 8: Derived SWAP soil-physical parameters.

Θ_{res} cm ³ /cm ³	Θ_{sat} cm ³ /cm ³	α 1/cm	n -	K_{sat} cm/d	λ -
0.05	0.50	0.1139	1.4068	22.09	2.0213

Schematization

The soil profile in SWAP is schematized by the vertical discretization of the soil profile. In addition to the natural soil layers with different hydraulic functions, the thickness and number of calculation compartments should be defined. For the correct simulation of infiltration and evaporation fluxes near the soil surface, the compartment thickness near the soil surface should be ≤ 1 cm (Van Dam, 2000). Deeper in the soil profile, where the soil water flow is less dynamic, the compartment thickness may increase to 10 cm (Van Dam, 2000). As the soil texture gradient is mainly North-South (Kotb et al., 1999) and the studied areas are East-West oriented and located within a few km of each other, the soil profile in SWAP for all three areas was schematized as one soil type with one set of parameters (Table 8). For numerical stability, the soil profile was discretized as shown in Table 9.

Table 9: Schematization of the SWAP soil profile.

Soil sub layer	Depth [cm below surf.]	Height soil compartment [cm]	Number of soil compartments
1	0 - 10	1.0	10
2	10 - 30	5.0	4
3	30 - 60	5.0	6
4	60 - 200	10.0	14

An exception to the schematization is made for the simulation of rice. Because rice is grown in ponded conditions, some pre-measures are taken in the field that allow for ponded conditions. These measures result in a top-soil layer that is less permeable, which results in a reduced infiltration rate and subsequently more surface runoff. Bunds around the rice field prevent surface runoff from flowing out of the field. Therefore, for the correct simulation of rice in SWAP the following changes were made in the schematization:

- The saturated hydraulic conductivity (K_{sat} , Table 8) was reduced to create ponding conditions. This parameter was tuned during the calibration process.
- The ponding thickness parameter was increased during the calibration process; this parameter is the minimum thickness of the water ponding layer before surface runoff takes place.

2.3.2.3 Crops

For the simulation of transpiration, SWAP uses a crop growth model that represents a green canopy that intercepts precipitation, transpires water vapor and shades the ground. Therefore, the user has to specify as function of the development stage (Figure 19) the Leaf Area Index (LAI), crop factor (Kc), and rooting depth. In this project, crop yield is not estimated by SWAP, but from seasonal SEBAL biomass production combined with surveyed farm yields.

Parameterization

For each crop, the LAI and Kc during the growing season is retrieved from the remote sensing imagery and SEBAL results. These LAI and Kc values are used as input into the SWAP model, allowing for the use of information that is determined specifically for the area and period under consideration, instead of general literature values. The root development stages for each crop were obtained from Allen et al. (1998). The maximum root water extraction rate, integrated over the rooting depth, is equal to the potential transpiration, which is governed by atmospheric conditions and plant characteristics. Stresses due to dry or wet conditions and/or high salinities may reduce this root water extraction rate, which subsequently leads to a reduction in the transpiration.

Water shortage and too wet conditions are the result of the hydrological / meteorological conditions. The current study also involves the effect of irrigation modernization on salinity levels for the selected crops. SWAP uses a response function for salinity stress. Below salinity concentrations of EC_{max} (dS/m) no salinity stress is assumed. The EC_{max} definition in SWAP is equal to the EC-threshold as defined by FAO-56. At salinity levels above EC_{max} the root water uptake declines at a rate of EC_{slope} (dS/m). Salinity stress levels are crop specific and were obtained from Allen et al. (1998).

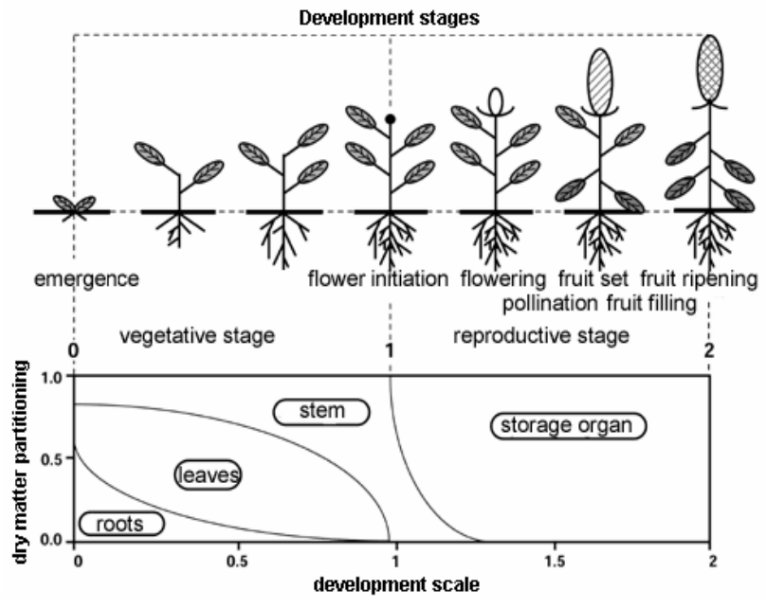


Figure 19: Typical partitioning of assimilated dry matter among leaves, stem, roots and storage organs as function of development stage (Van Dam, 2000).

The crop parameters for each crop are specified in the tables below. The beginning and ending of the growing cycles per crop are determined from remote sensing observations (see Section 3.1).

Table 10: Rice crop parameters (Allen et al., 1998).

Crop characteristic	Development stage			
	Initial	Crop development	Mid-season	Late
Root depth [m]	0.10	>>	>>	0.55
EC _{max} [dS/m]	3.0			
EC _{slope} [dS/m]	12.0			

Table 11: Maize crop parameters (Allen et al., 1998).

Crop characteristic	Development stage			
	Initial	Crop development	Mid-season	Late
Root depth [m]	0.30	>>	>>	1.00
EC _{max} [dS/m]	1.7			
EC _{slope} [dS/m]	12.0			

Table 12: Cotton crop parameters (Allen et al., 1998).

Crop characteristic	Development stage			
	Initial	Crop development	Mid-season	Late
Root depth [m]	0.30	>>	>>	1.40
EC _{max} [dS/m]	7.7			
EC _{slope} [dS/m]	5.2			

Table 13: Wheat crop parameters (Allen et al., 1998).

Crop characteristic	Development stage			
	Initial	Crop development	Mid-season	Late
Root depth [m]	0.30	>>	>>	1.20
EC _{max} [dS/m]	6.0			
EC _{slope} [dS/m]	7.1			

Table 14: Berseem crop parameters (Allen et al., 1998).

Crop characteristic	Development stage			
	Initial	Crop development	Mid-season	Late
Root depth [m]	0.0	>>	>>	0.60
EC _{max} [dS/m]	1.5			
EC _{slope} [dS/m]	5.7			

2.3.2.4 Drainage

The amount of drainage water is a function of crop type and irrigation management, meteorological conditions, and soil characteristics. The current study evaluates the effect of irrigation modernization on both drainage water quantity and quality (e.g. salinity levels). In the Nile Delta, drainage water from the upstream part of a branch area is often reused as irrigation water by a downstream farmer. For SWAP, several drainage characteristics are needed, such as the drain spacing, drain depth, wet perimeter, and entrance resistance.

Schematization and parameterization

Unfortunately, no field-specific drainage fluxes or drainage water salinities are measured for the three branch canal command areas within the existing measurement campaigns. However, there is enough information available regarding the “classic” drainage systems in Egypt. According to Amer and De Ridder (1989) and Bastiaanssen et al. (1996), drainage depths in Egypt can vary between 1.5 m and 0.6 m. For the current study we applied a drainage depth of 1.0 m, which is within the classical ranges often found in Egypt. A commonly used drain spacing in Egypt is 20 m (Amer and de Ridder (1989); Bastiaanssen et al. (1996)). According to the final report of technical support for on-farm improvements in W-10 (Mohamed, 2008), this drain spacing is also commonly used in the W-10 branch canal area. Therefore, a drain spacing of 20 m is used for all simulations. Figure 20 gives an illustration of the ‘traditional’ drainage system which is often found in Egypt.

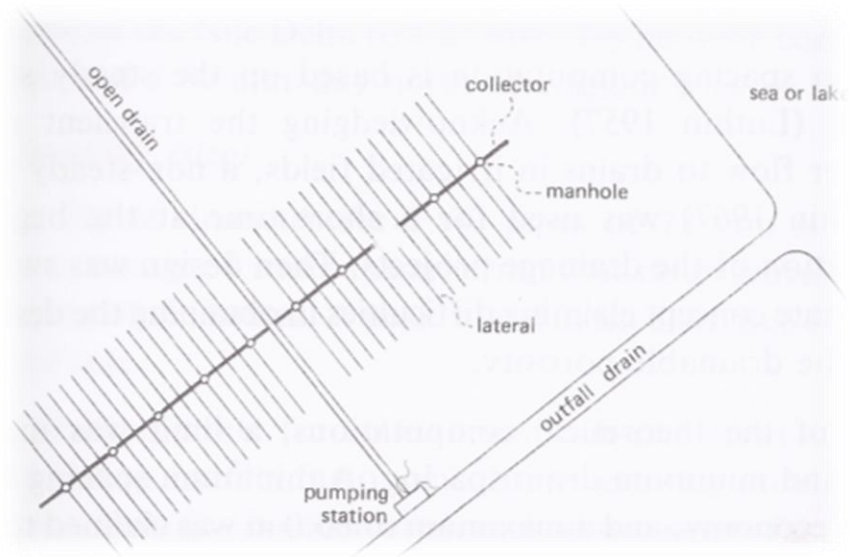


Figure 20: Illustration of a traditional drainage system in Egypt (Amer and de Ridder, 1989).

2.3.2.5 Irrigation scheduling

The current study evaluates the effects of irrigation modernization in three branch canal areas: El Gemeza, Daqalt, and W-10. One of the main components of this modernization is the transition from a traditional “rotational” schedule (where water availability is fixed at certain days) to a “continuous flow” system (where the timing of the irrigation application will be determined by the farmers’ interpretation of crop water stress). The application of irrigation water, together with the meteorological conditions, is part of the upper model boundary condition.

Schematization and parameterization

Average irrigation frequency per branch canal area and per crop has been obtained during field surveys (see Table 22). It is known that W-10 is the only branch canal that is modernized up to the *marwa* level, while Daqalt is modernized up to the *mesqa* level, and El Gemeza is still supplied according to the traditional rotational flow system at branch canal level. Therefore, it was decided to use the “fixed” irrigation option in SWAP for El Gemeza and Daqalt, using the frequencies as described in Table 22. To analyze the effect of the modernization up to the farm-level in W-10, however, we used the T_{stress} option (Section 2.3.1) in SWAP to trigger irrigation if there is a demand for irrigation. This option enables the distinction between the traditional rotational flow system (El Gemeza and Daqalt), in which irrigation is set as fixed (frequencies based on fieldwork), and the continuous flow system (W-10, demand driven). The applied irrigation depth is used as a calibration parameter (Section 2.3.3.1).

It should be noted that the model set-up as described above cannot be based on farm-level flow measurements, as these are not being recorded under existing measurement campaigns. The assumptions on irrigation water availability rely on the statements made by the World Bank regarding the degree of modernization in the studied command areas. Available flow data at the branch canal level (Section 2.1.2) during summer 2011 correspond with these statements.

During the fieldwork, it was established that the prevailing irrigation types in the study area are basin, border and furrow irrigation. SWAP differentiates between surface and sprinkler irrigation. Therefore, the irrigation type in SWAP is schematized as surface irrigation. This is relevant, because if surface irrigation

is applied, no interception of water by leaves will be calculated, which is also the case for furrow irrigation.

Besides the irrigation frequencies, irrigation depth, and irrigation type, the solute concentration of irrigation water is required. This is described in detail in Section 2.3.2.8.

2.3.2.6 Initial soil water conditions (quantitative)

For the initial soil water conditions a prescribed initial groundwater level should be given. Water table depths in the Nile Delta in Egypt are quite shallow, and are often within 1 m from the surface (Bastiaanssen et al., 1996; Amer and de Ridder, 1989). For the current study SWAP was initialized with an initial groundwater depth of -1 m. For the summer simulation, defined for 1 May 2011 through 31 October 2011, SWAP was initialized with the period 1 November 2009 through 30 April 2011 (3 growing seasons). Because of the presence of drains (100 cm below the surface), the groundwater table flattens out to approach drainage levels, and therefore this is a faster responding systems then if no drains were present. Therefore, the defined initialization period gives the model sufficient time to reach a representative water table depth and initial conditions for soil water pressure heads and soil water contents. This is also shown in Figure 21, which represents the groundwater level for the summer growing season (2011 through 31 October 2011) for Maize in Daqalt. It is shown that initialization time is sufficient to reach a groundwater level of -83 cm at the beginning of the growing season. During summer season the groundwater level increases due to irrigation, and eventually decreases again to approach drain depth.

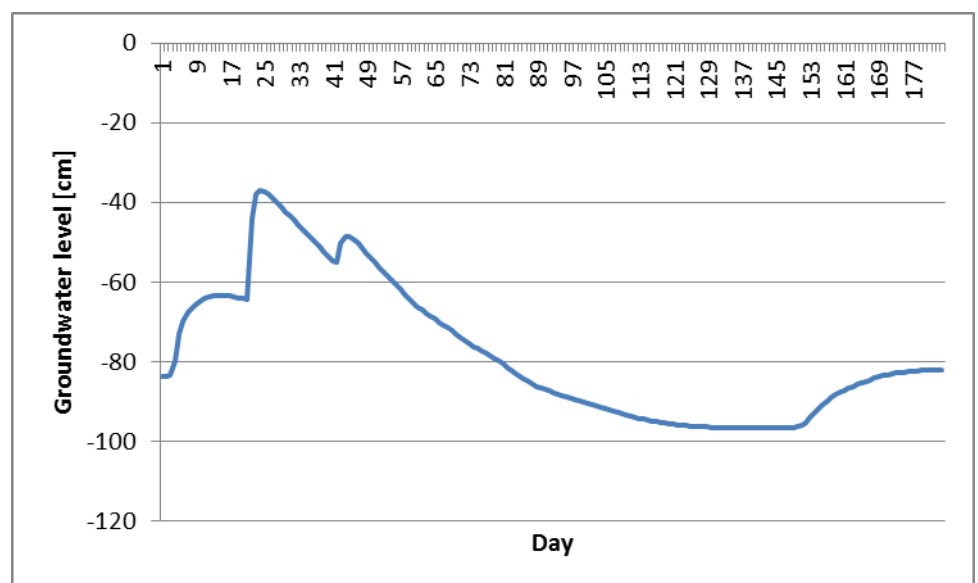


Figure 21: Groundwater level for the summer growing season (2011 through 31 October 2011) for Maize in Daqalt.

2.3.2.7 Bottom boundary condition

The bottom boundary condition has a quantitative and a qualitative aspect. The quantitative aspect is described in this section. The qualitative aspect considers the solutes concentration in the groundwater, which is described in Section 2.3.2.8. SWAP has several options for defining the bottom boundary

condition. These options describe the relation between saturated shallow soil layers with the deep groundwater. According to Amer and de Ridder (1989), the study area is located in a zone with an upward seepage rate of 0.2 mm/d. SWAP offers the option to define a prescribed bottom flux (q_{bot}), which is positive upwards and negative downwards.

Schematization and parameterization

Because of the upward seepage of 0.2 mm/d, a prescribed bottom flux of 0.2 mm/d was defined as bottom boundary condition. Based on the information that is available on the degree of modernization of the three areas, this value was assumed to either be valid for both upstream and downstream areas in case of lined or piped canals, or higher in downstream areas due to canals being not yet modernized, where seepage losses add up to the bottom boundary flux. Following this reasoning, it was assumed that seepage losses in W-10 between the upstream and downstream part are negligible due to the lining of the canals (Figure 3), resulting in a bottom boundary flux of 0.2 mm/day both upstream and downstream. For Daqalt a difference of 10% was introduced due to the occurrence of seepage losses from canals, and for El Gemeza this difference was assumed at 25%. These canal seepage losses are estimates based on expert knowledge, due to the absence of field measurements. A study by Wachyan and Rushton (1987) showed that unlined canals have 30% more seepage losses than lined canals. Although there is a degree of uncertainty regarding the assumed seepage losses, the relevance of the current study lies in evaluating the relative differences in seepage losses between the branch canals, rather than establishing the exact seepage values for each field.

2.3.2.8 Initial solute concentrations (salinity)

The current study involves the effect of irrigation modernization on salinity levels. High salinity levels result in reduced root water uptake, causing reduced crop yields at the end of the growing season. For the correct simulation of salinities, SWAP requires an initial condition (Section 2.3.2.6) and boundary conditions (Section 2.3.2.7).

Schematization and parameterization

As an initial condition (1-Nov-2009), the user needs to specify the solute concentrations in the soil. Amer and de Ridder (1989) studied the salinity levels in the soil and groundwater for the entire Nile Delta. These values are shown in Table 15. According to Amer and de Ridder (1989), the soil salinity in the study area is 3 dS/m on average, which is equal to 1920 mg/l or 1.92 mg/cm³, which are the required SWAP units. Thus for the initial solute concentration in SWAP a value of 1.92 mg/cm³ is chosen, which is assumed to be homogeneous through the soil profile. Since solute concentrations in irrigation water vary per location, one may suggest that it is better to assume different initial solute condition for the three branch canals. However, irrigation water solute concentrations (-0.6 dS/m) that have been measured in all three areas are considerably lower than the initial solute concentration in the soil. In combination with the good working drains, which leads to a non-uniform salinity concentration in the soil profile at the start of the summer season 2011 (see Results section).

The boundary condition consists of an upper and bottom boundary condition. For the top boundary condition, the solute concentrations in irrigation and rain water needs to be specified. It is assumed that the solute concentration of rain water is zero. Salinity levels in the irrigation canals were obtained from the PMU IIIIMP (Figure 7). Analysis showed that there is no clear seasonal pattern in the irrigation water salinity level. This holds for all three branch canal areas. Therefore, the average irrigation water salinity throughout the year is used as input in SWAP. A distinction, however, is made between the upstream and

downstream irrigation water salinities, as salinity levels are observed to increase with distance from the inlet point of the branch canal command area.

For the bottom boundary condition, SWAP uses the flux through the bottom of the soil profile (Section 2.3.2.7) with the average solute concentration in the groundwater. The average solute concentration in the groundwater was obtained from Amer and de Ridder (1989). They studied the salinity levels in the soils, and groundwater for the entire Nile Delta. Therefore, we used their salinity levels for groundwater (Table 15).

Table 15: Salinity levels used for the SWAP model (Amer and de Ridder, 1989).

Parameter	Concentration [mg/l]	Concentration [dS/m]
Rainfall salinity	0	0.0
Initial soil profile salinity	1920	3.0
Average groundwater salinity	2550	3.5

2.3.2.9 Leaching with additional water-supply

As described in the previous section, solutes enter the soil profile through irrigation water (-0.6 dS/m) and through the bottomflux (3.5 dS/m). A certain part of these solutes will leave the soil profile by drainage. However, solutes may still accumulate in the soil profile. Leaching with large amounts of additional water may prevent solutes from accumulating in the soil profile. Unfortunately, no field-specific information (e.g. frequencies and volumes) regarding these possible leaching practices was available for the current study. Therefore, leaching with additional water-supply is not considered in the current study.

2.3.3 Calibration and model runs

Before the effects of farm-level irrigation modernization on water availability and crop yields can be evaluated, the SWAP model needs to be calibrated. The calibrated SWAP model should be capable of simulating the average farm-level water and solute balance. The calibration methodology and results are described in Section 2.3.3.1. The model is calibrated using the data, schematizations and parameterizations as described in the previous section. Subsequently, the calibrated model is used to assess the effects of farm-level irrigation modernization on water availability and crop yields. This is described in Section 2.3.3.2.

2.3.3.1 Calibration

Methodology

The SWAP model is calibrated for the average farm-level field for each branch canal area and for each crop. For the summer season, this results in 9 calibrated SWAP models (3 branch canal areas x 3 crops). For the winter season, this results in 6 calibrated SWAP models (3 branch canal areas x 2 crops). SWAP was calibrated on two targets:

- Match the SWAP ET_a with the average of the SEBAL ET_a distributions (Figure 22, Figure 23, and Figure 24 for summer and Figure 25 and Figure 26 for winter) on a seasonal basis;

- Match the SWAP ET_a/ET_p with the SEBAL ET_a/ET_p (Table 16) on a seasonal basis.

The current study focuses on assessing seasonal differences between the non-modernized, and mesqa and marwa modernized fields in e.g. water consumption, yields, etc. To meet these goals, it is not required to calibrate on a smaller time scale. Also, the reliability of SEBAL results is higher on a seasonal basis, due to the canceling out of a random error factor occurring for smaller time steps (Appendix E). The added value of daily or weekly calibration would become particularly high once measured daily drainage fluxes and salinity levels come available.

Due to the spatial heterogeneity of the study area, a substantial amount of pixels classified as a certain crop, in fact contain a mix of land use types. A correlation was found between low SEBAL ET_a values and distance to built-up areas (villages, individual houses, roads, canals). Pixels where such influence is visible were disregarded in the SWAP calibration procedure, as their reduced ET_a or LAI values are not representative of crop water conditions, but merely a consequence of a discrepancy between the spatial resolution of the modeling exercise and the highly variable land use patterns.

As further explained in Section 3.1, it proved difficult to distinguish maize in El Gemeza in the summer crop classification procedure. Therefore, SWAP could not be calibrated for maize in El Gemeza. It was decided to use the calibrated SWAP model for maize in Daqalt, to simulate the water and solute balance in El Gemeza. It should be noted that field data that was available for maize in El Gemeza (e.g. soils, salinities, irrigation frequencies), are logically used to simulate the water and solute balance for maize in El Gemeza, as is described in Section 2.3.3.2.

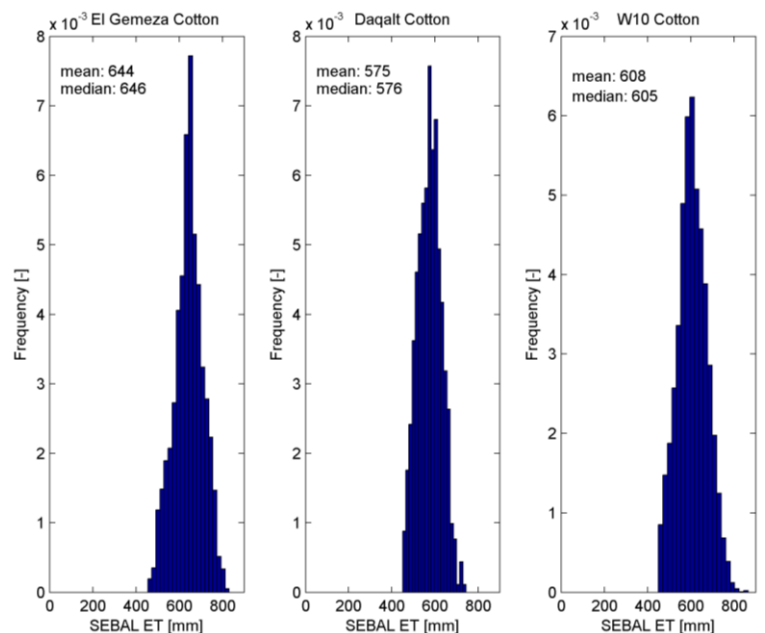


Figure 22: Calculated SEBAL ET distributions for cotton for each of the branch canal areas.

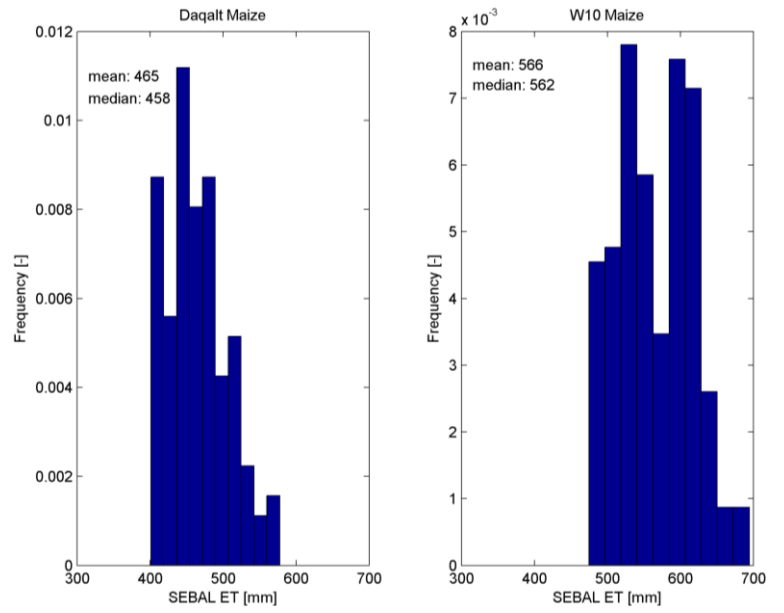


Figure 23: Calculated SEBAL ET distributions for maize for Daqalt and W-10.

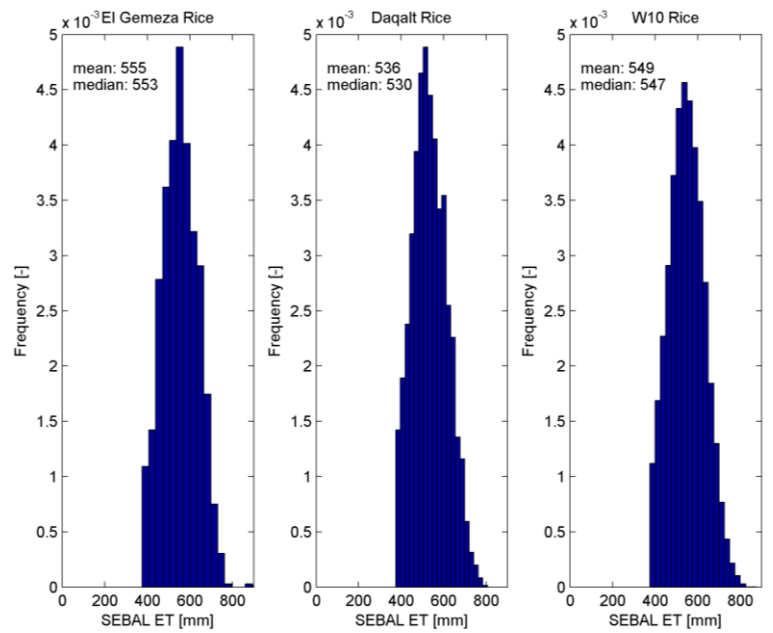


Figure 24: Calculated SEBAL ET distributions for rice for each of the branch canal areas.

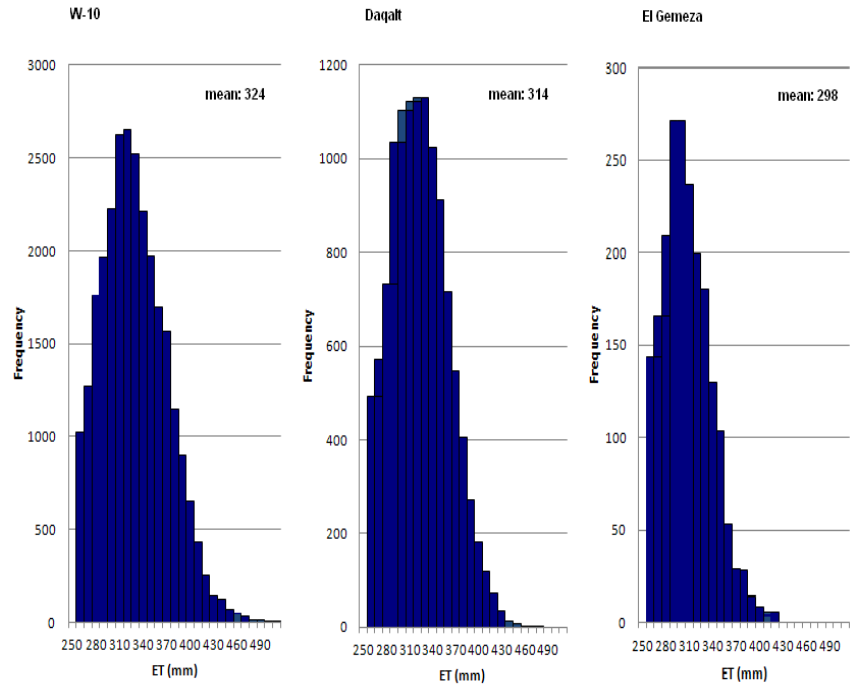


Figure 25: Calculated SEBAL ET distributions for wheat for each of the branch canal areas.

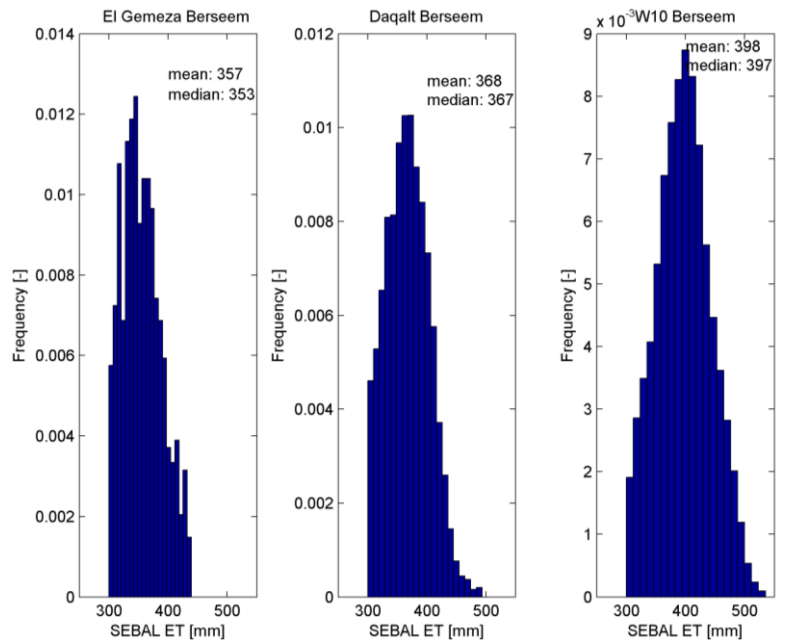


Figure 26: Calculated SEBAL ET distributions for berseem for each of the branch canal areas.

Table 16: Ratio between SEBAL ET_a and ET_p per branch canal and per crop.

Branch canal	Cotton	Maize	Rice	Wheat	Berseem
El Gemeza	0.79	-	0.87	0.64	0.66
Daqalt	0.72	0.71	0.80	0.68	0.73
W-10	0.76	0.88	0.84	0.70	0.79

Because most model parameters were obtained from field data (Section 2.3.2), the largest uncertainty exists for the applied irrigation depth. Therefore this parameter is used as a calibration parameter. Because irrigation in W-10 is triggered by the demand for irrigation, the T_{stress} parameter is an additional calibration parameter in W-10. For rice one additional calibration parameter is required to allow for ponding conditions. This is the K_{sat} parameter.

Table 17: Calibration parameters for each branch canal and crop for the summer season.

Branch canal	Cotton	Maize	Rice
El Gemeza	Irrigation depth	-	Irrigation depth, K_{sat}
Daqalt	Irrigation depth	Irrigation depth	Irrigation depth, K_{sat}
W-10	Irrigation depth, T_{stress}	Irrigation depth, T_{stress}	Irrigation depth, T_{stress} , K_{sat}

Table 18: Calibration parameters for each branch canal and crop for the winter season.

Branch canal	Wheat	Berseem
El Gemeza	Irrigation depth	Irrigation depth
Daqalt	Irrigation depth	Irrigation depth
W-10	Irrigation depth, T_{stress}	Irrigation depth, T_{stress}

Calibration results summer season

By tuning the parameters, as shown in Table 17, SWAP was calibrated for each branch canal and crop. Table 19 shows the summary of calibration results for each branch canal and crop for the summer season. The maximum error between the SWAP ET_a and SEBAL ET_a is 6%. It should be noted that all the simulated ET_a sums fall within the SEBAL distributions (Figure 22, Figure 23, and Figure 24). Also the ratios between ET_a and Etp of SWAP and SEBAL are very comparable. Based on these results it is clear that the SWAP results compare well with the SEBAL values. The resulting calibration parameters are shown in Table 21. It should be realized that the irrigation depths on an individual field would be much higher in reality. But since SWAP simulates an average field, not all farmers irrigate on the same day and time. Therefore the irrigation depths, as shown in Table 19, should be seen as the area average irrigation depth.

Table 19: Summarized calibration results for each branch canal and crop for the summer season. The error term shows the % difference between the average SEBAL ET_a and SWAP ET_a , thus the error introduced in the analysis by the calibration procedure.

Field	Crop	SEBAL ET_a/ET_p [-]	SWAP ET_a/ET_p [-]	SEBAL ET_a [mm]	SWAP ET_a [mm]	Error [%]
El Gemeza	Cotton	0.79	0.77	644	669	4
El Gemeza	Rice	0.87	0.87	555	579	4
Daqalt	Cotton	0.72	0.71	575	604	5
Daqalt	Maize	0.71	0.69	465	473	2
Daqalt	Rice	0.80	0.80	536	546	2
W-10	Cotton	0.76	0.75	608	644	6
W-10	Maize	0.88	0.80	566	549	3
W-10	Rice	0.84	0.86	549	578	5

Calibration results winter season

By tuning the parameters, as shown in Table 18, SWAP was calibrated for each branch canal and crop. Table 20 shows the summarized calibration results for each branch canal and crop for the winter season. The maximum error between the SWAP ET_a and SEBAL ET_a is 3%. It should be noted that all the simulated ET_a sums fall within the SEBAL distributions (Figure 25 and Figure 26). Also the ratios between ET_a and ET_p of SWAP and SEBAL are very comparable. Based on these results it is clear that the SWAP results correspond well with the SEBAL values. The resulting calibration parameters are shown in Table 21. It should be realized that the irrigation depths on an individual field would be much higher in reality. But since SWAP simulates an average field, not all farmers irrigate on the same day and time. Therefore the irrigation depths, as shown in Table 19, should be seen as the area average irrigation depth.

Table 20: Summarized calibration results for each branch canal and crop for the winter season. The error shows the % difference between the average SEBAL ET_a and SWAP ET_a .

Field	Crop	SEBAL ET_a/ET_p [-]	SWAP ET_a/ET_p [-]	SEBAL ET_a [mm]	SWAP ET_a [mm]	Error [%]
El Gemeza	Wheat	0.64	0.67	298	308	3
El Gemeza	Berseem	0.66	0.70	357	354	1
Daqalt	Wheat	0.68	0.69	314	314	0
Daqalt	Berseem	0.73	0.74	368	368	0
W-10	Wheat	0.70	0.71	324	322	0
W-10	Berseem	0.79	0.81	398	412	3

In addition to the summarized results, the water balance gives a good indication of whether the calibrated SWAP model approaches reality. The water balance, which is defined as:

$$\frac{dS}{dt} = Q_{in} - Q_{out} \quad (8)$$

with dS/dt the change in storage, Q_{in} the total inflow, and Q_{out} the total outflow. The total inflow is:

$$Q_{in} = R + Ir + Q_b \quad (9)$$

with R the rainfall, Ir the amount of applied irrigation, and Q_b the bottom flux which is positive upwards. The outflow is defined as:

$$Q_{out} = Run + T_a + E_a + Q_{drain} \quad (10)$$

with Run the runoff, T_a the actual transpiration, E_a the actual evaporation, and Q_{drain} the drainage. The change in storage should be close to zero if the simulation time is 1 year. This means that the total inflow should be more or less equal to the outflow. Another check is that the simulated groundwater table should be shallow (ca. 1 m below surface) (Bastiaanssen et al., 1996; Amer and de Ridder, 1989) and that the groundwater level is not substantially different from its initial state. Analysis of the water balance of the 1-year simulation showed that for all crops and branch canals the change in storage is close to zero, and that the average groundwater table is shallow. An example of the groundwater table throughout the summer season is shown in Figure 21 for maize in Daqalt. A one-year water balance for maize in Daqalt is shown in Appendix C. Based on these numbers, the average shallow and stable groundwater table, and the ET_a and ET_a/ET_p simulations, it can be concluded that the SWAP calibration is successful given the goals of the current study. The appendix shows that the largest model uncertainty exists within the applied irrigation (CV 11%).

Table 21: Final SWAP calibration parameters for each branch canal and crop. No value indicates that this parameter is not used during the calibration process.

Field	Crop	Irr. Depth [mm]	T_{stress} [-]	K_{sat} top layer [mm/d]
El Gemeza	Cotton	16	-	-
El Gemeza	Rice	22	-	1.2
El Gemeza	Wheat	55	-	-
El Gemeza	Berseem	9	-	-
Daqalt	Cotton	42	-	-
Daqalt	Maize	70	-	-
Daqalt	Rice	7	-	1.2
Daqalt	Wheat	60	-	-
Daqalt	Berseem	12		
W-10	Cotton	9	0.92	-
W-10	Maize	8	0.97	-
W-10	Rice	8	0.95	1.2
W-10	Wheat	55	0.81	-
W-10	Berseem	14	0.94	-

2.3.3.2 Model runs

Several SWAP runs were defined that represent the situation in the field, with a clear distinction between the upstream and downstream conditions. Upstream is defined as the 10% of the total area that is closest to the inlet point, while the downstream portion is the final 10% along the canal length. These values are

20% for the El Gemeza command area, due to its very small size. This distinction was made because it is very likely that in El Gemeza (not modernized) due to seepage losses, the downstream farmer has less irrigation water available than the upstream farmer. In addition to this, the salinity levels in irrigation water are higher downstream than upstream (Figure 7). Since there are three summer crops, two winter crops, three branch canal areas, and an upstream and downstream part, 30 model runs have been defined. These model runs are differentiated in:

- Irrigation frequencies;
- Canal seepage losses;
- Salinity levels.

The irrigation frequencies for El Gemeza and Daqalt are fixed according the irrigation intervals obtained from the summer and winter fieldwork. Irrigation frequencies in W-10 are “demand driven”, and are based on the T_{stress} threshold as determined during the calibration process. Seepage losses are translated into having less irrigation water available downstream, and an increase in the bottom boundary flux. Seepage losses were determined based on expert knowledge and on a study by Wachyan and Rushton (1987). The irrigation water salinity levels upstream and downstream have been obtained from the IIIMP PMU. The SWAP model simulations are presented in Table 22.

Table 22: Defined SWAP simulations (30 model runs).

Field	Crop	Location	Irrigation frequency	Seepage losses [%]	Salinity [dS/m]
El Gemeza	Cotton	Upstream	4 days on, 6 days off	0	0.61
El Gemeza	Cotton	Downstream	4 days on, 6 days off	25	0.85
Daqalt	Cotton	Upstream	Every 20 days	0	0.50
Daqalt	Cotton	Downstream	Every 20 days	10	0.62
W10	Cotton	Upstream	Demand driven	0	0.46
W10	Cotton	Downstream	Demand driven	0	0.69
El Gemeza	Maize	Upstream	4 days on, 6 days off	0	0.61
El Gemeza	Maize	Downstream	4 days on, 6 days off	25	0.85
Daqalt	Maize	Upstream	Every 20 days	0	0.50
Daqalt	Maize	Downstream	Every 20 days	10	0.62
W10	Maize	Upstream	Demand driven	0	0.46
W10	Maize	Downstream	Demand driven	0	0.69
El Gemeza	Rice	Upstream	4 days on, 6 days off	0	0.61
El Gemeza	Rice	Downstream	4 days on, 6 days off	25	0.85
Daqalt	Rice	Upstream	Every 2 days	0	0.50
Daqalt	Rice	Downstream	Every 2 days	10	0.62
W10	Rice	Upstream	Demand driven	0	0.46
W10	Rice	Downstream	Demand driven	0	0.69
El Gemeza	Wheat	Upstream	3 times during the season	0	0.61
El Gemeza	Wheat	Downstream	3 times during the season	25	0.85
Daqalt	Wheat	Upstream	3 times during the season	0	0.50
Daqalt	Wheat	Downstream	3 times during the season	10	0.62
W10	Wheat	Upstream	Demand driven	0	0.46
W10	Wheat	Downstream	Demand driven	0	0.69
El Gemeza	Berseem	Upstream	Every 10 days	0	0.61
El Gemeza	Berseem	Downstream	Every 10 days	25	0.85
Daqalt	Berseem	Upstream	Every 10 days	0	0.50
Daqalt	Berseem	Downstream	Every 10 days	10	0.62
W10	Berseem	Upstream	Demand driven	0	0.46
W10	Berseem	Downstream	Demand driven	0	0.69

2.4 Capacity building

As described in Section 1.3, the project includes the objective of capacity building for the key local counterparts, in particular the different Agricultural Research Centers (ARC) of the MALR and the Water Management Research Institute (WMRI) and IIIMP office of the MWRI.

A kickoff workshop was organized in Cairo at the office of the Executive Authority for Land Improvement Projects (EALIP), part of the MALR, on 26-27 October 2011. A list of workshop participants is included as Appendix D. As the attendants were coming from a variety of backgrounds, the training course commenced with an introduction on the principles of the different tools that are applied in the project. This included the basic theory of remote sensing interpretation for water resource management and the functioning of the SEBAL and SWAP models. The main part of the training course focused on explaining the integrated methodological approach of fieldwork, remote sensing interpretation and simulation modeling, and how the data obtained from one component feeds into another. Results of earlier projects conducted in Egypt and abroad were used to clarify the added value of the proposed methodology and illustrate the type of results that will be obtained from this project. The content of the workshop was provided to the attendants as course material.

The final workshop took place on September 26th at the EALIP office in Cairo. The project results as described in the interim report were presented and discussed with an audience coming from various agencies of the MALR and MWRI, as well as attendants affiliated with the World Bank and the International Water Management Institute (IWMI). A special focus was put on the limitations of data availability and of the technical approach, to define a number of lessons that need to be dealt with in a future study. Inputs from workshop attendants have been incorporated in this report.



Figure 27: Kickoff workshop at the EALIP office, October 26-27 2011.

3 Results summer 2011

3.1 Cropping pattern

Based on the crop identification performed in the field and the selected satellite images (Section 2.2.2), a supervised classification was performed, while accounting for the acreages delivered by the PMU IIIMP. The end result of this procedure is a land use map, with a special focus on the distinction of the different crop types. For rice and cotton, the performed fieldwork in W-10 and Daqalt and the available satellite imagery proved to be enough basis for distinguishing the different crops in all three areas. However, the small portion of fields classified as maize during the fieldwork (which was not performed in El Gemeza), in combination with spectral reflectance characteristics derived from the available satellite images, was insufficient to produce a reliable maize classification for El Gemeza. Therefore, remote sensing derived spatial results for maize in El Gemeza, which comprises a total acreage of just 59 ha (Table 3), are not available. As mentioned in paragraph 2.3.3.1, the SWAP model calibrated for Daqalt was used to compute the water and solute balance for maize in El Gemeza, using the appropriate input data specific for El Gemeza.

Figure 28 depicts the summer 2011 land use map resulting from the supervised classification procedure.

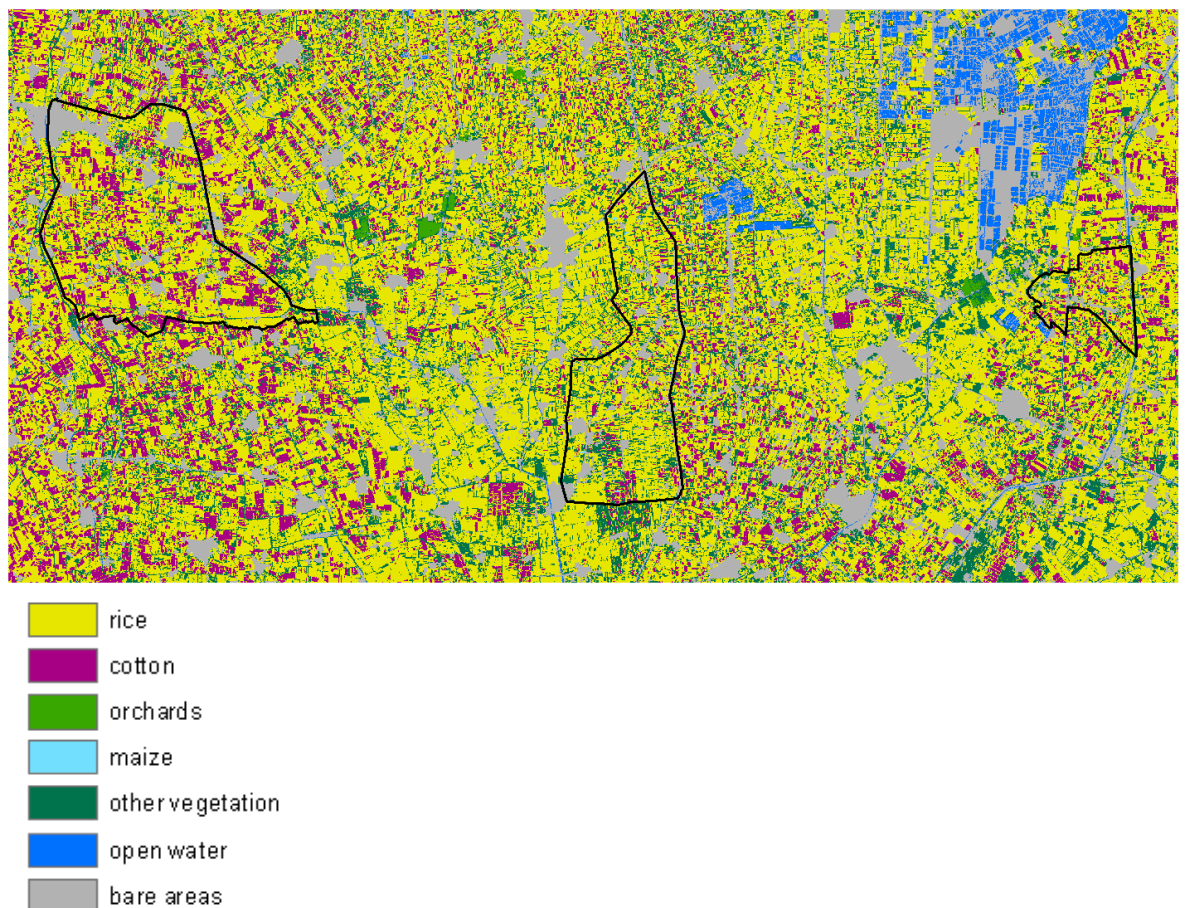


Figure 28: Summer 2011 land use map of the study areas.

Although the main summer cropping season was defined as ranging from May 1st to October 31st, it was observed that the length of the actual growing cycle is crop-specific. Figure 29 presents a comparison of average NDVI values per agricultural land use class as derived from the collected satellite imagery. Especially for rice it is important to fully cover the early phase of the growing season in the current analysis, since ponding conditions will already account for substantial water consumption early in the season. While all crop types show a similar vegetation curve during the early summer months, particularly the harvest date is crop dependent. It should be noted that the temporal coverage of satellite imagery is better in the final months than in the early months of the season (Table 4), thus yielding a more reliable and representative NDVI profile for the months July to October. June NDVI values are based on MODIS imagery. 1). MODIS NDVI's are included in Figure 29, resulting in a less fluent curve for the first part of the season, and more mixing of crop types due to the lower spatial resolution. Timely programming of a high resolution satellite would ensure more regular coverage of the area and thus help in avoiding this problem.

Maize and rice already show a sharp decrease in vegetation cover in late August, whereas many cotton fields still have high NDVI values on October 8th (the date of the final high-resolution image available). Based on the time profile of vegetation indices derived from additional MODIS 250m images for late October and early November, it was determined that the cotton season in fact lasts until the end of October, covering the full generally defined summer season of 184 days. For maize and rice, the end of the growing season was set at October 1st, yielding a total season length of 153 days. This period is longer than the growing season for an individual field, but is necessary to include the land preparation period and harvest time of the majority of the fields in the time range.

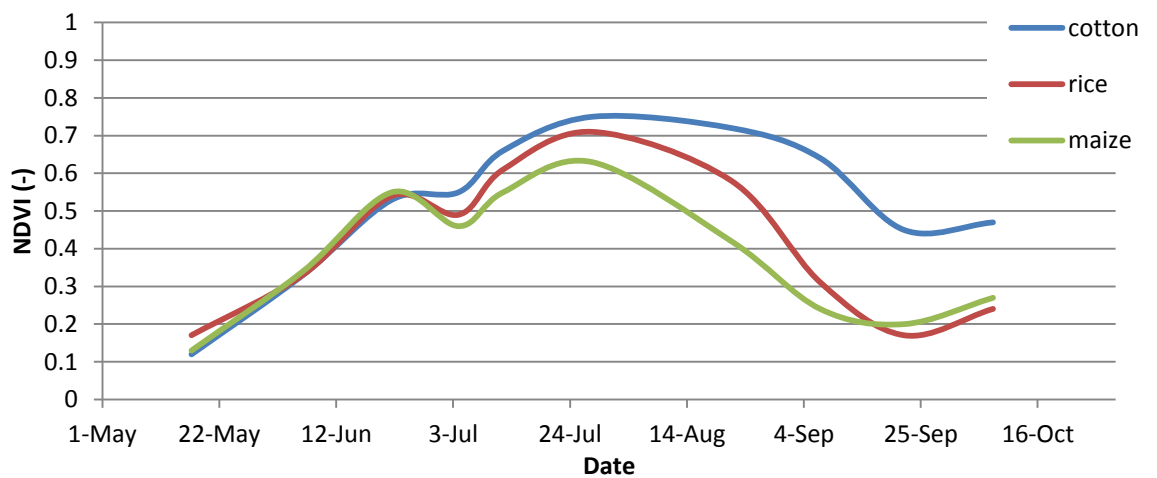


Figure 29: Temporal evolution of the vegetation index (NDVI) for the summer agricultural classes based on the available high-resolution satellite data (combined with MODIS data for June).

3.2 Water consumption

3.2.1 Rice

Figure 30 depicts maps of seasonal water consumption for rice in W-10, Daqalt and El Gemeza. Water consumption in this figure is accumulated for the crop specific growing season (as discussed in the previous section).

The water consumption results for rice are summarized per branch canal in Table 23. As the table shows, ET_a in summer 2011 is higher in El Gemeza than in the other two areas. This possible effect of branch canal modernization efforts is also present when comparing seasonal ET_a of 2011 in W-10 and Daqalt to the same areas in earlier years 1995 and 2002, which also shows a decrease in water consumption. However, it should be noted that all differences are within the range of the error bars of the SEBAL model, and could also be related to minor differences in meteorological conditions.

The final step of farm-level modernization is less prevalent in the water consumption figures for rice, with water consumption in W-10 being higher than in Daqalt. The spatial variability in ET_a , as expressed by the coefficient of variation (CV), is equal for all areas. The head-tail analysis (Figure 31) shows that there is a slightly decreasing trend in water consumption along the branch canal, with the decline being somewhat sharper in Daqalt. This could be an indication of less irrigation water availability downstream.

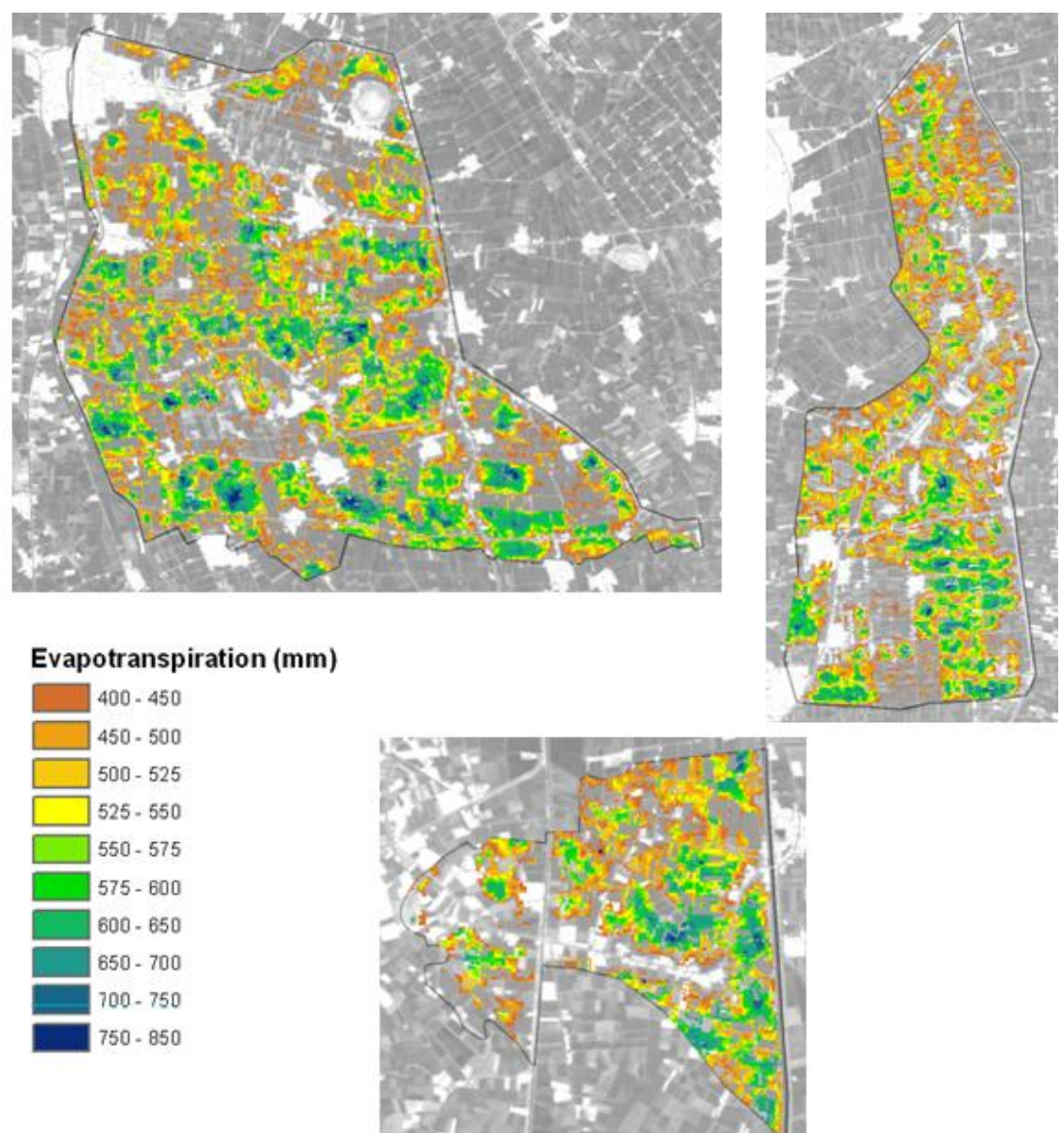


Figure 30: Spatial distribution of seasonal water consumption (ET_a) of rice in W-10, Daqalt and El Gemeza (clockwise) during summer 2011.

Table 23: Average rice water consumption during the 2011, 2002 and 1995 growing seasons.

	2011			2002	1995
	ET_a (mm)	σ	CV	ET_a (mm)	ET_a (mm)
W-10	549	83.2	0.152	566	555
Daqalt	536	81.0	0.151	560	548
El Gemeza	555	83.6	0.151	-	-

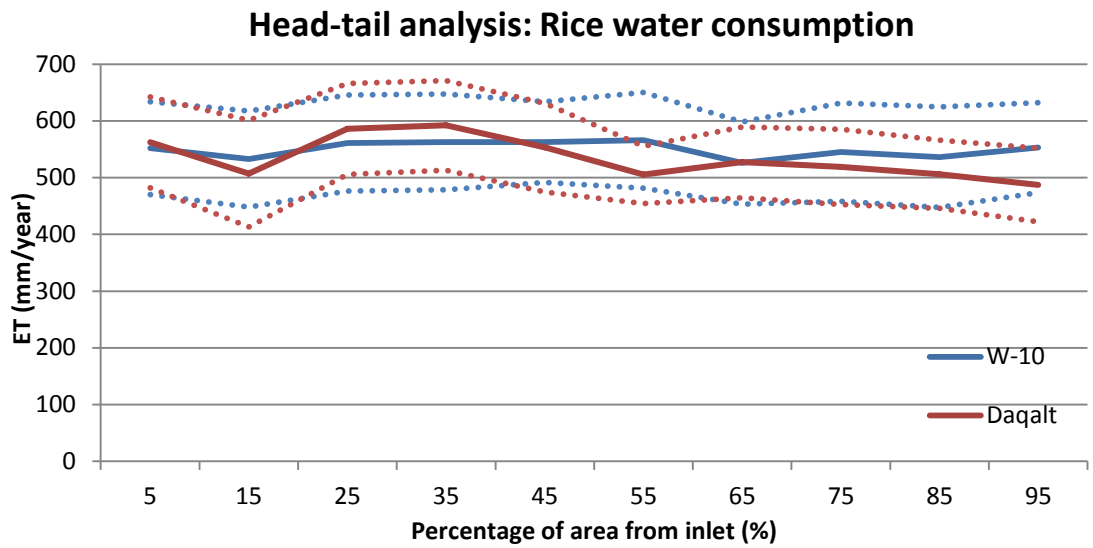


Figure 31: Head-tail analysis of water consumption from rice fields in W-10 and Daqalt. Dashed lines indicate a variability range (mean plus and minus standard deviation per 10% section)

Table 24 shows the water consumption for rice per branch canal and upstream/downstream location, with the distinction between T_a and E_a as computed with SWAP. All branch canals and upstream/downstream fields show comparable results, with approximately 80% of water used for transpiration and 20% water lost through evaporation. Soil evaporation under rice production is high when compared to other crops, due to ponded conditions. However, an underestimation of E_a could still be occurring due to the availability of only one image during the rice preparation phase (May 17th, Table 4). Availability of more high-resolution imagery by sensor programming could resolve this issue (see Paragraph 5.2.2). However, this is not expected to affect the minor relative differences between command areas that are listed in Table 24.

Table 24: Applied irrigation volumes, transpiration (T_a) and water losses through evaporation (E_a) for rice per branch canal and upstream/downstream location.

Field	Crop	Location	Irrigation [m ³ /ha]	ET _a [m ³ /ha]	T _a [m ³ /ha]	T _a /ET _a [%]	E _a [m ³ /ha]	E _a /ET _a [%]
El Gemeza	Rice	Upstream	6720	5938	4802	81%	1136	19%
El Gemeza	Rice	Downstream	5600	5592	4456	80%	1136	20%
Daqalt	Rice	Upstream	5180	5557	4438	80%	1119	20%
Daqalt	Rice	Downstream	4690	5385	4266	79%	1119	21%
W10	Rice	Upstream	6240	5774	4623	80%	1151	20%
W10	Rice	Downstream	6320	5766	4615	80%	1151	20%

Figure 32 shows the rice water stress due to water shortage through time, where the amount of stress is expressed as a percentage of T_p . Water shortage stress for rice can occur even under ponded conditions. This is related to the fact that, under ponded conditions, a thin soil layer with low water permeability is created. Therefore, water will mainly stay in the paddies, while a part of the water slowly infiltrates into the soil layer below. This creates unsaturated conditions just below the surface (negative suction). Therefore, the roots may experience water shortage due to the slow infiltration of water into the soil. This phenomenon has been described in various publications (eg. Bouman et al., 2001). Based on Figure 32, water stresses in Daqalt are higher than in the other two branch canals. This is likely to be related to the high irrigation frequency (every two days) in combination with a small irrigation depth per application. This results in a smaller total irrigation sum for rice in Daqalt (see also Table 37).

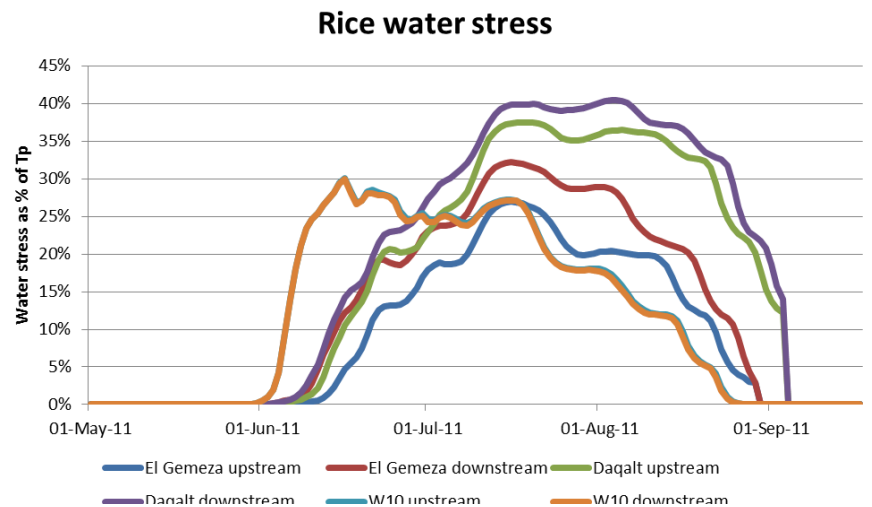


Figure 32: Rice water stress for each branch canal and upstream/downstream location. Rice water stress is expressed as percentage water of potential transpiration.

3.2.2 Cotton

Figure 33 depicts the water consumption for cotton in W-10, Daqalt and El Gemeza. Water consumption in this figure is accumulated for the crop specific growing season (as discussed in Section 3.1).

The water consumption results for cotton are summarized per crop in Table 24. As the table shows, ET_a in summer 2011 is higher in El Gemeza than in the other two areas. This possible effect of branch canal and

mesqa modernization efforts is also present when comparing seasonal ET_a of 2011 in W-10 and Daqalt to the same areas in earlier years 1995 and 2002, which also shows a decrease in water consumption. For cotton this decrease is particularly sharp, and this trend continues toward 2011. Regarding the effect of *marwa* level modernizations, no further decrease in water consumption is observed, with ET_a being even somewhat higher in W-10 than in Daqalt.

Similar to what is observed for rice, field level irrigation modernization has not led to a decrease in water consumption for cotton, as more water is consumed in W-10 compared to Daqalt. Differences in the variability in ET_a , as expressed by the coefficient of variation (CV), are negligibly small. The head-tail analysis does not show a clear trend, and thus does not indicate that water consumption would be limited by irrigation water availability decreasing in downstream direction.

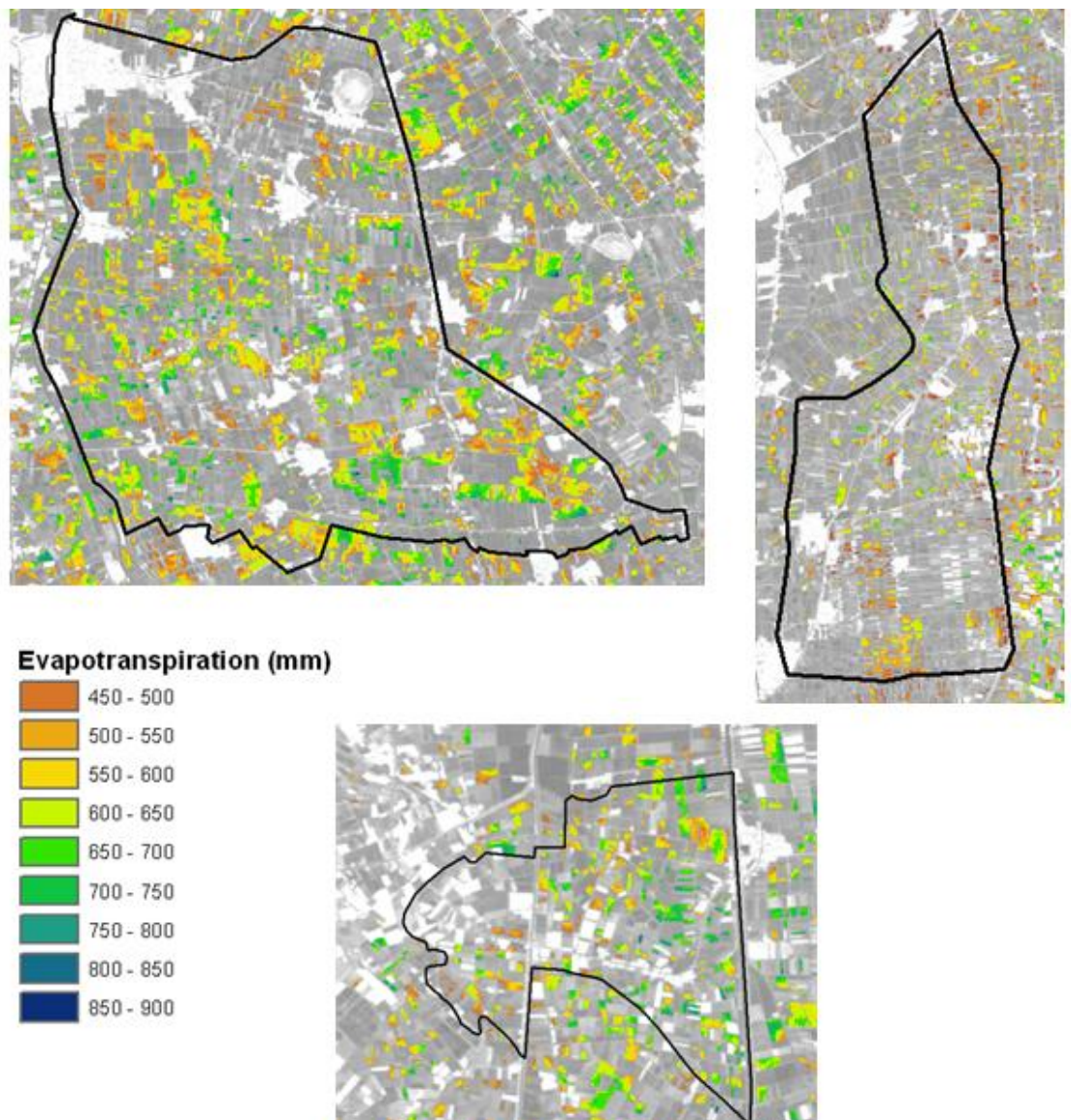


Figure 33: Spatially distributed water consumption of cotton in W-10, Daqalt and El Gemeza (clockwise).

Table 25: Average cotton water consumption during summer seasons 2011, 2002 and 1995.

	2011			2002	1995
	ET _a (mm)	σ	CV	ET _a (mm)	ET _a (mm)
W-10	608	67.6	0.111	735	848
Daqalt	575	58.0	0.101	745	869
El Gemeza	644	66.5	0.103	-	-

Head-tail analysis: Cotton water consumption

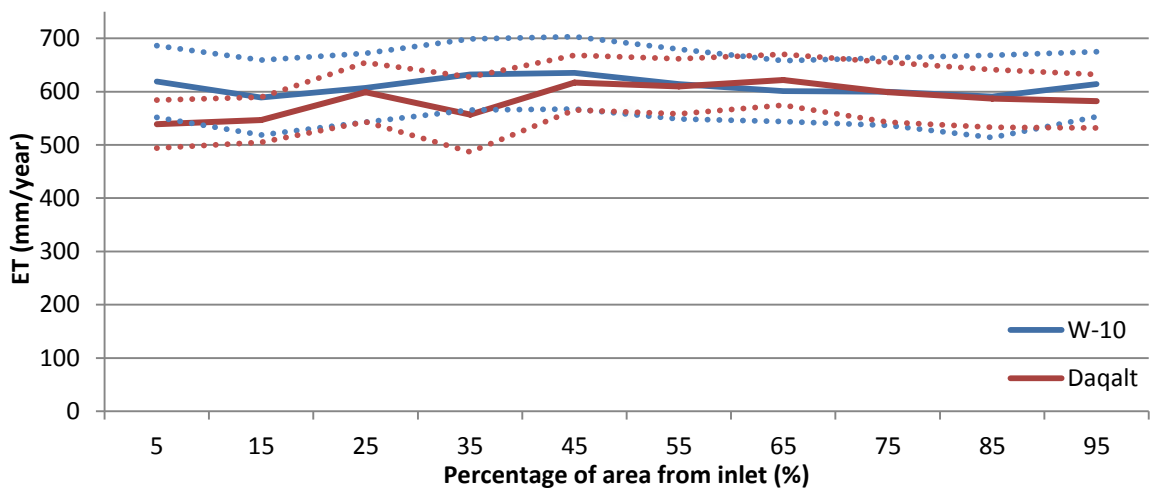


Figure 34: Head-tail analysis of water consumption from cotton fields in W-10 and Daqalt. Dashed lines indicate a variability range (mean plus and minus standard deviation per 10% section)

Table 26 shows location water consumption for cotton, per branch canal and upstream/downstream locations, with the distinction between T_a and E_a as computed by SWAP. It should be noted that the sum of T_a and E_a (ET_a) can be larger than the total amount of applied irrigation water. This is due to the initial soil water conditions and rainfall. Therefore, the amount of water that is used for crop transpiration is expressed as percentage of the ET_a sum. Table 26 shows that the higher consumptive use in the traditional irrigation system of El Gemeza (Table 25) for a relatively large part consists of non-productive soil evaporation (~20%). The percentage of water that is used for crop transpiration is largest for W-10 (90%), which corresponds with the relatively high crop yields (Table 1). Here, only a small fraction of water (10%) is lost through soil evaporation. This possibly indicates a beneficial effect of implemented *marwa* level irrigation modernizations.

As can be observed in Table 26, the amount of applied irrigation water is relatively high in upstream El Gemeza, especially when compared to the applied irrigation depths in the downstream portion of the same area. This is attributed to the reuse of drainage water that occurs downstream, causing the downstream farmers to suffice with smaller additional irrigation depths. As discussed in Section 3.9, the other areas experience less seepage losses from upstream to downstream, resulting in a smaller difference in upstream and downstream irrigation.

Table 26: Water consumption (T_a) and water losses through evaporation (E_a) for Cotton per branch canal and upstream/downstream location.

Field	Crop	Location	Irrigation [m ³ /ha]	ETa [m ³ /ha]	Ta [m ³ /ha]	Ta/ETa [%]	Ea [m ³ /ha]	Ea/ETa [%]
El Gemeza	Cotton	Upstream	6840	7033	5699	81%	1334	19%
El Gemeza	Cotton	Downstream	5320	6316	4983	79%	1333	21%
Daqalt	Cotton	Upstream	5720	6163	5375	87%	788	13%
Daqalt	Cotton	Downstream	5200	5910	5126	87%	784	13%
W10	Cotton	Upstream	5670	6477	5816	90%	661	10%
W10	Cotton	Downstream	5670	6445	5813	90%	631	10%

Figure 35 shows the cotton water stress due to water shortage, where the amount of stress is expressed as percentage of T_p . Water shortage stress is computed to be highest for the downstream El Gemeza and Daqalt fields (~30%). Since some uncertainty exists around these curves (~10%), stresses for Daqalt and the downstream El Gemeza fields are comparable, while the upstream El Gemeza fields and W-10 fields show the lowest stresses (~10%).

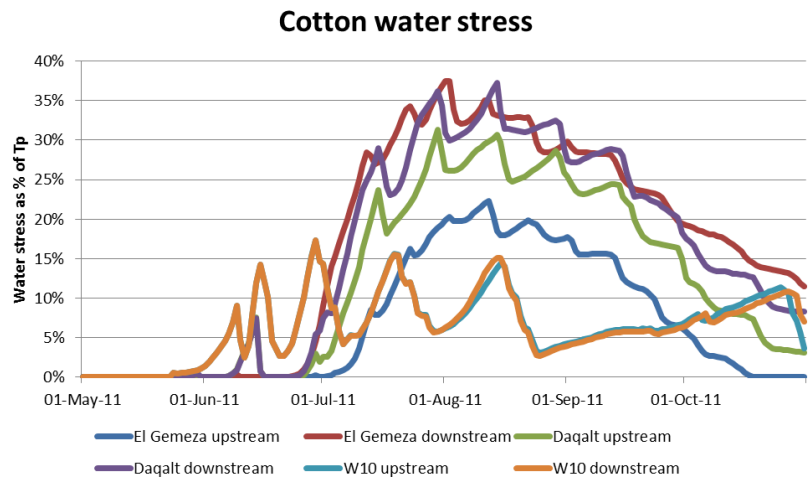


Figure 35: Cotton water stress for each branch canal and upstream/downstream location. Cotton water stress is expressed as percentage water of potential transpiration.

3.2.3 Maize

For maize, it is not feasible to spatially present and analyze the data in a meaningful way, due to the very small amount of pixels classified as maize (see Section 3.1).

What is striking is the relatively large difference in water consumption between W-10 and Daqalt (Table 27). It would, however be wrong to conclude that the additional consumed water in W-10 is wasted, as Table 1 indicates a markedly higher maize yield in W-10 compared to Daqalt. These figures suggest that maize farmers in Daqalt may be limited in their production by the irrigation water supply, although there may other causes for these observations, such as a difference in terms of the maize cultivar that is grown. Also, due to the small amount of maize pixels and the pixel size relative to the field size, the occurrence of mixed pixels may have a larger influence on the remote sensing analysis.

Table 27: Maize evapotranspiration during summer 2011.

	2011			2002	1995
	ETa (mm)	σ	CV	ETa (mm)	ETa (mm)
W-10	566	55.0	0.097	-	-
Daqalt	465	42.0	0.090	-	-

SWAP calculates that, of all water consumed in Daqalt and W-10, 83% is used for transpiration, and 17% is lost through evaporation (Table 28). A substantial amount of water is lost through evaporation in the El Gemeza simulations (ca. 30%). These simulations suggest that irrigation modernization at the *mesqa* level has a positive effect on the amount of water that is effectively used for crop growth, whereas further improvements from *marwa* modernization are not yet achieved. However, It should be kept in mind that maize results for El Gemeza are reported with a higher degree of uncertainty than for the other areas, as the model could not be specifically calibrated for this area (Section 2.3.3.1).

Table 28: Water consumption (T_a) and water losses through evaporation (E_a) for maize per branch canal and upstream/downstream location.

Field	Crop	Location	Irrigation [m3/ha]	ETa [m3/ha]	Ta [m3/ha]	Ta/ETa [%]	Ea [m3/ha]	Ea/ETa [%]
El Gemeza	Maize	Upstream	6080	5494	3899	71%	1595	29%
El Gemeza	Maize	Downstream	4800	5029	3440	68%	1589	32%
Daqalt	Maize	Upstream	5920	4719	3935	83%	784	17%
Daqalt	Maize	Downstream	5360	4699	3917	83%	782	17%
W10	Maize	Upstream	5280	5367	4449	83%	919	17%
W10	Maize	Downstream	6320	5383	4439	82%	944	18%

3.3 Crop yield

3.3.1 Rice

SEBAL biomass production per pixel (kg/ha) is accumulated for the crop-specific growing season, and related to the crop yield data from the field by means of a harvest index (as described in Section 2.2). Since no fieldwork was performed in the El Gemeza area during the summer period, the harvest index here was taken from a WaterWatch study performed for an earlier year (2008) in the same area.

Figure 36 spatially depicts the summer 2011 rice yield derived from fieldwork data and SEBAL biomass production in the three areas, allowing for the distinction of strongly and weakly performing fields.

Table 29 summarizes the area-averaged results for the rice yields, and also reports the obtained harvest indices obtained from the relation between computed biomass production and yield statistics. The harvest index in Daqalt is higher than in the other two areas (0.42 vs. 0.38), possibly indicating a difference in rice cultivar (Paragraph 2.1.1). However, this difference could also be a reflection of uncertainties in biomass production computations or surveyed yields. Both numbers are plausible as they are within the range found by Badawi (1995), who reports HI of 0.3 - 0.4 for lower yielding varieties and a maximum of 0.48-0.49 for high yielding varieties.

As for rice water consumption, differences in rice yield between the areas do not exceed a few %, both when intercomparing the different areas for summer 2011 and when looking at the performance of W-10 and Daqalt compared to 2002. Compared to 1995, however, rice yields have increased substantially. This suggests that, so far, IIP interventions have led to greater improvements in crop yield than recent, farm-level modernization. This is to be expected however, as the period between 1995 and 2002 marks the introduction of a different, high-yielding rice variety in the area.

Table 29 shows that the spatial variability of crop yields is higher in El Gemeza than in the other areas. This suggests that the applied modernizations at the branch canal and *mesqa* level in W-10 and Daqalt have led to an increased equity in the crop yields that are achieved. The head-tail analysis of rice yields (

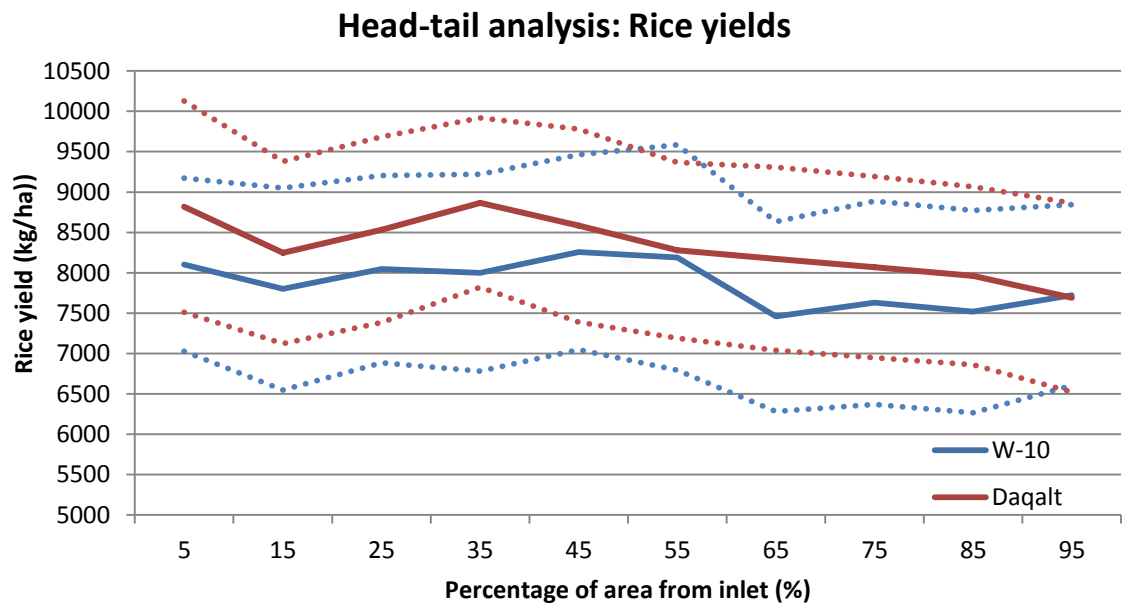


Figure 37) shows that, both for W-10 and Daqalt, higher yields typically occur in the upstream part of the branch canal command area, with lower yields typically occurring further downstream. Full equity between upstream and downstream areas is apparently not yet achieved by the *marwa* level modernizations.

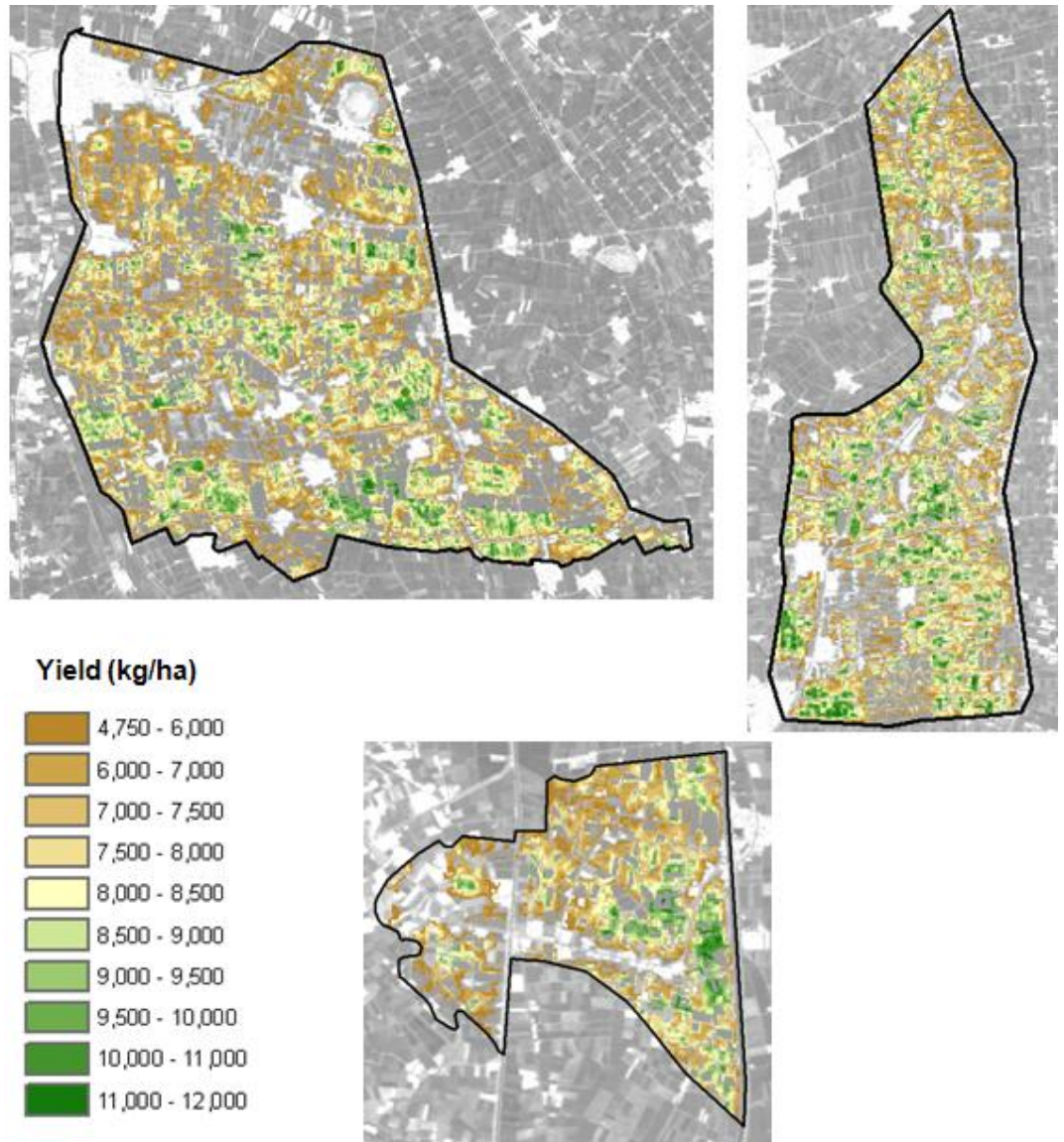


Figure 36: Spatially distributed rice yield for summer 2011 in W-10, Daqalt and El Gemeza (clockwise).

Table 29: Rice yield statistics for summer seasons 2011, 2002 and 1995. Harvest indices are based on a moisture content of 0.14.

	2011				2002	1995
	Y (kg/ha)	σ	CV	HI	Y (kg/ha)	Y (kg/ha)
W-10	7857	1245	0.158	0.38	8035	5167
Daqalt	8333	1229	0.147	0.42	7981	4688
El Gemeza	8091	1367	0.169	0.38	-	-

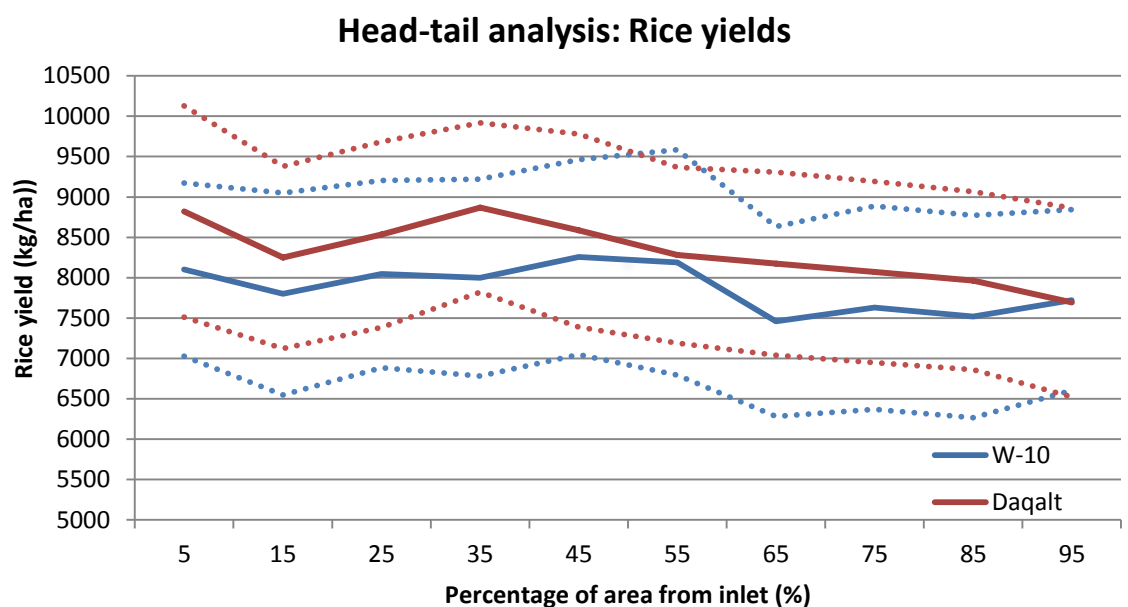


Figure 37: Head-tail analysis of rice yields in W-10 and Daqalt. Dashed lines indicate a variability range (mean plus and minus standard deviation per 10% section)

3.3.2 Cotton

The reported cotton yields in Daqalt are very low, and are lagging far behind the reported yields in W-10, the calculated yield in El Gemeza, the historical yield number for Daqalt in 2002, and general cotton yields in the Nile Delta found in FAOSTAT. Also, such a large difference between W-10 and Daqalt is not observed when looking at average seasonal SEBAL biomass production, which is only slightly lower for Daqalt than for W-10 (20226 kg/ha vs. 21168 kg/ha). To investigate this discrepancy, Figure 38 depicts a dataset of different combinations of cotton yield and ETa from locations around the world, both for seed cotton yield and cotton lint yield (Zwart, 2010). The combination of 575 mm ETa and 1964 kg/ha of yield illustrates that the Daqalt figures are far below the curve for seed cotton, and are in fact closer to the curve for cotton lint. This would imply that the reported cotton yield for Daqalt (and thus the yields for Daqalt depicted in Figure 39) is an underestimation of the actual seed cotton yield. There may be several causes for this, one being the confusion of lint yield and seed yield by the interviewees. GeoMAP reports

that an alternative reason may be the deliberate underestimation of crop yield by the farmers, who are known to be skeptic toward government inspection campaigns as tax rates are related to crop production.

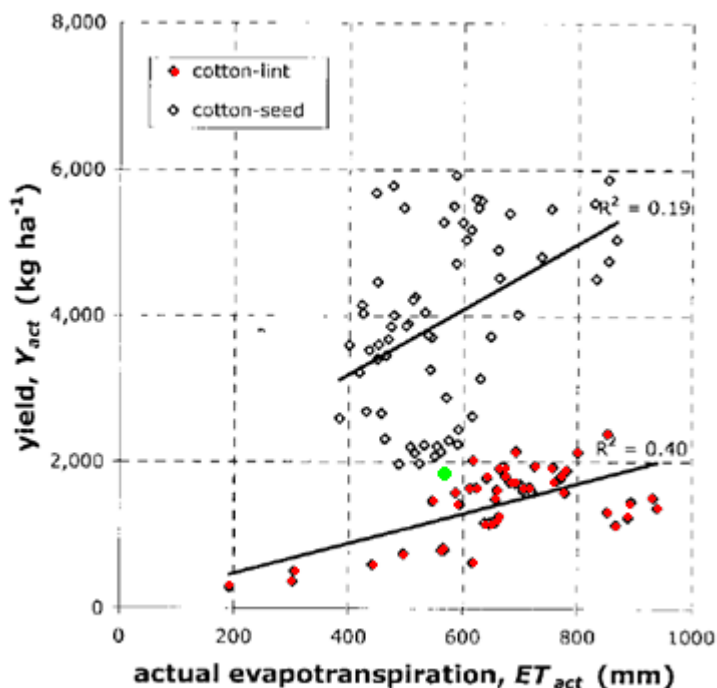


Figure 38: Literature values of cotton ET_a plotted against the achieved cotton lint and seed cotton yield (adopted from Zwart, 2010). The green dot indicates the combination of Daqalt average ET_a and yield, which falls outside the range of seed cotton observed globally.

Based on this analysis, it was decided that the reported cotton yield for Daqalt is in fact unreliable, and Daqalt cotton yield was calculated based on the harvest index found for W-10, in combination with the actual seasonal biomass production in Daqalt as computed by SEBAL. This results in a seed cotton yield for 2011 that is very close to the one recorded in 2002 (see Table 30).

Figure 39 spatially depicts the summer 2011 cotton yield derived from fieldwork data and SEBAL biomass production in the three areas, allowing for the distinction of strongly and weakly performing fields. Table 30 summarizes the area-averaged results for the cotton yields. The table shows that W-10 crop yields are the largest, followed by Daqalt and El Gemeza. Also, cotton yield in W-10 is higher (10%) than in 2002, a possible effect of *marwa* level improvements. A low harvest index of 0.13 is required to tune the computed seasonal biomass production to surveyed yields, using a moisture content of 8%.

In terms of spatial variability, no improvements from the irrigation modernizations are observed. The head-tail analysis for both areas (Figure 38) does not show a clear spatial pattern with an increasing distance from the inlet point.

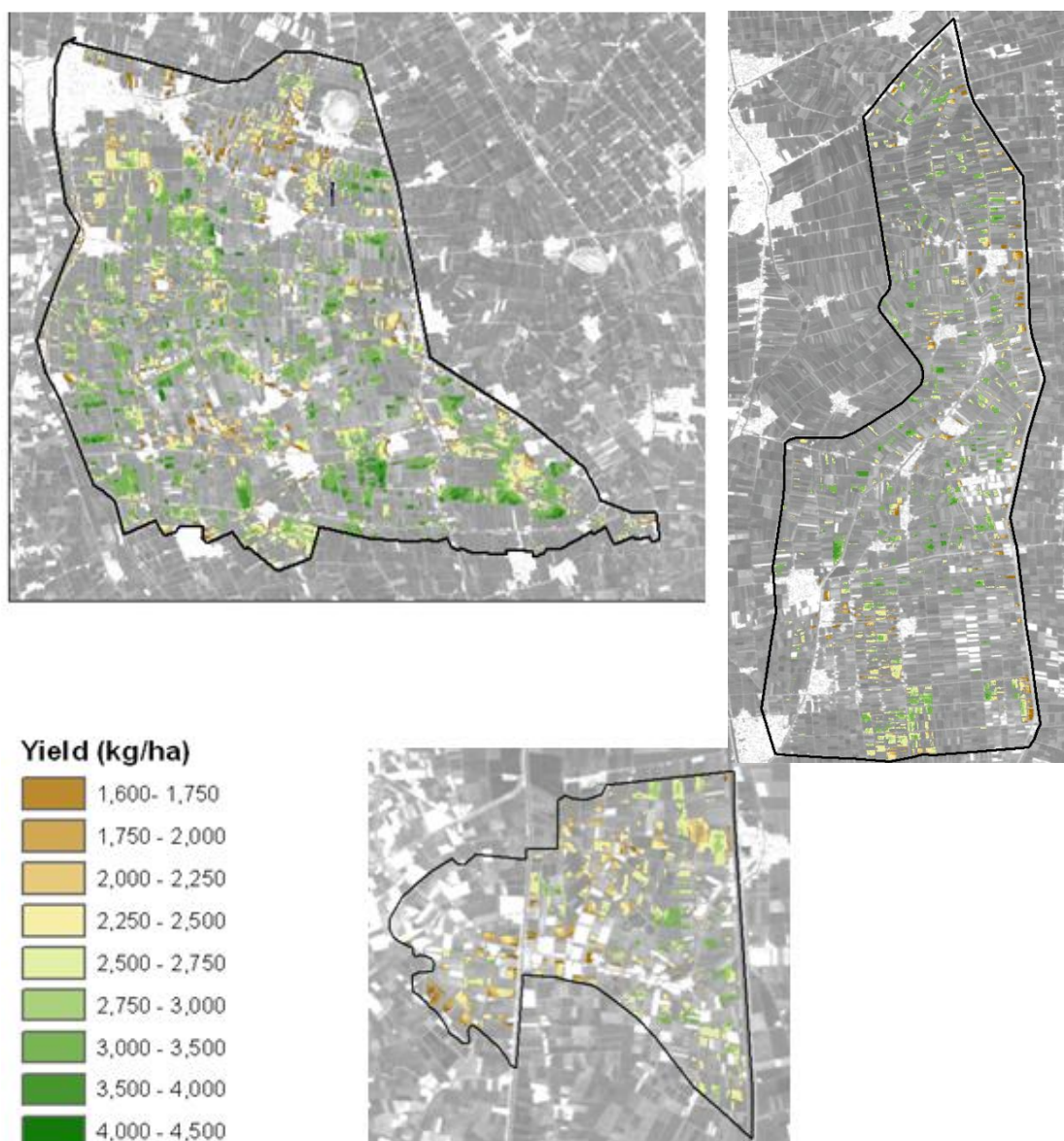


Figure 39: Spatially distributed seed cotton yield in W-10, Daqalt and El Gemeza (clockwise).

Table 30: Average seed cotton yield during summer seasons 2011, 2002 and 1995. Harvest indices are based on a seed cotton moisture content of 0.08 (Baskin et al.).

	2011				2002	1995
	Y (kg/ha)	σ	CV	HI	Y (kg/ha)	Y (kg/ha)
W-10	3036	422	0.139	0.13	2780	1838
Daqalt	2900	399	0.137	0.13	2906	1986
El Gemeza	2634	321	0.122	0.13	-	-

Head-tail analysis: Cotton yields

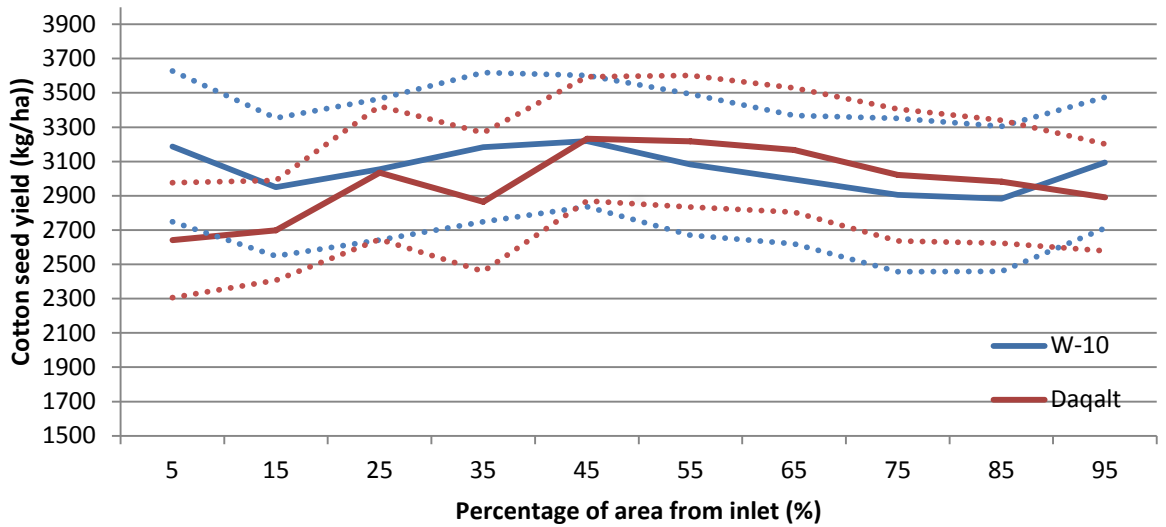


Figure 40: Head-tail analysis of seed cotton yield in W-10 and Daqalt. Dashed lines indicate a variability range (mean plus and minus standard deviation per 10% section)

3.3.3 Maize

For maize, it is not feasible to spatially present and analyze the data in a meaningful way, due to the very small amount of pixels classified as maize (see Section 3.1).

Table 31 summarizes the area-averaged results for the maize yields. As shown in Table 1, reported maize yields in Daqalt are very low. This corresponds with the low ET_a that was found in the remote sensing analysis (Paragraph 3.2.3), and may thus be the consequence of limited irrigation water availability. There could, however, be other causes of these observations, both related to on-farm conditions and the applied methodology and data availability (as described in Paragraph 3.2.3). Therefore, maize results should be interpreted with a higher degree of uncertainty than the results for the other crops.

Table 31: Maize yields during summer 2011. Harvest indices are based on a moisture content of 0.15 (Willcutt, 2010)

	2011			HI	2002	1995
	Y (kg/ha)	σ	CV		Y (kg/ha)	Y (kg/ha)
W-10	6667	771	0.116	0.31	-	-
Daqalt	3833	451	0.118	0.22	-	-

3.4 Crop water productivity

3.4.1 Rice

Figure 41 spatially depicts the summer 2011 rice water productivity derived from actual yields and SEBAL consumptive use. Table 32 summarizes the area-averaged results. With Daqalt having a higher average rice water productivity than W-10, this result does not indicate a beneficial effect of recent farm-level irrigation modernization. However, it should be kept in mind that this difference between areas is the result of two small differences (~5%) in consumptive use and crop yield. It is observed that El Gemeza has a higher spatial variability in water productivity than the other two areas, which is a result of the higher variability in rice yield discussed in 3.3.1. Overall, water productivity of the two areas has increased somewhat since 2002 and substantially since 1995.

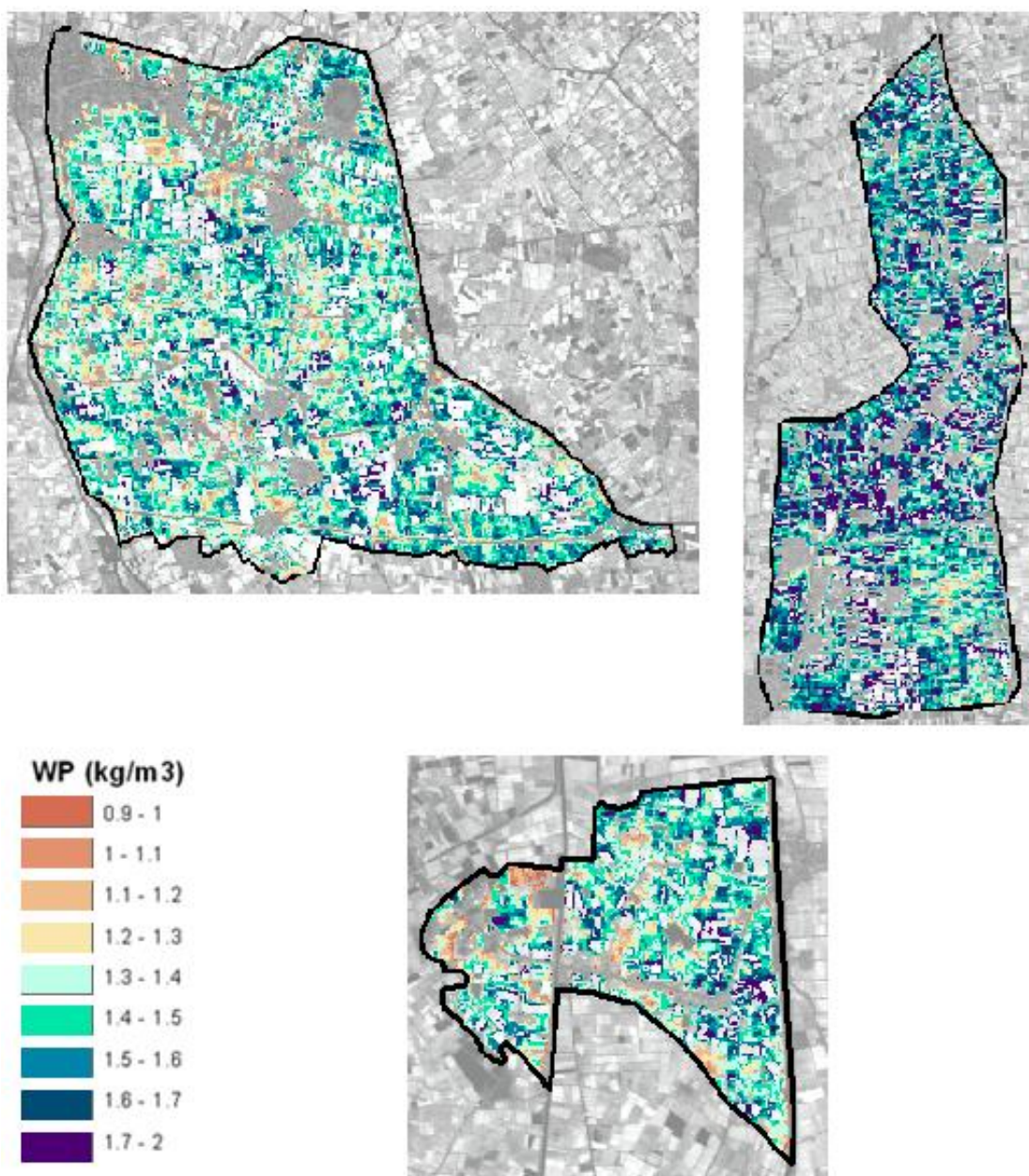


Figure 41: Spatially distributed rice crop water productivity in W-10, Daqalt and El Gemeza (clockwise).

Table 32: Average rice crop water productivity during summer seasons 2011, 2002 and 1995.

	2011			2002	1995
	WP (kg/m ³)	σ	CV	WP (kg/m ³)	WP (kg/m ³)
W-10	1.44	0.15	0.104	1.42	0.93
Daqalt	1.56	0.16	0.103	1.42	0.86
El Gemeza	1.46	0.18	0.123	-	-

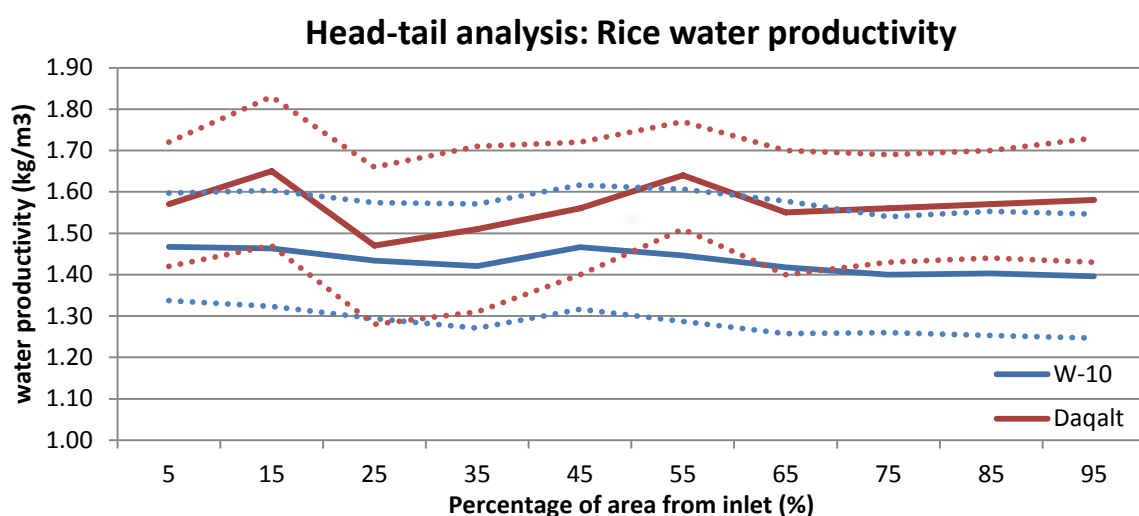


Figure 42: Head-tail analysis of rice water productivity in W-10 and Daqalt. Dashed lines indicate a variability range (mean plus and minus standard deviation per 10% section)

3.4.2 Cotton

Figure 43 spatially depicts the summer 2011 seed cotton water productivity derived from actual yields and SEBAL consumptive use.

Table 33 summarizes the area-averaged results for the cotton yields. Daqalt and W-10 cotton water productivity values are equal and have increased substantially compared to 2002 and 1995, which corresponds with the IIIMP goals. The head-tail analysis does not show an obvious trend (Figure 44). El Gemeza performs weaker in terms of water productivity. Based on values found in Zwart (2010), it can be concluded that 2011 cotton water productivity in W-10 and Daqalt is now up to speed from an international perspective, with values similar to averages for cotton fields in areas in Turkey and Pakistan. Productivity values computed for 2002 and 1995 lag behind international averages, and the increase over recent years could be attributed to irrigation modernization efforts on the branch canal and *mesqa* levels.

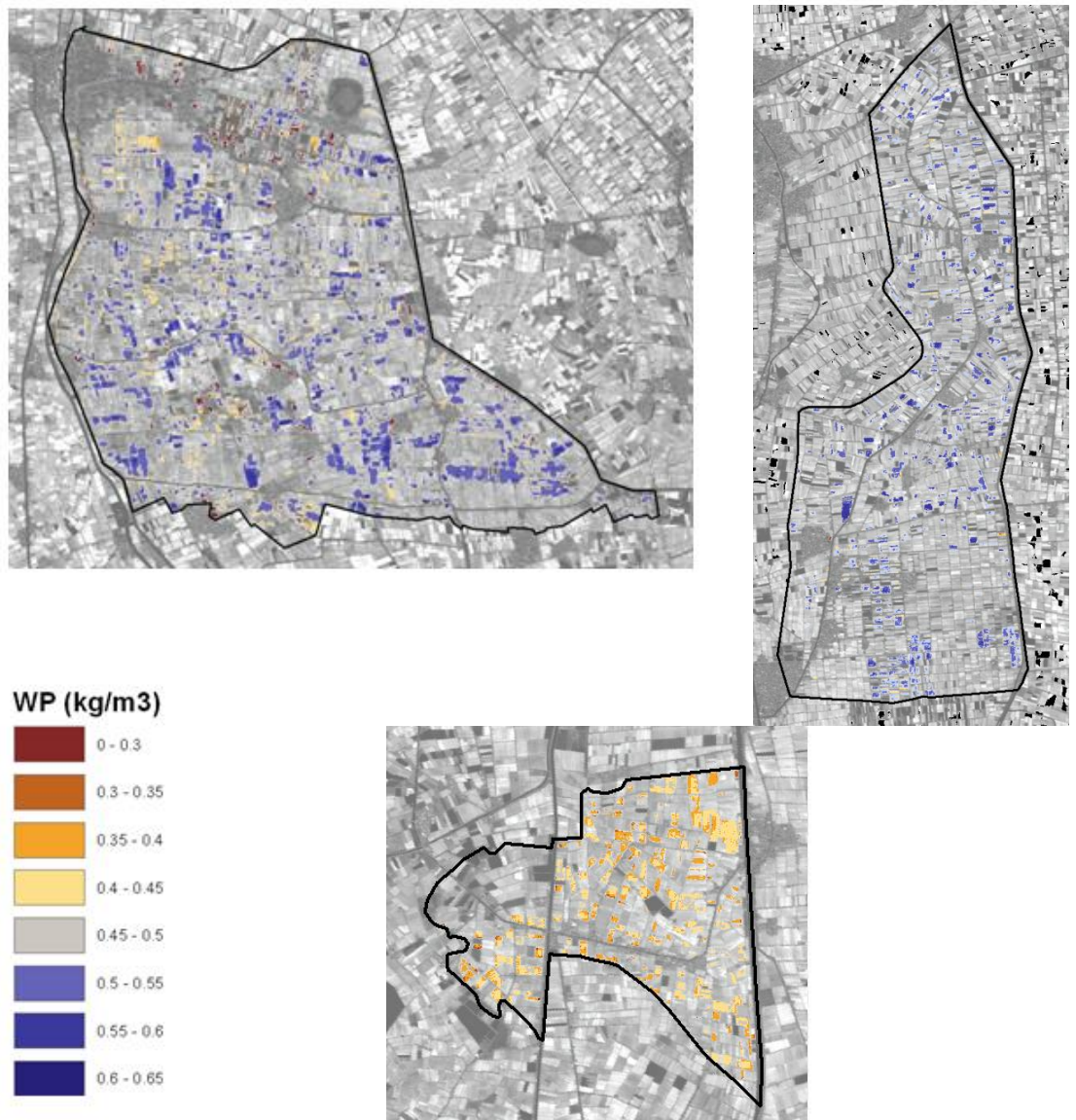


Figure 43: Spatially distributed seed cotton water productivity for summer 2011 in W-10, Daqalt and El Gemeza (clockwise).

Table 33: Average seed cotton water productivity during summer seasons 2011, 2002 and 1995.

	2011			2002	1995
	WP (kg/m ³)	σ	CV	WP (kg/m ³)	WP (kg/m ³)
W-10	0.5	0.0338	0.068	0.33	0.25
Daqalt	0.5	0.0345	0.069	0.33	0.27
El Gemeza	0.41	0.0268	0.065	-	-

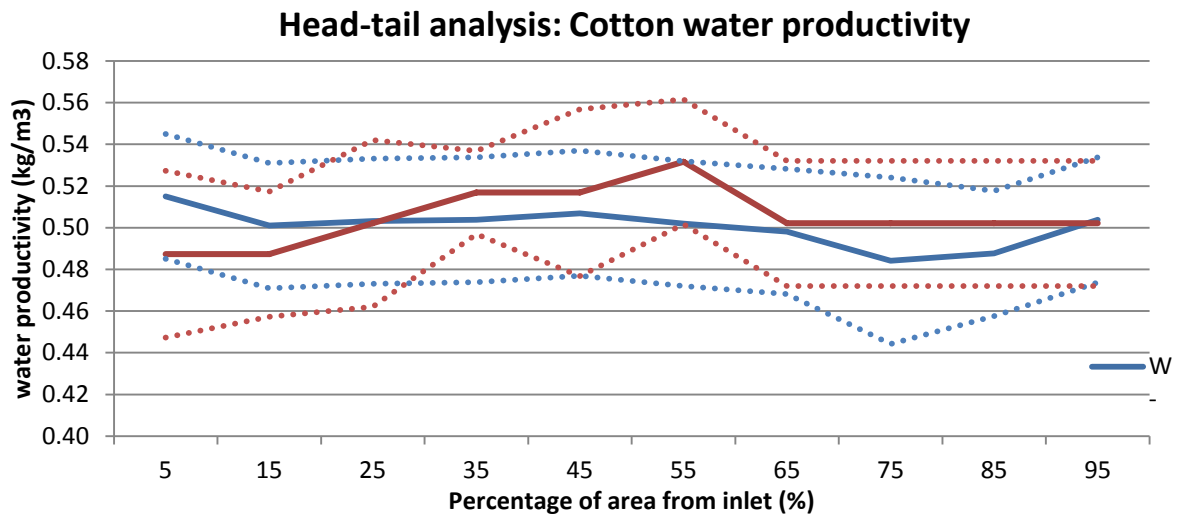


Figure 44: Head-tail analysis of seed cotton water productivity in W-10 and Daqalt. Dashed lines indicate a variability range (mean plus and minus standard deviation per 10% section)

3.4.3 Maize

For maize, it is not feasible to spatially present and analyze the data in a meaningful way, due to the very small amount of pixels classified as maize (see Section 3.1). The reported yield in Daqalt leads to a lower maize water productivity compared to W-10. However, the water productivity of 1.2 kg/m³ under *marwa* level modernized conditions is still in the low range of water productivity values internationally reported (Zwart, 2010), possibly indicating scope for improvement.

Table 34: Average maize water productivity during summer season 2011.

	2011 WP (kg/m ³)	σ	CV	2002 WP (kg/m ³)	1995 WP (kg/m ³)
W-10	1.2	0.0925	0.077	-	-
Daqalt	0.83	0.0735	0.089	-	-

3.5 Gross return

Hellegers et al. (2009) describe the value of economic water productivity as an indicator for water resources management. By computing spatially variable economic water productivity for an irrigation system, the performance of the irrigation system can be examined per pixel from a financial perspective. Economic water productivity is then defined as the crop water productivity multiplied by the market price of the crop, while subtracting variable and fixed costs that are required for offering the crop on the market (eg. production, transport, etc.). As these costs are currently unknown, and can be assumed constant for a specific crop at the local scale, in this study the combination of crop water productivity and crop market price is adopted as a performance indicator (*gross return to water*).

For rice, market prices in Egypt have been fluctuating during recent years. These fluctuations are related to many factors, including the government policy of reducing the extent of rice cultivation in Egypt, and related governmental control of prices of domestic rice and imported rice, as well as reductions of exported quantities of rice. In this study, as an indication of gross return of rice per cubic meter of water, a price of 3 Egyptian Pounds (LE) per kg of rice is adopted. This was reported as a reasonable value to represent the price of rice for the customer. It should be noted that the actual benefit to the farmer may be far lower, and could be a factor of 2 or 3 lower than the price for which the rice is sold on the market.

As well as for rice, cotton market prices in Egypt are strongly coupled to the political situation. It was reported that, in 2011, extra long staple (ELS) cotton prices reached record heights of LE 18 (3\$) per kg due to political unrest, with prices generally under \$2 / kg. As summer 2011 is evaluated in this study, the high price of LE 18 / kg is adopted to evaluate gross return. Averaged gross return for rice is found to be LE 4.32 / m³ for W-10, LE 4.68 / m³ for Daqalt and LE 4.38 for El Gemeza. For cotton, gross return is around 9.00 LE / m³ both for W-10 and Daqalt, while 1 m³ delivers LE 7.40 in El Gemeza. As there is a linear relation between crop water productivity and gross return to water, spatial variability of gross return is equal to the coefficient of variance of crop water productivity presented in the previous section, and the spatial pattern of gross return to water is equal to that of crop water productivity as displayed in the previous section.

3.6 Reliability of irrigation water availability

In an IWMI research report (IWMI, 1999), a number of irrigation system performance indicators is analyzed. One of these is *adequacy*, which is defined as the sufficiency of water use in an irrigation system, such that there is enough water to fulfill the crop needs. As relative evapotranspiration provides direct information on crop stress conditions, evaporative fraction (EF) is taken as a measure of adequacy. Subsequently, the temporal variability of adequacy is an indication of the reliability of water delivery in the irrigation system. The average of absolute deviations of spatially distributed EF pixels from their mean value (AVEDEV) is selected as the measure of temporal variability:

$$AVEDEV_{EF} = (1 / n) \sum |EF - EF_{mean}| \quad (8)$$

A set of five consecutive fortnight periods is chosen for AVEDEV calculations (June 26th - September 3rd). This time period coincides with the optimum of the growing season, and has a good coverage of high-resolution satellite images to ensure the quality of the analysis.

Figure 45 presents the results of the reliability analysis for the summer season. It is found that, for the examined time series, the AVEDEV for all three areas is low (in comparison to eg. the original IWMI research area in Pakistan), indicating an overall reliable water delivery service both in the traditional irrigation system and the modernized, continuous flow system. When rounded off to two decimal digits, the AVEDEV is 0.13 for all three branch canal command areas. Thus, although water is delivered to the farmer in increments in the rotational flow system, this does not lead to a higher temporal variability in the adequacy of water supply when looking at two-weekly periods. To perform a more accurate and direct analysis of reliability of irrigation water delivery, a *marwa* flow measuring campaign would be required.

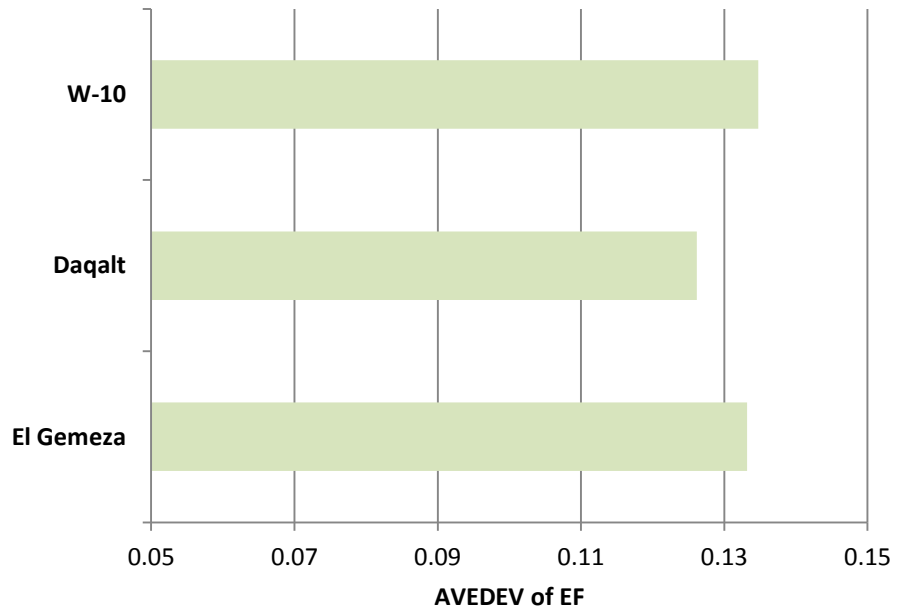


Figure 45: Reliability of irrigation water delivery, expressed in the absolute average deviation from the mean (AVEDEV) per branch canal command area.

3.7 Canal seepage losses

The irrigation depth per application is shown in Table 35 for cotton for each branch canal and upstream/downstream location. Due to seepage losses, which are assumed to be the highest for El Gemeza (Section 2.3.3.2), the downstream farmer in El Gemeza has less irrigation water available in our simulations. Due to the lower irrigation frequency in Daqalt, the irrigation depth per application is considerably higher than in W-10 and El Gemeza. Seepage losses in Daqalt also result in less irrigation water for the downstream farmer, although the effect is smaller than for El Gemeza. In W-10 no seepage losses are assumed to occur, meaning that the amount of irrigation water per application is equal for the upstream and downstream farmer.

Table 35: Total irrigation, number of irrigation applications, and irrigation depth per irrigation application for Cotton per branch canal and upstream/downstream location.

Field	Crop	Location	Irrigation [mm]	Number of irrigation applications	Irrigation depth [mm]
El Gemeza	Cotton	Upstream	684	38	18.0
El Gemeza	Cotton	Downstream	532	38	14.0
Daqalt	Cotton	Upstream	572	13	44.0
Daqalt	Cotton	Downstream	520	13	40.0
W10	Cotton	Upstream	567	63	9.0
W10	Cotton	Downstream	567	63	9.0

Table 36 shows the irrigation depth per application for Maize per branch canal and upstream/downstream location. Also for maize it is clear that seepage losses result in less irrigation water for the downstream farmer in El Gemeza. Seepage losses in Daqalt are less substantial and therefore the difference between

the upstream and downstream amount of irrigation water per application is smaller. Again W-10 shows the same irrigation depths for both the upstream and downstream field, due to the absence of seepage losses.

Table 36: Total irrigation, number of irrigation applications, and irrigation depth per irrigation application for Maize per branch canal and upstream/downstream location.

Field	Crop	Location	Irrigation [mm]	Number of irrigation applications	Irrigation depth [mm]
El Gemeza	Maize	Upstream	608	32	19.0
El Gemeza	Maize	Downstream	480	32	15.0
Daqalt	Maize	Upstream	592	8	74.0
Daqalt	Maize	Downstream	536	8	67.0
W10	Maize	Upstream	528	66	8.0
W10	Maize	Downstream	632	79	8.0

Finally, Table 37 represents the irrigation depth per application for rice per branch canal and upstream/downstream location. Again seepage losses are most substantial between the upstream and downstream field in El Gemeza, resulting in less irrigation water per application for the downstream farmer. The upstream and downstream farmers in W-10 have the same amount of irrigation water available, and in Daqalt these differences are smaller.

Table 37: Total irrigation, number of irrigation applications, and irrigation depth per irrigation application for Rice per branch canal and upstream/downstream location.

Field	Crop	Location	Irrigation [mm]	Number of irrigation applications	Irrigation depth [mm]
El Gemeza	Rice	Upstream	672	28	24.0
El Gemeza	Rice	Downstream	560	28	20.0
Daqalt	Rice	Upstream	518	70	7.4
Daqalt	Rice	Downstream	469	70	6.7
W10	Rice	Upstream	624	78	8.0
W10	Rice	Downstream	632	79	8.0

The seepage losses and corresponding lower amount of available irrigation water for the downstream farmer in El Gemeza, and to a smaller extent also in Daqalt, can affect the scope for drainage water recycling and salinity levels in the soil. This is discussed in detail in the following sections.

3.8 Drainage water recycling

As described in Section 2.3.2.4, the drainage situation for all fields is equal. Therefore, the amount of drainage water is a function of climate, irrigation depth, irrigation frequency, crop type, solute concentrations, and bottom flux. Too high salinity levels for example, can result in less root water uptake and therefore more water will leave the system as drainage water. Unfortunately, drainage fluxes and drainage water salinity levels were not measured in the study area. Therefore, SWAP could not be calibrated for observed drainage fluxes. Compared to the other SWAP water balance terms, the sensitivity of drainage results to varying input parameters is relatively small (Appendix C).

For El Gemeza and Daqalt drainage water can be re-used by the downstream farmer. Since W-10 is modernized up to the farm-level, irrigation water in W-10 is not likely to be recycled because the farmers have their “fresh” water source at the farm-level. Recycled drainage water may contain higher solute concentrations. This is discussed in detail in Section 3.9.

3.8.1 Rice

Table 38 shows for rice the amount of drainage water that is produced per branch canal and upstream/downstream location. The amount of drainage water is computed to be a small fraction of the total outflow ($T_a + E_a + \text{drainage}$), for all branch canals and upstream/downstream locations. This is a result of the fact that rice is grown under ponded conditions, where more water is lost through open water evaporation than through drainage. The amount of drainage water is approximately 8-9% of the total outflow for all branch canals and upstream/downstream locations. This means that 8-9% of the total outflow can be used as recycled drainage water downstream. Since this amount is equal for all branch canals and upstream/downstream locations, the irrigation modernization does not have an effect on the scope for recycling drainage water from rice fields.

Table 38: Drainage flux for each branch canal and upstream/downstream location where Rice is grown. Drainage is expressed in mm as well as percentage of the total outflow flux ($Q_{out} = T_a + E_a + \text{Drainage}$).

Field	Crop	Location	Drainage [mm]	Qout [mm]	Drainage [%]
El Gemeza	Rice	Upstream	45	564	8%
El Gemeza	Rice	Downstream	47	532	9%
Daqalt	Rice	Upstream	41	516	8%
Daqalt	Rice	Downstream	40	499	8%
W10	Rice	Upstream	47	542	9%
W10	Rice	Downstream	48	543	9%

Figure 46 shows a time-series of drainage for Rice per branch canal and upstream/downstream location. The maximum drainage flux is close to 0.6 mm/day. The drainage patterns for all branch canals and upstream downstream fields are more or less equal. The high irrigation frequencies lead to a uniform drainage flux throughout the season.

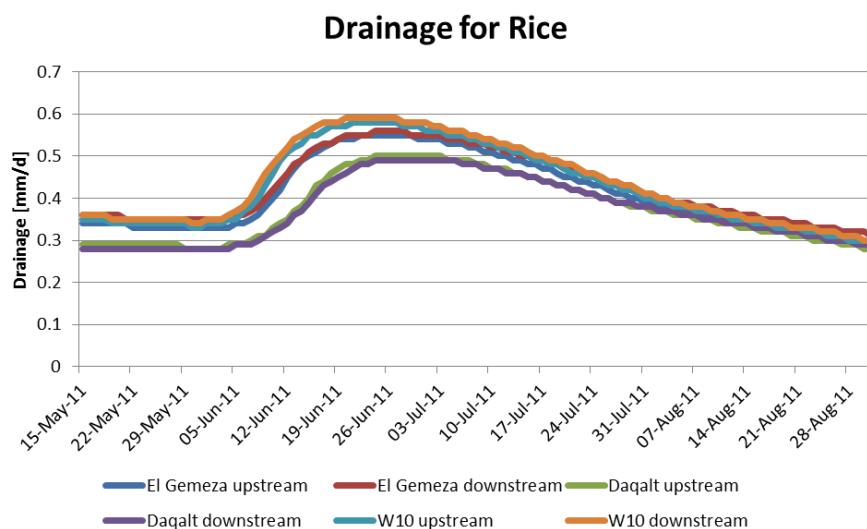


Figure 46: Drainage flux of Rice for each branch canal and upstream/downstream location.

3.8.2 Cotton

Table 39 shows for cotton the amount of drainage water that is produced per branch canal and upstream/downstream location. Results are shown for the growing season without the last month, as irrigation is normally not applied during this period, which means that drainage approaches zero. The drainage flux is shown as total flux in mm, as well as the percentage of total water outflow. The amount of drainage water is computed at 8% or less from the total water outflow. Especially for W-10 the drainage flux is very small, meaning that water is used efficiently at the farm-level modernized field. El Gemeza has the largest drainage flux and most convincing difference between the upstream and downstream drainage flux; a part of this upstream drainage water will be recycled by the downstream farmer in El Gemeza. There is no clear difference between the upstream drainage flux from El Gemeza and Daqalt. Therefore the amount of drainage water that can be recycled is more or less equal for the downstream farmers in El Gemeza and Daqalt.

Table 39: Drainage flux for each branch canal and upstream/downstream location where Cotton is grown. Drainage is expressed in mm as well as percentage of the total outflow flux ($Q_{out} = T_a + E_a + \text{Drainage}$).

Field	Crop	Location	Drainage [mm]	Qout [mm]	Drainage [%]
El Gemeza	Cotton	Upstream	50	671	7%
El Gemeza	Cotton	Downstream	15	571	3%
Daqalt	Cotton	Upstream	47	598	8%
Daqalt	Cotton	Downstream	32	559	6%
W10	Cotton	Upstream	15	572	3%
W10	Cotton	Downstream	17	574	3%

Figure 47 shows a time-series of drainage for Cotton per branch canal and upstream/downstream location. The maximum drainage flux is close to 1 mm/day. The drainage patterns of the upstream fields in El Gemeza and Daqalt are more or less equal. Drainage is increasing at the beginning of the growing season, because the soil moisture builds up since the crop uses more water in the middle of the growing season. Due to the irrigation modernization up to the farm-level in W-10, irrigation depths are smaller and irrigation takes place more frequently. This results in a more uniform drainage flux throughout the season.

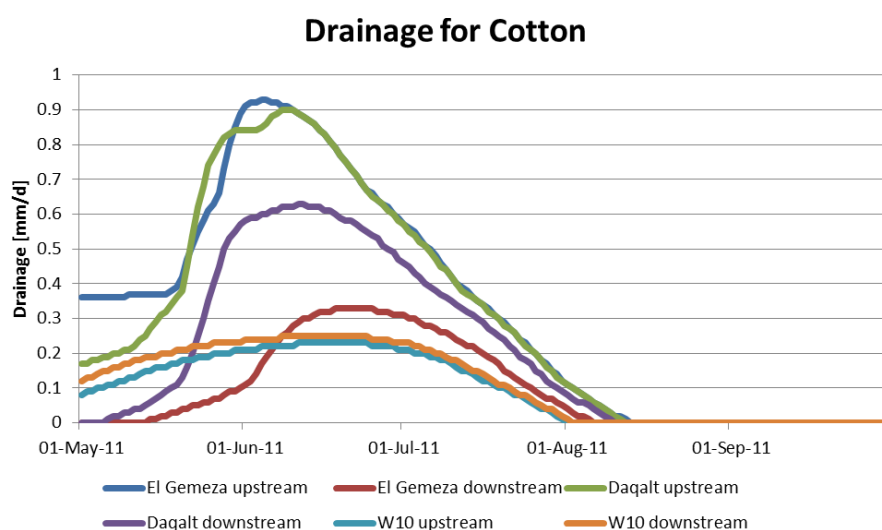


Figure 47: Drainage flux of cotton for each branch canal and upstream/downstream location.

3.8.3 Maize

Table 40 shows for maize the amount of drainage water that is produced per branch canal and upstream/downstream location. It is clear that the amount of drainage water in Daqalt is considerably higher than for El Gemeza and W-10. This is related to the lower reported irrigation frequency and larger irrigation depth in Daqalt. Here, 20% of the total outflow is drainage water that could potentially be reused downstream, as compared to 11% for an upstream El Gemeza field. Note that the difference in simulated irrigation behavior leads to relatively high water losses through E_a (Table 28). Thus, *mesqa* level modernizations keep more water in the system, increasing the potential for reuse. The difference between upstream and downstream drainage water is more or less equal for El Gemeza and Daqalt. The drainage flux from W-10 is very small and is only 6% of the total water outflow.

Table 40: Drainage flux for each branch canal and upstream/downstream location where maize is grown. Drainage is expressed in mm as well as percentage of the total outflow flux ($Q_{out} = T_a + E_a + \text{Drainage}$).

Field	Crop	Location	Drainage [mm]	Qout [mm]	Drainage [%]
El Gemeza	Maize	Upstream	63	570	11%
El Gemeza	Maize	Downstream	46	507	9%
Daqalt	Maize	Upstream	113	560	20%
Daqalt	Maize	Downstream	95	540	18%
W10	Maize	Upstream	30	517	6%
W10	Maize	Downstream	31	517	6%

Figure 48 shows a time-series of drainage for maize per branch canal and upstream/downstream location. The maximum drainage flux is close to 2 mm/day. Again drainage increases at the beginning of the growing season, because the soil moisture builds up since the crop uses more water in the middle of the growing season. The drainage pattern for Daqalt can be described as erratic, which is the result of the low irrigation frequency in combination with the large irrigation depths. The drainage patterns for El Gemeza and W-10 are more or less equal, with W-10 showing the most uniform drainage flux throughout the season.

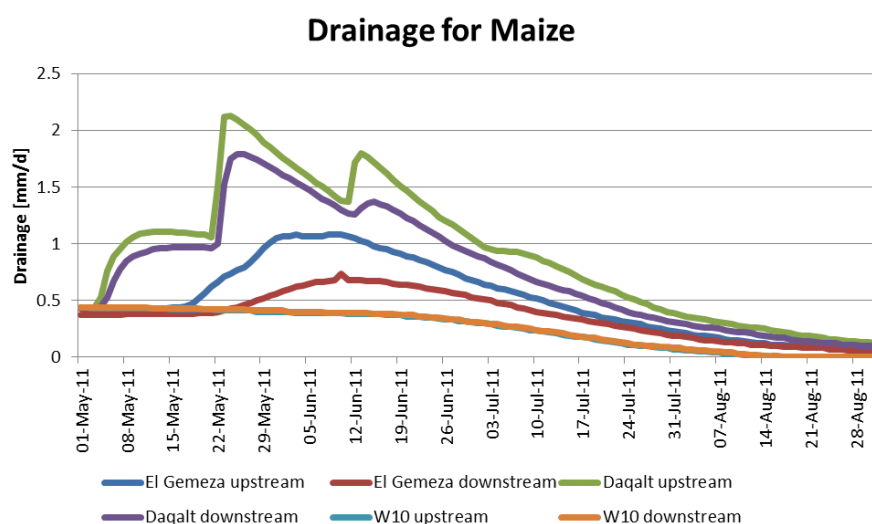


Figure 48: Drainage flux of maize for each branch canal and upstream/downstream location.

3.9 Salinity

High salinity levels can result in reduced root water uptake, subsequently leading to reduced crop yields at the end of the growing season. Solutes enter the field by irrigation and a bottom flux. Therefore, the solute balance is a function of the irrigation water solute concentration, irrigation depth, irrigation frequency, bottom flux, and crop type. The following paragraphs describe the solute balance per crop for each of the branch canals and upstream/downstream locations. SWAP provides the user with a solute balance output file, in which solutes are shown in mg/cm². For the analysis in the following sections, these numbers are converted to kg/ha. The current study does not consider additional leaching with large amounts of water (see also Section 2.3.2.9).

3.9.1 Rice

The total amount of solutes in kg/ha is shown in Table 41 for each branch canal and upstream/downstream location where rice is grown. Solute accumulations are most evident for the downstream El Gemeza and downstream W-10 fields. Therefore, for rice fields the *marwa* level irrigation modernization has not lead to a smaller accumulation of solutes in the soil than for the modernization up to *mesqa* level. The larger solute accumulations for the downstream fields in El Gemeza and W-10 are due to the higher solute concentrations in irrigation water. Solute accumulations are smallest for the upstream Daqalt and W-10 fields. The overall lower solute accumulation in Daqalt is mainly due to the low irrigation solutes concentration in combination with the total irrigation sum, which is the lowest of all branch canals. Since all fields show substantial solute accumulations, it is recommended to leach the soils in these fields with additional water-supply, especially in the downstream El Gemeza and W-10 fields.

Table 41: Solute balance for rice for each branch canal and upstream/downstream location. Solutes enter the field by irrigation and a bottom flux, and leave the field by drainage. Solutes are shown in kg/ha.

Field	Crop	Location	Irrigation [kg/ha]	Drainage [kg/ha]	Bottomflux [kg/ha]	dS [kg/ha]
El Gemeza	Rice	Upstream	3206	1154	683	2735
El Gemeza	Rice	Downsteam	3834	1216	878	3496
Daqalt	Rice	Upstream	2138	1044	683	1776
Daqalt	Rice	Downsteam	2476	1046	753	2183
W10	Rice	Upstream	2390	1227	683	1845
W10	Rice	Downsteam	3661	1279	718	3100

SWAP provides the user with a separate “stress” file, in which the mm of stress due to i) dry conditions, ii) wet conditions, iii) salinity, and iv) frost is shown. Therefore, for each day the amount of salinity stress (mm) can be related to T_p (mm). Figure 49 shows that rice experiences some salinity stress throughout the growing season in all branch canals and upstream/downstream locations, except for an upstream W-10 field. These stresses are, however, relatively small. Since some stress is present in Figure 49, it means that salinity concentrations can be above the EC_{max} threshold for rice (3.0 dS/m). Since solutes accumulate (Table 41) if additional leaching is not applied, the concentrations may become more substantial on the long-term. The higher solute concentration in the downstream El Gemeza irrigation water is the reason for the higher solute stress in this area.

Rice salinity stress

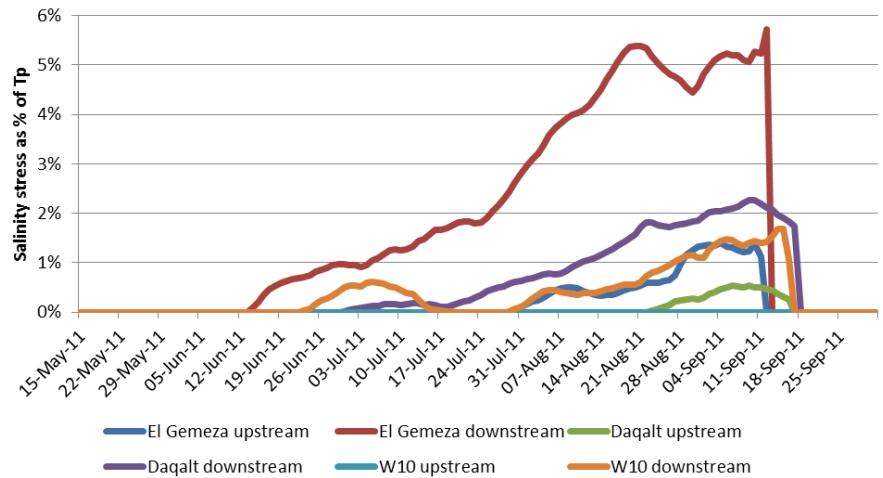


Figure 49: Rice salinity stress expressed as percentage of potential transpiration.

3.9.2 Cotton

The total amount of solutes in kg/ha is shown in Table 42 for each branch canal and upstream/downstream location where cotton is grown. El Gemeza was measured to have the highest solute concentrations in its irrigation water, both upstream and downstream (see Section 2.1.3). Due to the higher solute concentration in the downstream irrigation water and a smaller drainage flux, the change in solute storage is quite large for a downstream El Gemeza field. This is also true for a downstream W-10 field. It appears that, despite the irrigation modernization up to farm-level (W-10), the solute concentrations at the downstream W-10 field are considerably higher than an upstream W-10 field. Therefore, also for the downstream W-10 field, solutes are computed to be accumulating in the soil profile. Due to the high load of drainage solutes in combination with a small load of irrigation solutes, the upstream Daqalt field shows the lowest accumulation of solutes. Therefore, it can be summarized that modernization up to the farm-level, and associated changes in irrigation behavior, does in our simulations not lead to a smaller accumulation of solutes in the soil than observed for the *mesqa* level modernized area.

Analysis shows that cotton does not experience any stress due to too high solute concentrations. This is due to the fact that cotton is quite resistant to solutes ($EC_{max} = 7.7$ dS/m, Table 12). Based on the solute accumulations, as shown in Table 42, it is recommended to leach with additional water to reduce solute accumulations and prevent salinity stress on the long-term. It is expected that solute stress will be most evident in the downstream El Gemeza fields and downstream W-10 fields.

Table 42: Solute balance for cotton for each branch canal and upstream/downstream location. Solute enter the field by irrigation and a bottom flux, and leave the field by drainage. Solute are shown in kg/ha.

Field	Crop	Location	Irrigation [kg/ha]	Drainage [kg/ha]	Bottomflux [kg/ha]	dS [kg/ha]
El Gemeza	Cotton	Upstream	2597	1107	817	2307
El Gemeza	Cotton	Downstream	2797	315	1050	3533
Daqalt	Cotton	Upstream	1690	1034	817	1472
Daqalt	Cotton	Downstream	1920	670	901	2150
W10	Cotton	Upstream	1644	313	817	2147
W10	Cotton	Downstream	2495	359	859	2995

3.9.3 Maize

The total amount of solutes in kg/ha is shown in Table 43 for each branch canal and upstream/downstream location where maize is grown. Due to the large drainage fluxes in Daqalt, and the low solute concentration in irrigation water, the accumulation of solutes is very small for Daqalt. In fact, the amount of solutes in an upstream Daqalt field decreases throughout the growing season. The large drainage flux is a result of the low irrigation frequency in combination with a large irrigation depth per application. This shows that leaching with large amounts of additional water helps to prevent solute accumulations. It is not observed that *marwa* level modernizations (W-10) lead to a smaller accumulation of solutes in the soil compared to conditions in Daqalt.

Table 43: Solute balance for Maize for each branch canal and upstream/downstream location. Solute enter the field by irrigation and a bottom flux, and leave the field by drainage. Solute are shown in kg/ha.

Field	Crop	Location	Irrigation [kg/ha]	Drainage [kg/ha]	Bottomflux [kg/ha]	dS [kg/ha]
El Gemeza	Maize	Upstream	2297	1354	683	1626
El Gemeza	Maize	Downstream	2511	956	878	2432
Daqalt	Maize	Upstream	1658	2347	683	-7
Daqalt	Maize	Downstream	1876	2017	753	612
W10	Maize	Upstream	1531	626	683	1588
W10	Maize	Downstream	2781	1393	718	2106

Figure 50 shows that maize experiences some salinity stress throughout the growing season in all branch canals and upstream/downstream locations. This is due to the fact that the EC_{max} for maize (1.7 dS/m) is considerably lower than e.g. for cotton. The salinity stresses as shown in Figure 50, however, are not resulting in considerable yield decreases. The higher salinity stress in a downstream El Gemeza field is the result of the measured higher irrigation water salinity concentration in these fields. Based on the solute accumulations, as shown in Table 43, it is recommended to leach with additional water to reduce solute accumulations and prevent increased salinity stress on the long-term. This holds especially for El Gemeza and W-10.

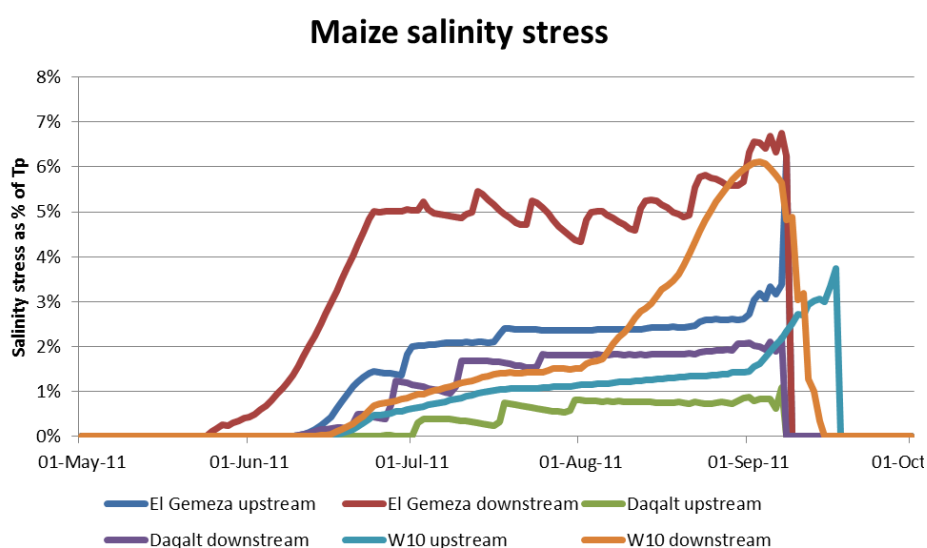


Figure 50: Maize salinity stress expressed as percentage water of potential transpiration.

Figure 51 illustrates the solute concentration in the soil profile on various depths throughout the growing season. The higher solute concentrations are located shallower in the downstream El Gemeza field than in the downstream W-10 field. After approximately 100 days the solutes in a downstream W-10 field build up and become shallower, which clarifies the pattern as shown in Figure 50. The effect of irrigation frequencies is noticeable for El Gemeza and Daqalt, whereas the irrigation pattern for W-10 is more continuous.

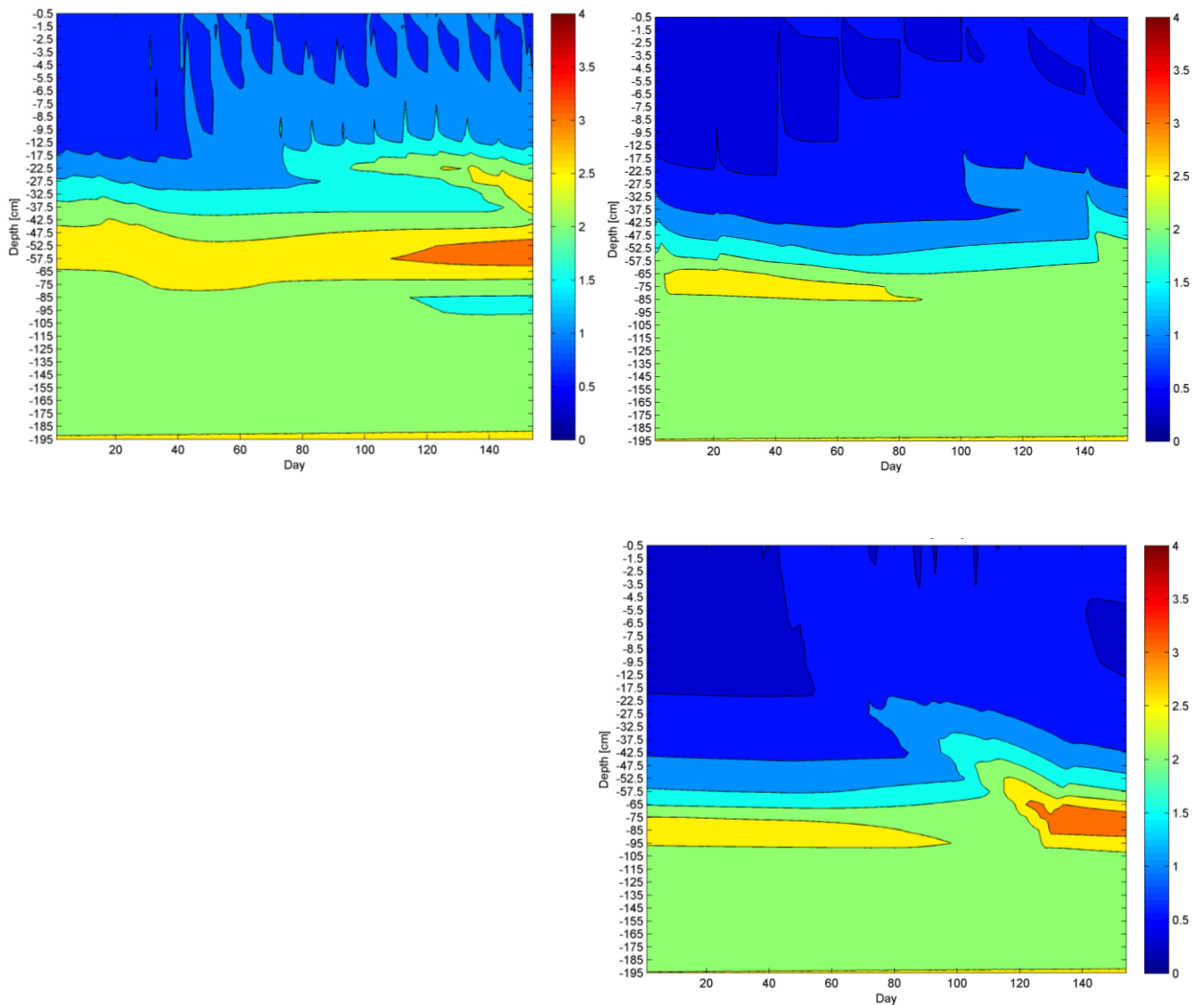


Figure 51: Maize solute concentrations [dS/m] throughout the soil profile for the downstream El Gemeza field (top left), the downstream Daqalt field (top right), and the downstream W-10 field (bottom). The x-axis represents the day of the growing season, while the y-axis represents the soil depth. It should be noted that the discretization of soil depth is smaller in the top soil.

4 Results winter 2011-2012

4.1 Cropping pattern

Based on the crop identification performed in the field and the available satellite images a supervised classification was performed, while accounting for the relative abundance of the main crops as observed in the field (see Section 2.2.2 for a more detailed description). The end result of this procedure is a land use map, with a special focus on the distinction of the main winter crops, i.e. wheat and berseem. Other crops are taken together in a lump class, as these were not selected for further analysis.

Figure 52 depicts the final land use classification for the winter season 2011/2012.



Figure 52: Land use in W-10, Daqalt and El Gemeza (in clockwise order) during winter 2011/2012.

Based on satellite imagery and fieldwork observations, it was concluded that the growing periods for both wheat and berseem extend beyond the end of the general winter growing season assumed prior to the analysis (November 1st - April 30th), as NDVI values are still high on many fields at the end of April. Average NDVI values rapidly decline in the first half of May (Figure 53). Therefore, it was decided to extend the modeling period for both wheat and berseem with two weeks to account for harvest time, meaning that all wheat and berseem results described in this chapter correspond with a growing season ranging from November 1st, 2011, to May 14th, 2012.

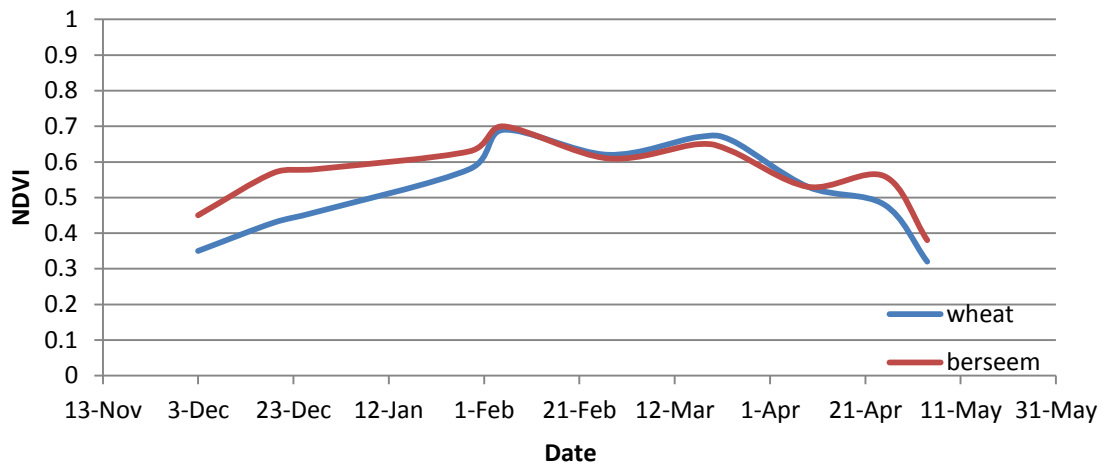


Figure 53: Temporal evolution of the average vegetation index (NDVI) for wheat and berseem based on the available high-resolution satellite data.

4.2 Water consumption

4.2.1 Wheat

Figure 54 depicts maps of seasonal water consumption for wheat in W-10, Daqalt and El Gemeza. Water consumption in this figure is accumulated for the winter growing season as defined in Section 4.1.

The water consumption results for wheat are summarized per crop in Table 44. As the table shows, ET_a in winter 2011/2012 is highest in W-10, followed by Daqalt, with the least water being consumed in El Gemeza. There are substantial differences between water consumption in 1998, 2003 and 2011 in both Daqalt and W-10. It should be noted that this is, to some extent, caused by meteorological conditions. ET_{ref} in 1997/1998 and 2002/2003 was calculated at 719 and 628 mm respectively, a 12% difference which is comparable to the difference in ET_a . ET_{ref} in 2011/2012 is 564 mm. Even when accounting for this 10% difference with 2002/2003, ET_a in 2011/2012 is clearly lower. This could be due to implemented modifications in the irrigation system since 2002/2003.

The head-tail analysis (Figure 55) shows that there is a slightly decreasing trend in water consumption from upstream to downstream in Daqalt. This could be an indication of less irrigation water availability downstream.

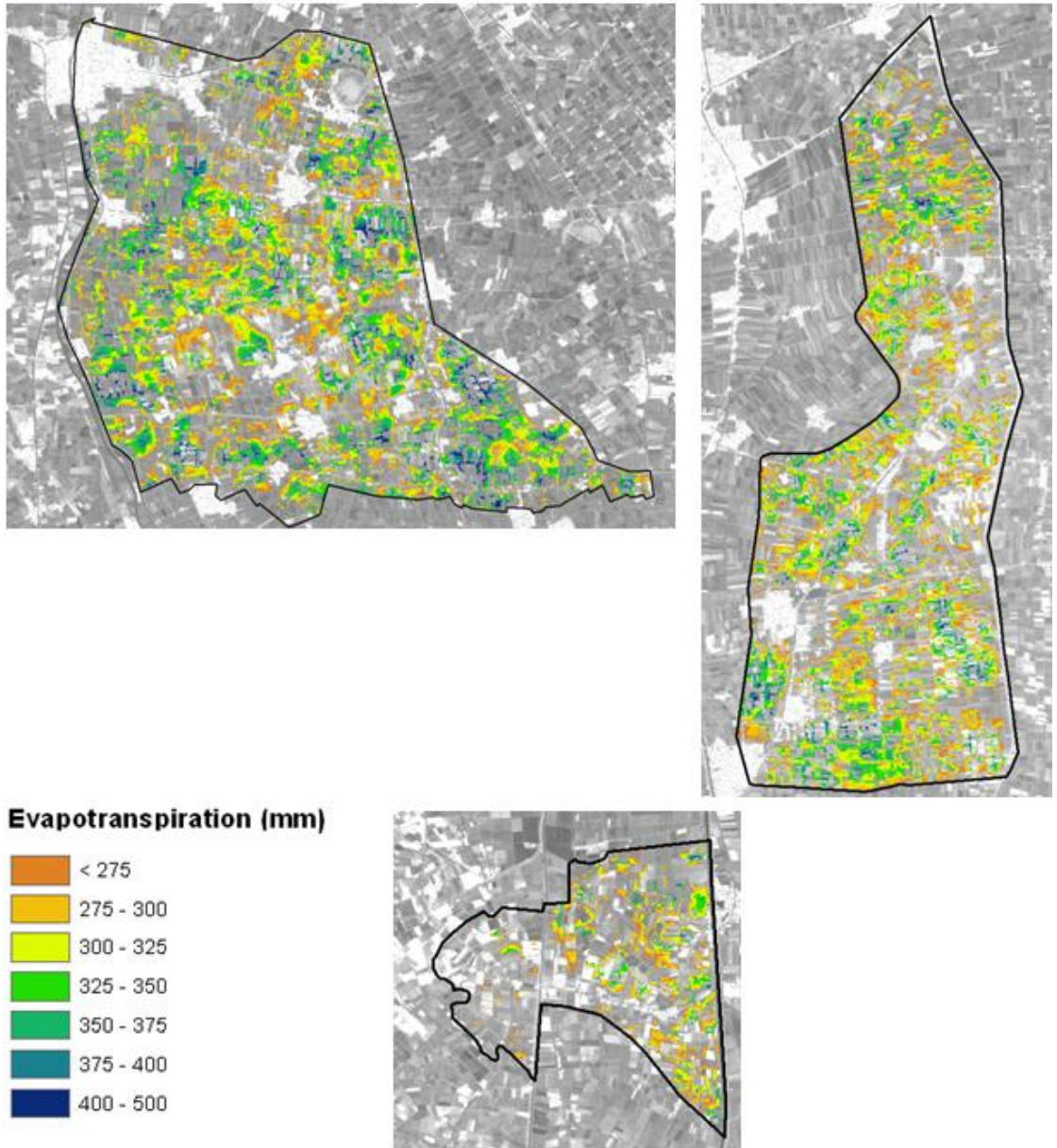


Figure 54: Spatially distributed seasonal water consumption of wheat fields in W-10, Daqalt and El Gemeza (clockwise).

Table 44: Average wheat water consumption for winter seasons 1997/1998, 2002/2003 and 2011/2012.

	2011/2012			2002/2003	1997/1998
	ET_a (mm)	σ	CV	ET_a (mm)	ET_a (mm)
W-10	324	40.9	0.126	468	524
Daqalt	314	35.1	0.112	465	523
El Gemeza	298	29.4	0.099	-	-

Head-tail analysis: Wheat water consumption

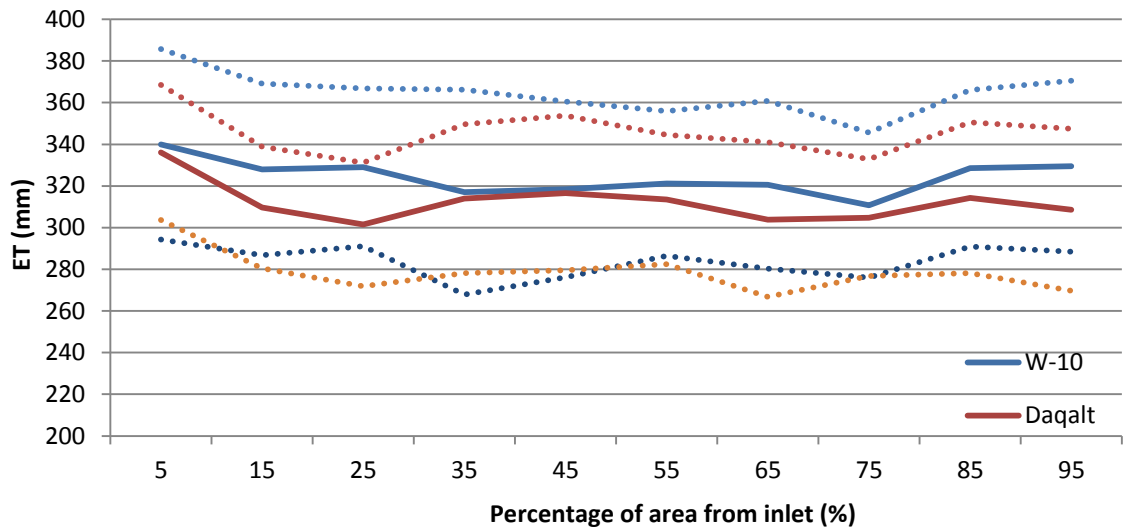


Figure 55: Head-tail analysis of wheat water consumption in W-10 and Daqalt during winter 2011/2012. Dashed lines indicate a variability range (mean plus and minus standard deviation per 10% section)

Table 45 shows the water consumption for wheat per branch canal and upstream/downstream location, with the distinction between T_a and E_a as computed with SWAP. It should be noted that the sum of T_a and E_a (ET_a) can be larger than the total amount of applied irrigation water. This is due to the initial soil water conditions and rainfall. Therefore, the amount of water that is used for crop transpiration is expressed as percentage of the ET_a sum. The upstream/downstream fields in El Gemeza and Daqalt show comparable results, with 88% of water used for transpiration, and 12% water lost through evaporation. In W-10, the T_a/ET_a ratio is lower, with 80% of water used for transpiration and 20% water lost through evaporation. This is due to the fact that the LAI values in W-10 are lower during the first half of the growing seasons when compared to El Gemeza and Daqalt, leading to more evaporation losses (non-beneficial). The lower LAIs can be a result of many factors, including nutrient deficiencies and diseases (see Section 5.2.4 for a discussion of the effects of such factors). Interestingly, there are no differences between the upstream and downstream T_a/ET_a ratios in each of the three branch canal areas. This is likely to be a result of the positive impact of rainfall, which minimizes the negative effect of seepage losses.

Table 45: Applied irrigation volumes, transpiration (T_a) and water losses through evaporation (E_a) for wheat per branch canal and upstream/downstream location.

Field	Crop	Location	Irrigation [m ³ /ha]	ET _a [m ³ /ha]	T _a [m ³ /ha]	T _a /ET _a [%]	E _a [m ³ /ha]	E _a /ET _a [%]
El Gemeza	Wheat	Upstream	1860	3084	2726	88%	358	12%
El Gemeza	Wheat	Downstream	1440	3080	2722	88%	359	12%
Daqalt	Wheat	Upstream	1890	3143	2755	88%	388	12%
Daqalt	Wheat	Downstream	1710	3136	2751	88%	385	12%
W10	Wheat	Upstream	1650	3224	2579	80%	645	20%
W10	Wheat	Downstream	1650	3224	2579	80%	645	20%

Figure 56 shows the wheat water stress due to water shortage through time, where the amount of stress is expressed as a percentage of T_p . Due to a sufficient amount of rainfall the amount of water stress is zero halfway through the growing season. The upstream/downstream non-modernized El Gemeza fields experience the highest water stress. This figure shows that stress to water shortage is lowest for the “demand driven” irrigation in W-10.

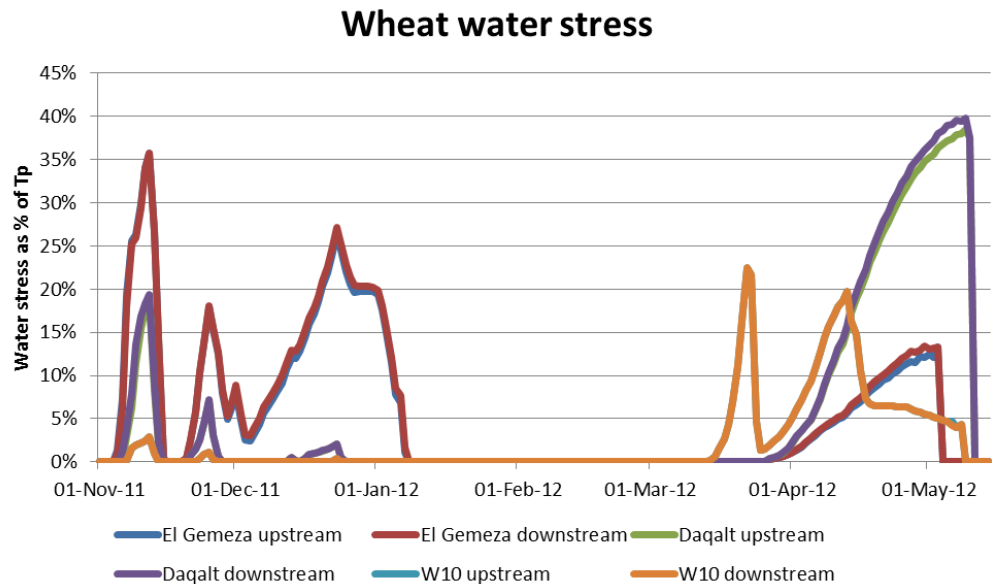


Figure 56: Wheat water stress for each branch canal and upstream/downstream location. Wheat water stress is expressed as percentage water of potential transpiration.

4.2.2 Berseem

Figure 57 depicts maps of seasonal water consumption for berseem in W-10, Daqalt and El Gemeza. Water consumption in this figure is accumulated for the winter growing season as defined in Section 4.1.

The water consumption results for berseem are summarized per crop in Table 46. As the table shows, ET_a in winter 2011/2012 is highest in W-10, followed by Daqalt, with the least water being consumed in El Gemeza. This is consistent with the pattern observed for water consumption of wheat (Paragraph 4.2.1). Berseem was not distinguished in the previous study, and current findings could therefore not be compared to historical values.

The head-tail analysis (Figure 58) shows that for Daqalt, there is a slightly decreasing trend in water consumption from upstream to downstream. In W-10, water availability is clearly not limiting to the down-stream farmers, as some of the highest water consumption figures occur near the tail end of the branch canal command area.

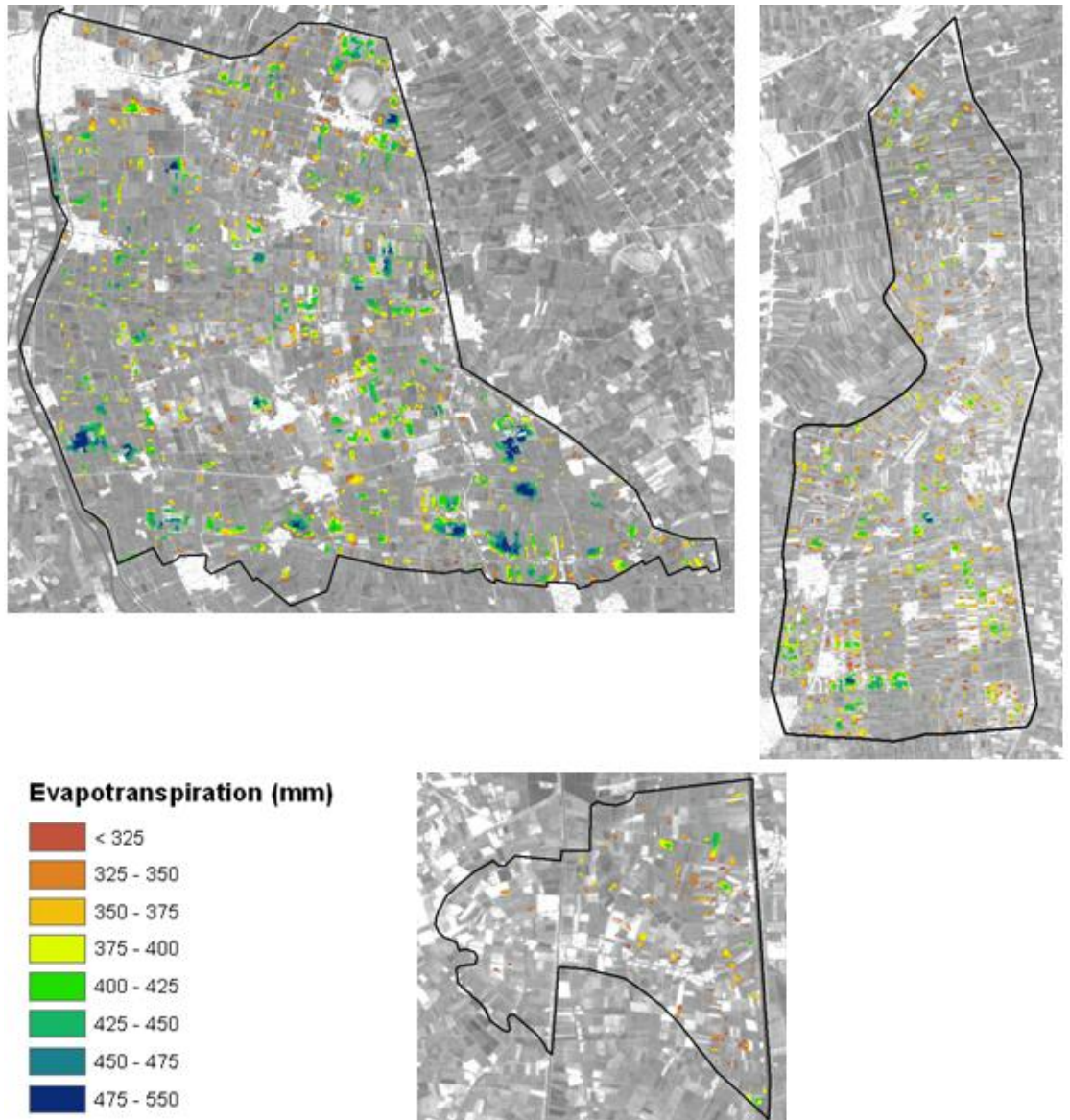


Figure 57: Spatially distributed seasonal water consumption of berseem fields in W-10, Daqalt and El Gemeza (clockwise) in winter 2011/2012.

Table 46: Average berseem water consumption in W-10, Daqalt and El Gemeza in winter 2011/2012.

	2011/2012		
	ET_a (mm)	σ	CV
W-10	398	45.4	0.114
Daqalt	368	36.1	0.098
El Gemeza	357	32.7	0.092

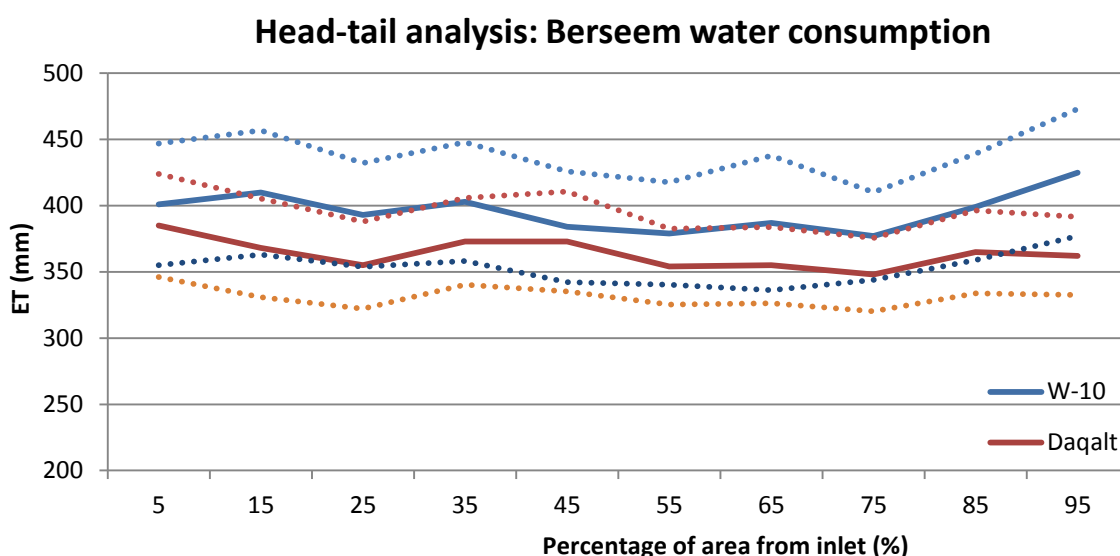


Figure 58: Head-tail analysis of berseem water consumption in W-10 and Daqalt during winter 2011/2012. Dashed lines indicate a variability range (mean plus and minus standard deviation per 10% section)

Table 47 shows the water consumption for berseem, per branch canal and upstream/downstream locations, with the distinction between T_a and E_a as computed by SWAP. In W-10, 84% of water is used for crop transpiration and 16% of water is lost through evaporation. In Daqalt, 22% of water is lost through evaporation and 78% is used for crop transpiration. This corresponds with a slightly lower LAI in Daqalt during the growing season. The non-modernized fields in El Gemeza use 81% of water for transpiration, while 19% of water is lost through evaporation in these fields. Similar to wheat, there are no differences between the upstream and downstream water consumption T_a/ET_a ratios for berseem in each of the three branch canal areas due to the effect of rainfall.

Table 47: Applied irrigation volumes, transpiration (T_a) and water losses through evaporation (E_a) for berseem per branch canal and upstream/downstream location.

Field	Crop	Location	Irrigation [m ³ /ha]	ET _a [m ³ /ha]	T _a [m ³ /ha]	T _a /ET _a [%]	E _a [m ³ /ha]	E _a /ET _a [%]
El Gemeza	Berseem	Upstream	1800	3627	2935	81%	692	19%
El Gemeza	Berseem	Downstream	1440	3395	2740	81%	655	19%
Daqalt	Berseem	Upstream	2340	3747	2923	78%	825	22%
Daqalt	Berseem	Downstream	1980	3613	2818	78%	795	22%
W10	Berseem	Upstream	2100	4117	3464	84%	653	16%
W10	Berseem	Downstream	2100	4115	3462	84%	653	16%

Figure 59 shows the berseem water stress due to water shortage, where the amount of stress is expressed as percentage of T_p . In the “demand driven” irrigation situation (W-10), irrigation water is continuously available to the farmer, meaning that they can irrigate whenever they think it is required. Therefore, water stress throughout the growing season is lowest for the upstream and downstream W-10 fields. Water stresses in El Gemeza and Daqalt are more or less equal, with the highest water stress experienced for a downstream El Gemeza field. Due to the assumed seepage losses, which are most substantial for a downstream El Gemeza field, the water stress is highest for a downstream El Gemeza field. Differences in

water stress between an upstream and downstream field are only present for El Gemeza and Daqalt, with the downstream field experiencing the highest water stress.

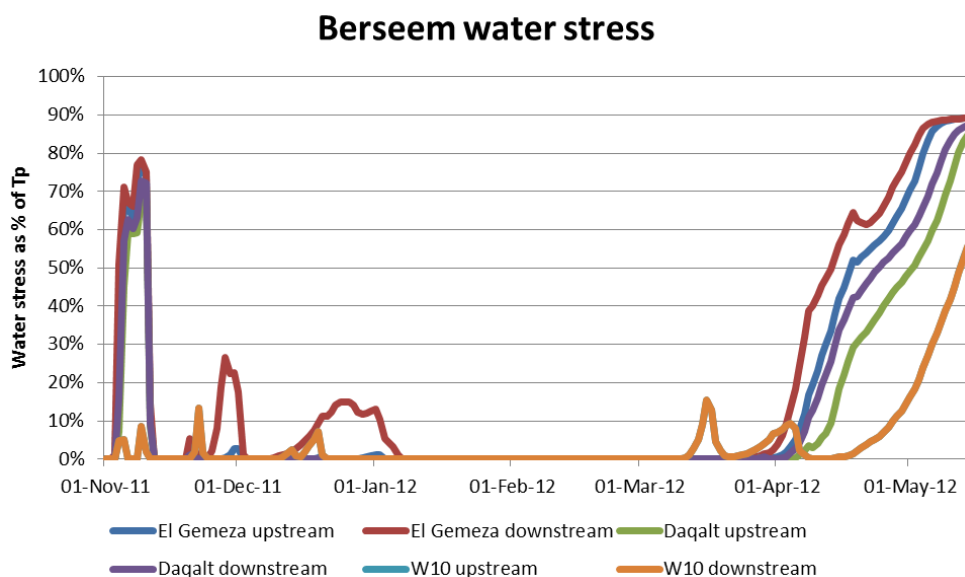


Figure 59: Berseem water stress for each branch canal and upstream/downstream location. Berseem water stress is expressed as percentage water of potential transpiration.

4.3 Crop yield

4.3.1 Wheat

SEBAL biomass production per wheat pixel (kg/ha) is accumulated for the winter growing season, and related to the fieldwork crop yield data by means of a harvest index (as described in Section 3.2). Figure 60 depicts the resulting maps of fresh yield for wheat in W-10, Daqalt and El Gemeza.

Table 48 presents the average crop yield values per branch canal command area, as well as the harvest indices obtained from the computed seasonal biomass production and reported field statistics. The spatial trend in crop yields is similar to the spatial pattern in water consumption (Table 44). This indicates that the higher water consumption in W-10 corresponds with a higher agricultural production, whereas a lower average wheat yield coincides with a lower average ETa (El Gemeza). Spatial variability is comparable in all three areas, as indicated by the negligible differences in the coefficient of variation (CV). Crop yields are lower when compared to the previous study, which is to be expected given the relatively low water consumption in 2011/2012. Also, the 2011/2012 crop yield results are believed to be more accurate, as these were calculated using locally calibrated harvest indices. In the previous study, wheat yields were calculated using harvest indices obtained from FAOSTAT yields, valid for all of Egypt. The relation between water consumption and wheat yield is further discussed in the analysis of crop water productivity (Paragraph 4.4.1).

The head-tail analysis (Figure 61) of wheat yield shows that there is a decreasing trend in wheat yield in both W-10 and Daqalt, with the slope being slightly steeper for Daqalt. This corresponds with the head-tail analysis of water consumption (Figure 51).

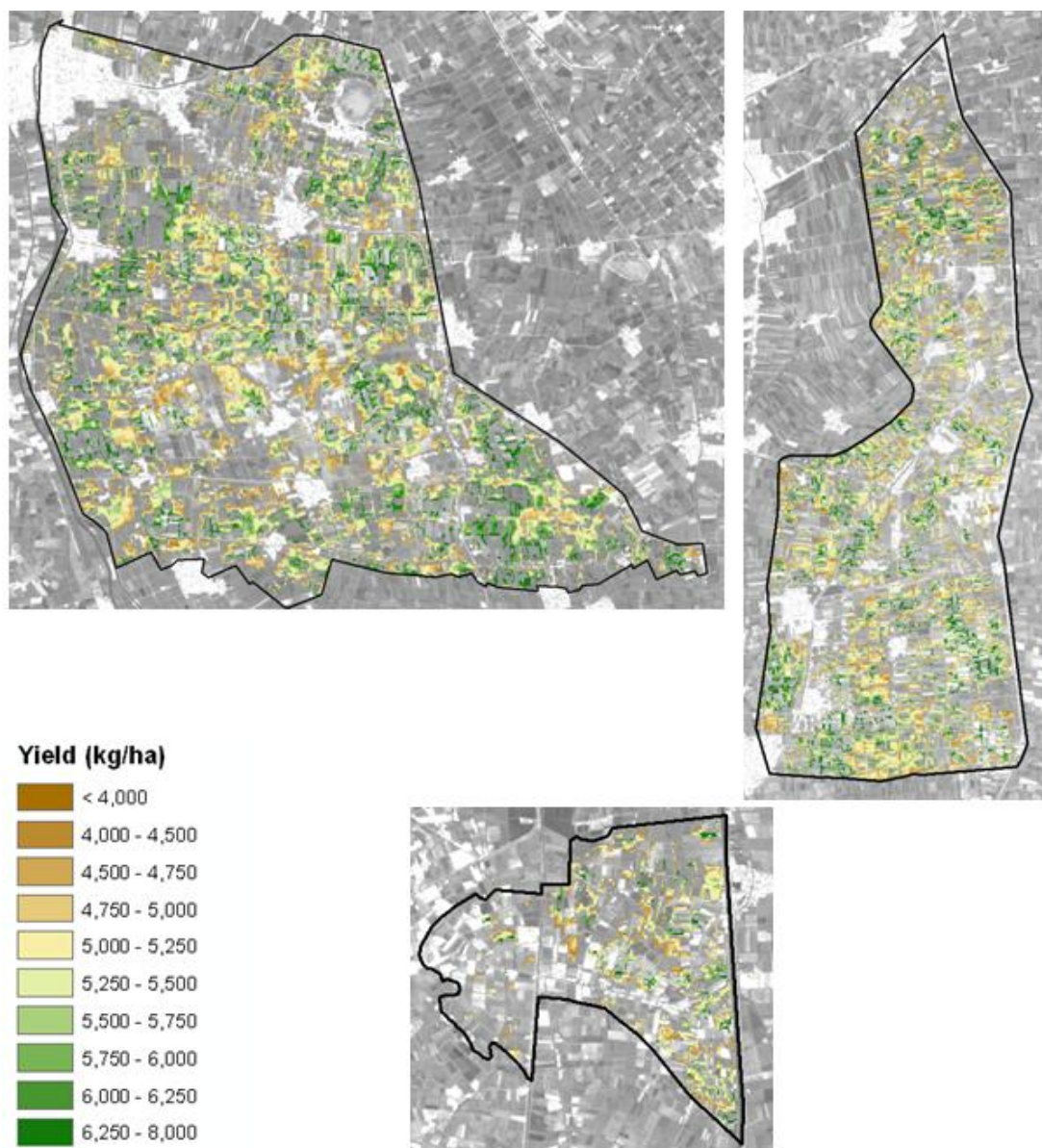


Figure 60: Spatially distributed wheat yield in W-10, Daqalt and El Gemeza (clockwise) in 2011/2012.

Table 48: Average wheat yield in W-10, Daqalt and El Gemeza in winter seasons 2011/2012, 2002/2003 and 1997/1998. Harvest indices are based on a moisture content of 0.14 (Van Gastel et al., 2002)

	2011/2012				2002/2003	1997/1998
	Y (kg/ha)	σ	CV	HI	Y (kg/ha)	Y (kg/ha)
W-10	5402	674.1	0.125	0.33	6787	6846
Daqalt	5344	653.5	0.122	0.33	6767	6889
El Gemeza	5146	597.2	0.116	0.33	-	-

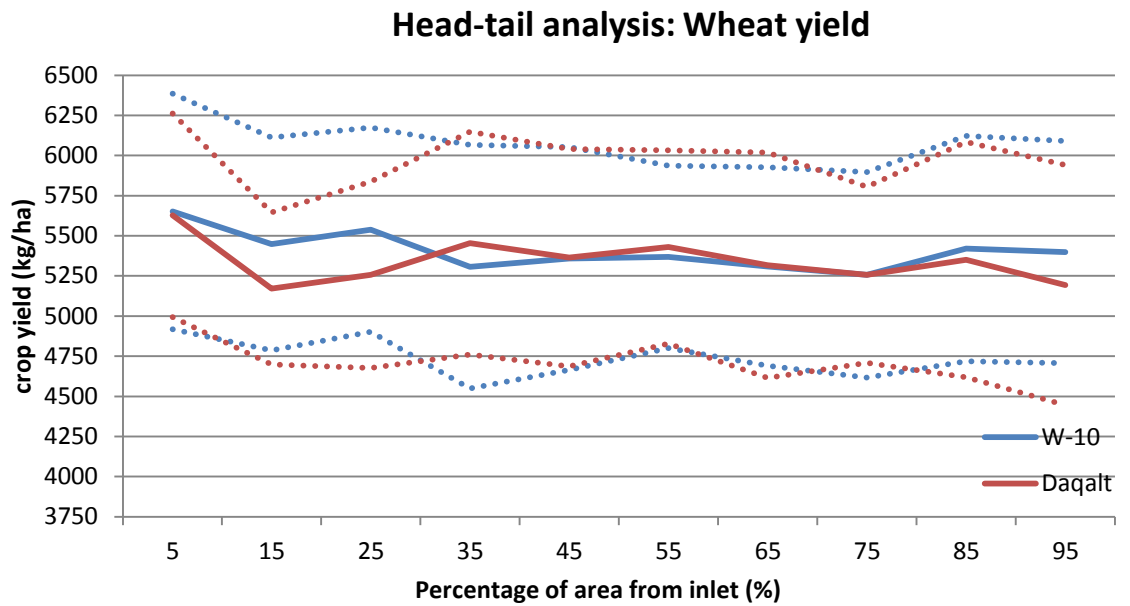


Figure 61: Head-tail analysis of wheat yield in W-10 and Daqalt for winter 2011/2012. Dashed lines indicate a variability range (mean plus and minus standard deviation per 10% section)

4.3.2 Berseem

As discussed more extensively in Paragraph 2.1.2, berseem is mainly grown as fodder for grazing cattle and for enrichment of the soil. Cutting of berseem hardly affects the NDVI as measured by a satellite, as only the crop height is reduced. Farmers seldom sell their harvested berseem crop or seeds, and they do not keep track of harvested amounts. For these reasons, an analysis of crop yields based on satellite imagery is not feasible, and the current study is limited to water and solute parameters as discussed in the other sections of this chapter.

4.4 Crop water productivity

4.4.1 Wheat

Figure 62 depicts the spatially distributed crop water productivity for wheat in W-10, Daqalt and El Gemeza. As can be seen from Table 49, the differences in water consumption and wheat yields presented in the previous sections, do not lead to marked changes in wheat productivity per unit of consumed water. For Daqalt, a value of 1.7 kg/m³ was found, with the other two areas lying in a range of 1 to 2 % from this value. Differences in spatial variability are similarly negligible. From a historical perspective, water productivity values have increased compared to 2002/2003 and 1997/1998. It should be noted that the wheat water productivity values found in this study, similar to the results of previous projects performed at a larger spatial scale, are in the high end of the global database presented by Zwart (2010), indicating an overall good performance of wheat irrigation in the Nile Delta.

The head-tail analysis of wheat water productivity (Figure 63) does not produce a clear declining trend in crop water productivity with distance from the branch canal inlet.

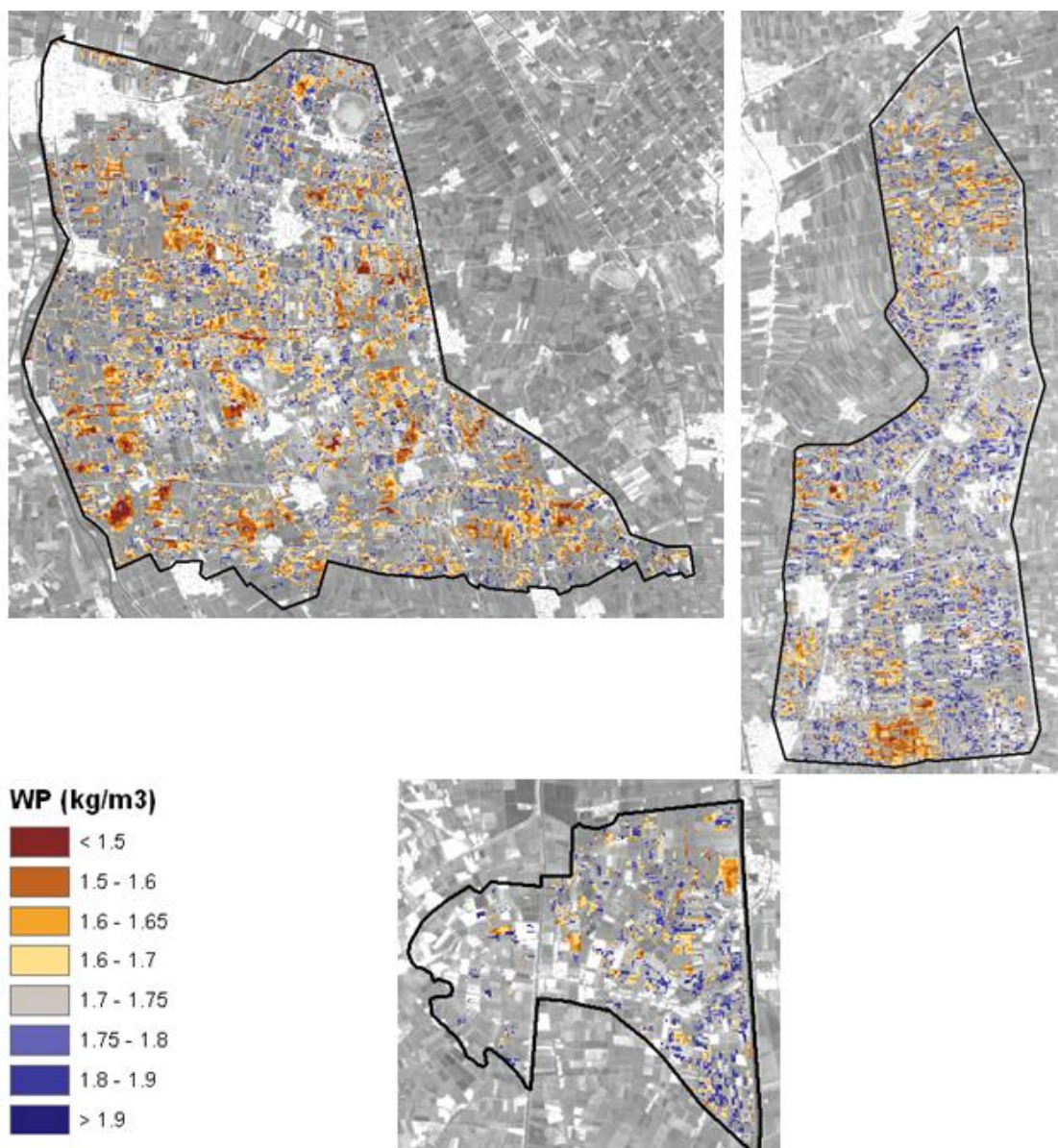


Figure 62: Spatially distributed wheat water productivity in W-10, Daqalt and El Gemeza (clockwise) for winter 2011/2012,

Table 49: Average wheat water productivity for W-10, Daqalt and El Gemeza in winter periods 2011/2012, 2002/2003 and 1997/1998.

	2011/2012 WP (kg/m ³)	σ	CV	2002/2003 WP (kg/m ³)	1997/1998 WP (kg/m ³)
W-10	1.67	0.089	0.053	1.46	1.31
Daqalt	1.70	0.089	0.052	1.48	1.32
El Gemeza	1.72	0.084	0.049	-	-

Head-tail analysis: Wheat water productivity

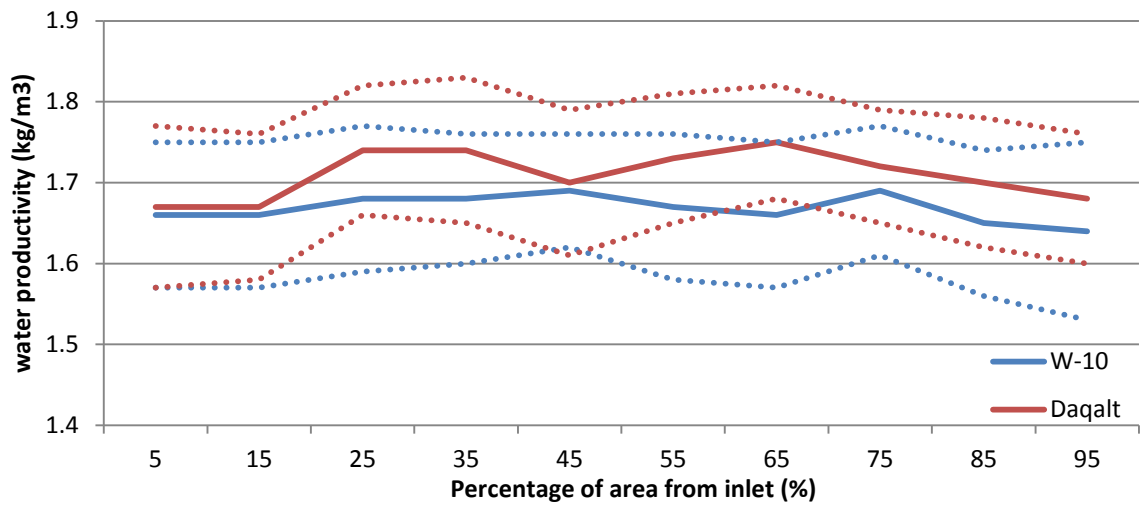


Figure 63: Head-tail analysis of wheat water productivity in W-10 and Daqalt for winter 2011/2012. Dashed lines indicate a variability range (mean plus and minus standard deviation per 10% section)

4.4.2 Berseem

As discussed more extensively in Paragraph 2.1.2, berseem is mainly grown as fodder for grazing cattle and for enrichment of the soil. Cutting of berseem hardly affects the NDVI as measured by a satellite, as only the crop height is reduced. Farmers seldom sell their harvested berseem crop or seeds, and they do not keep track of harvested amounts. For these reasons, an analysis of crop water productivity based on satellite imagery is not feasible, and the current study is limited to water and solute parameters as discussed in the other sections of this chapter.

4.5 Gross return

Based on the wheat water productivity values presented in Section 4.4.1, and locally prevailing market prices, the gross return to water for wheat in W-10, Daqalt and El Gemeza was calculated following the approach of Hellegers et al. (2009).

It was reported that, in 2011, the Egyptian government purchased wheat from the farmers at a price of LE 350 per ardebb, equal to LE 2.33 / kg (\$0.39 / kg). For 2012, figures were not available at the time of writing. Local wheat prices vary depending on government policy, harvested amounts and imported wheat. The price of LE 2.33 / kg was used in computing the gross return for wheat.

Because of the small differences in average wheat water productivity, the gross return for all three branch canals is also very similar. Values of LE 3.89 per m³, (W-10), LE 3.96 per m³ (Daqalt) and LE 4.01 per m³ (El Gemeza) are found when combining crop water productivity with the market price per kg. As there is a linear relation between crop water productivity and gross return to water, spatial variability of gross return is equal to the coefficient of variance of crop water productivity presented in Table 49.

4.6 Reliability of irrigation water availability

The reliability of irrigation water availability was evaluated following the IWMI (1999) approach (see Section 3.6, equation 8). A set of six consecutive fortnight periods is chosen for AVEDEV calculations (January 10th - April 16th). This time period coincides with the optimum of the winter growing season, and has a good coverage of high-resolution satellite images to ensure the quality of the analysis.

Figure 64 presents the results of the reliability analysis. It is found that, for the examined time series, the overall AVEDEV for all three areas is low, indicating an overall reliable water delivery both in the traditional irrigation system and the modernized, continuous flow system. This is similar to the reliability findings for the summer season (Section 3.6). Differences in the AVEDEV between the three areas are somewhat larger than during summer, with the highest variability occurring in the fully rotational system of El Gemeza. To perform a more accurate and direct analysis of reliability of irrigation water delivery to the farmer, a *marwa* flow measuring campaign is required.

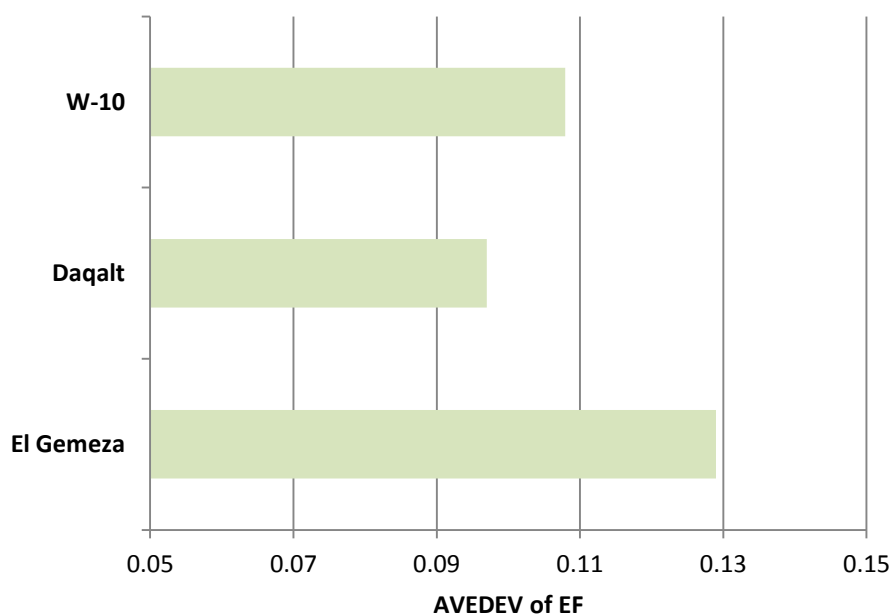


Figure 64: Reliability of irrigation water delivery per branch canal command area, expressed in the average absolute deviation from the mean (AVEDEV) of the evaporative fraction.

4.7 Canal seepage losses

The computed irrigation depth per application is shown in Table 50 for wheat for each branch canal and upstream/downstream location. It is clear that due to the assumed seepage losses, the downstream farmer in El Gemeza has less irrigation water available. Also for Daqalt seepage losses result in less irrigation water for the downstream farmer, although less evident than for El Gemeza. In W-10 no seepage losses occur, meaning that the amount of irrigation water per application is equal for the upstream and downstream farmer. Since there is a substantial amount of rainfall during the winter growing season, only three irrigation applications are required throughout the growing season (as reported in the farmer surveys).

Table 50: Total irrigation, number of irrigation applications, and irrigation depth per irrigation application for wheat per branch canal and upstream/downstream location.

Field	Crop	Location	Irrigation [mm]	Number of irrigation applications	Irrigation depth [mm]
El Gemeza	Wheat	Upstream	186	3	62
El Gemeza	Wheat	Downstream	144	3	48
Daqalt	Wheat	Upstream	189	3	63
Daqalt	Wheat	Downstream	171	3	57
W10	Wheat	Upstream	165	3	55
W10	Wheat	Downstream	165	3	55

Table 51 shows the irrigation depth per application for berseem per branch canal and upstream/downstream location. Also for berseem it is clear that seepage losses result in less irrigation water for the downstream farmer in El Gemeza. Assumed seepage losses in Daqalt are smaller and this affects the difference between the upstream and downstream amount of irrigation water per application. Again, W-10 shows the same irrigation depths for both the upstream and downstream field, due to the absence of seepage losses.

Table 51: Total irrigation, number of irrigation applications, and irrigation depth per irrigation application for berseem per branch canal and upstream/downstream location.

Field	Crop	Location	Irrigation [mm]	Number of irrigation applications	Irrigation depth [mm]
El Gemeza	Berseem	Upstream	180	18	10
El Gemeza	Berseem	Downstream	144	18	8
Daqalt	Berseem	Upstream	234	18	13
Daqalt	Berseem	Downstream	198	18	11
W10	Berseem	Upstream	210	15	14
W10	Berseem	Downstream	210	15	14

4.8 Drainage water recycling

As described in Paragraph 2.3.2.4, the drainage situation for all fields is assumed equal. Therefore, the amount of drainage water is a function of climate, irrigation depth, irrigation frequency, crop type, solute concentrations, and bottom flux. Too high salinity levels for example, can result in less root water uptake and therefore more water will leave the system as drainage water. Unfortunately, drainage fluxes and drainage water salinity levels were not measured in the study area. Therefore, SWAP could not be calibrated for observed drainage fluxes. Compared to the other SWAP water balance terms, the sensitivity of drainage results to varying input parameters is relatively small (Appendix C).

For El Gemeza and Daqalt, drainage water can be re-used by the downstream farmer. Since W-10 is modernized up to the farm-level, irrigation water in W-10 is not likely to be recycled because the farmers have their “fresh” water source at the farm-level. Recycled drainage water may contain higher solute concentrations. This is discussed in detail in Section 4.9.

4.8.1 Wheat

Table 52 shows the amount of drainage water from wheat fields that is produced per branch canal and upstream/downstream location. The drainage flux is shown as total flux in mm, as well as the percentage of total water outflow ($T_a + E_a + \text{drainage}$). The smallest amount of drainage is computed for the farm-level modernized fields in W-10 (only 6-7% of the total outflow). Since drainage is larger for El Gemeza

and Daqalt, it can be concluded that irrigation modernization up to farm-level reduces drainage, and thus decreases the scope for drainage water recycling. The upstream fields in Daqalt produce the largest amount of drainage (16%) that can be used as recycled drainage water downstream. Drainage in El Gemeza is more or less comparable to that of Daqalt, which means that irrigation modernization up to the *mesqa* level does not affect the scope for drainage water recycling for wheat.

Table 52: Drainage flux for wheat fields, per branch canal and upstream/downstream location. Drainage is expressed in mm as well as percentage of the total outflow flux ($Q_{out} = T_a + E_a + \text{Drainage}$).

Field	Crop	Location	Drainage [mm]	Qout [mm]	Drainage [%]
El Gemeza	Wheat	Upstream	48	357	14%
El Gemeza	Wheat	Downstream	33	341	10%
Daqalt	Wheat	Upstream	59	373	16%
Daqalt	Wheat	Downstream	51	365	14%
W10	Wheat	Upstream	22	344	6%
W10	Wheat	Downstream	23	345	7%

Figure 65 shows a time-series of drainage for wheat per branch canal and upstream/downstream location. The maximum drainage flux is close to 0.7 mm/day. Since irrigation in W-10 is demand driven, irrigation is only applied whenever a certain amount of water stress is experienced. Therefore, the drainage patterns for the upstream/downstream fields in W-10 are relatively smooth throughout the growing season. As the applied irrigation depths are largest for El Gemeza and Daqalt, the drainage fluxes are also largest for the fields in these branch canal areas. Due to the assumed seepage losses, the downstream drainage flux in El Gemeza is lower compared to an upstream field in El Gemeza.

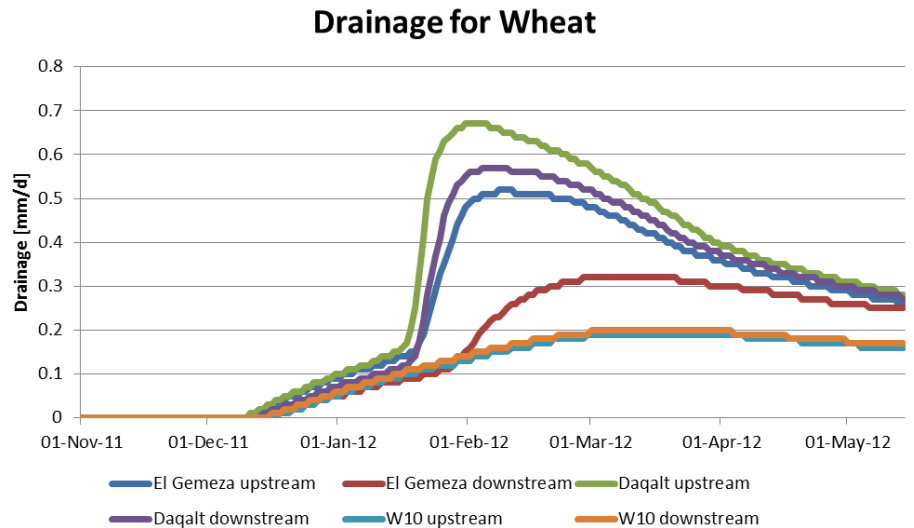


Figure 65: Drainage flux of wheat for each branch canal and upstream/downstream location.

4.8.2 Berseem

Table 53 shows the amount of drainage water that is produced from berseem fields per branch canal and upstream/downstream location. The drainage flux is shown as total flux in mm, as well as the percentage of total water outflow ($T_a + E_a + \text{drainage}$). Because irrigation for berseem is applied more frequently than for wheat, the corresponding irrigation depth per application is smaller. Daqalt is the branch canal where

the largest drainage volumes occur (9-11% of total outflow). Drainage water recycling in Daqalt is larger due to the larger irrigation depth per application. The scope for drainage water recycling in W-10 is smaller because of the demand driven irrigation system.

Table 53: Drainage flux for berseem fields, per branch canal and upstream/downstream location. Drainage is expressed in mm as well as percentage of the total outflow flux ($Q_{out} = T_a + E_a + \text{Drainage}$).

Field	Crop	Location	Drainage [mm]	Qout [mm]	Drainage [%]
El Gemeza	Berseem	Upstream	21	383	5%
El Gemeza	Berseem	Downstream	19	359	5%
Daqalt	Berseem	Upstream	48	423	11%
Daqalt	Berseem	Downstream	34	396	9%
W10	Berseem	Upstream	11	423	3%
W10	Berseem	Downstream	12	423	3%

Figure 66 shows a time-series of drainage for berseem per branch canal and upstream/downstream location. The maximum drainage flux is close to 0.6 mm/day and is therefore very small. Due to the demand driven irrigation in W-10, the drainage patterns for the upstream/downstream fields in W-10 are relatively smooth throughout the growing season and also very small. The figure shows that the simulated irrigation behavior of berseem farmers in Daqalt leads to the highest volumes of drainage water, whereas the difference between the traditional and the *marwa* modernized simulations is relatively small.

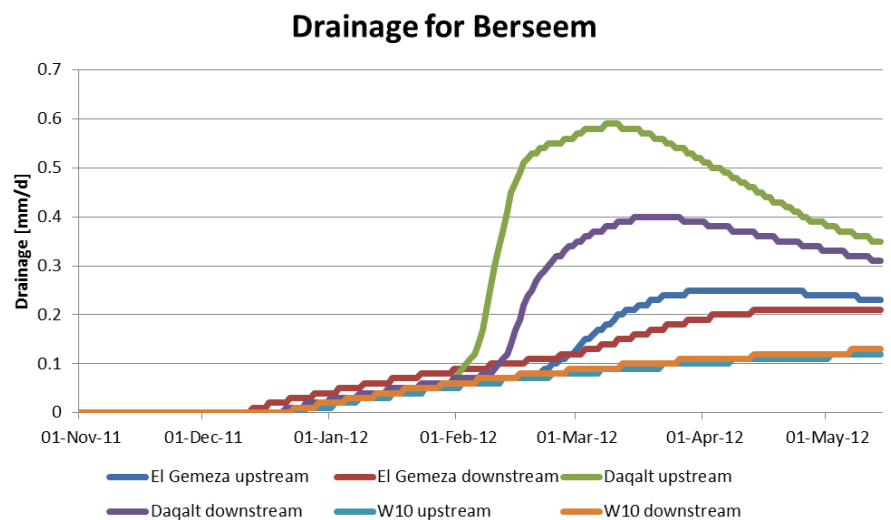


Figure 66: Drainage flux of Berseem for each branch canal and upstream/downstream location.

4.9 Salinity

High salinity levels can result in reduced root water uptake, subsequently leading to reduced crop yields at the end of the growing season. As described in detail in Section 2.3.2.8, solutes enter the field by irrigation and a bottom flux. Therefore, the solute balance is a function of the irrigation water solute concentration, irrigation depth, irrigation frequency, bottom flux, and crop type. The following paragraphs describe the solute balance per crop for each of the branch canals and upstream/downstream locations. SWAP provides the user with a solute balance output file, in which solutes are shown in mg/cm^2 . For the analysis in the following sections, these numbers are converted to kg/ha . The current study does not consider additional leaching with large amounts of water (see also Section 2.3.2.9).

4.9.1 Wheat

The total amount of solutes in kg/ha is shown in Table 54 for each branch canal and upstream/downstream location where wheat is grown. Solute accumulations are computed to be the largest for the downstream El Gemeza and downstream W-10 fields. These findings indicate that, for wheat fields, the *marwa* level irrigation modernization has not lead to a smaller accumulation of solutes in the soil than observed in ther *mesqa* level modernized area. The larger solute accumulations for the downstream fields in El Gemeza and W-10 are due to the measured higher irrigation water solute concentrations, in combination with a smaller drainage flux. Since an upstream Daqalt field has a low solute concentration in its irrigation water, and the drainage flux in these fields is quite large, most solutes leave the soil profile by drainage and therefore solute accumulations are smallest for an upstream Daqalt field. Since irrigation water solute concentrations in an upstream El Gemeza field and a downstream Daqalt field are comparable, and drainage fluxes as well, solute accumulations are similar for these fields.

Table 54: Solute balance for Wheat for each branch canal and upstream/downstream location. Solutes enter the field by irrigation and a bottom flux, and leave the field by drainage. Solutes are shown in kg/ha.

Field	Crop	Location	Irrigation [kg/ha]	Drainage [kg/ha]	Bottomflux [kg/ha]	dS [kg/ha]
El Gemeza	Wheat	Upstream	725	1121	875	479
El Gemeza	Wheat	Downstream	778	710	1125	1192
Daqalt	Wheat	Upstream	605	1395	875	85
Daqalt	Wheat	Downstream	684	1185	965	464
W10	Wheat	Upstream	479	465	875	888
W10	Wheat	Downstream	726	490	920	1155

Analysis shows that for all branch canals and upstream/downstream fields, wheat does not experience any salinity stress throughout the growing season. This is due to the fact that wheat is quite resistant to solutes ($EC_{max} = 6.0$ dS/m, Table 13). It should be noted, however, that since solutes accumulate for all wheat fields, wheat may be experiencing solute stress on the long-term if no additional water is supplied to leach these soils. If no additional leaching occurs, solute stress will be most substantial in the downstream El Gemeza fields and downstream W-10 fields.

4.9.2 Berseem

The total amount of solutes in kg/ha is shown in Table 55 for berseem fields per branch canal and upstream/downstream location. Solute accumulations are again most evident for the downstream El Gemeza and downstream W-10 fields. Therefore, also for berseem fields the *marwa* level irrigation modernization has not decreased the accumulation of solutes in the soil. Due to the large drainage fluxes in an upstream Daqalt field, and the measured low solute concentration in irrigation water, the accumulation of solutes is smallest for an upstream Daqalt field.

Table 55: Solute balance for berseem for each branch canal and upstream/downstream location. Solutes enter the field by irrigation and a bottom flux, and leave the field by drainage. Solutes are shown in kg/ha.

Field	Crop	Location	Irrigation [kg/ha]	Drainage [kg/ha]	Bottomflux [kg/ha]	dS [kg/ha]
El Gemeza	Berseem	Upstream	702	444	875	1133
El Gemeza	Berseem	Downstream	778	418	1125	1484
Daqalt	Berseem	Upstream	749	1135	875	488
Daqalt	Berseem	Downstream	792	760	965	997
W10	Berseem	Upstream	609	230	875	1254
W10	Berseem	Downstream	924	252	920	1592

Berseem experiences minor salinity stress (max 3% reduction in T_a) during the growing season. This is due to the fact that the EC_{max} for berseem (1.5 dS/m) is lower than for wheat. Based on the calculated solute accumulations, as shown in Table 55, it is recommended to leach with additional water to reduce solute accumulations and prevent increased salinity stress on the long-term.

Figure 67 illustrates the solute concentration in the soil profile on various depths throughout the growing season. The highest solute concentrations can be found in a downstream El Gemeza field, while the lowest concentrations are found in Daqalt.

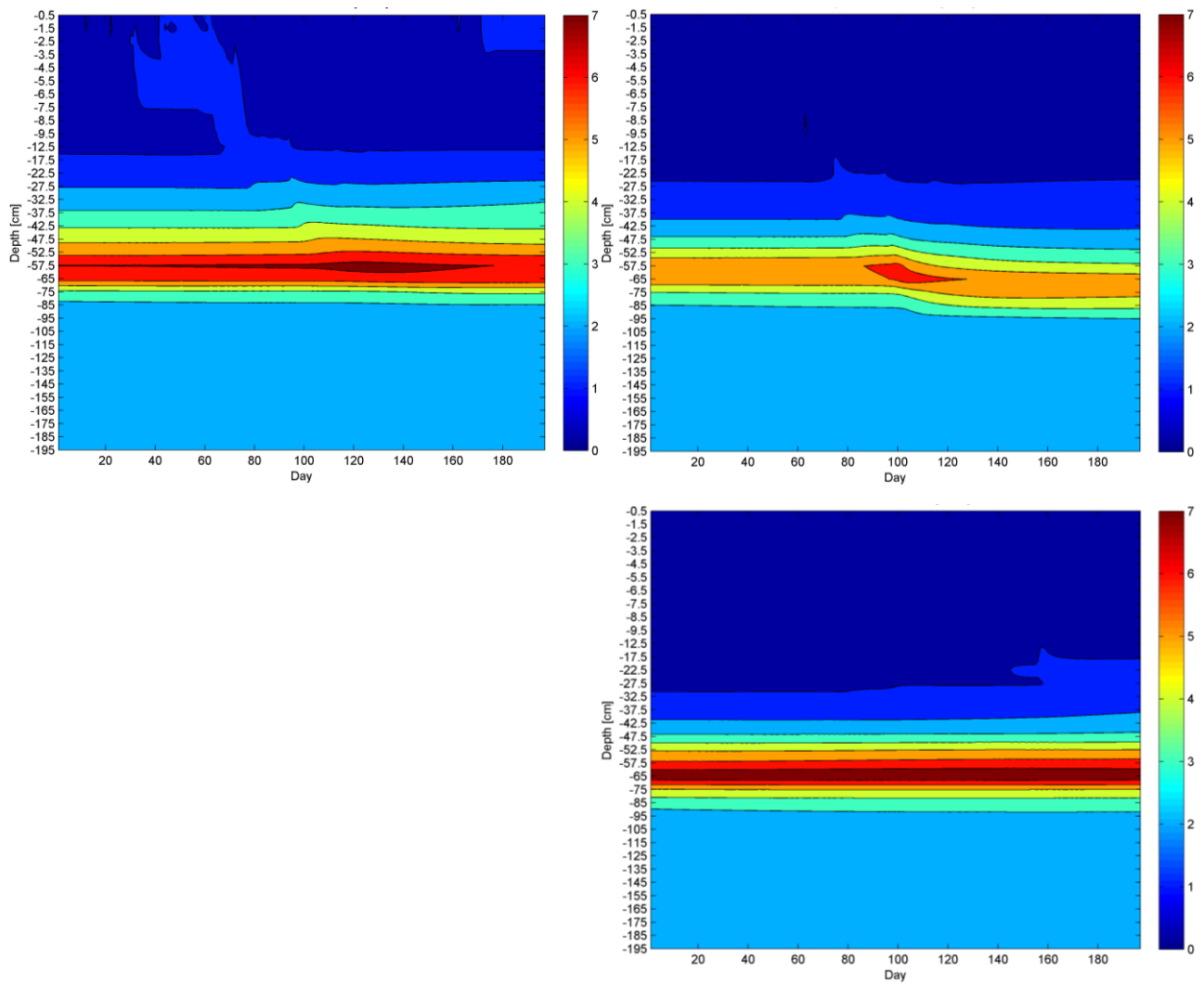


Figure 67: Berseem solute concentrations [dS/m] in the soil profile for the downstream El Gemeza field (top left), the downstream Daqalt field (top right), and the downstream W-10 field (bottom). The x-axis represents the day of the growing season, while the y-axis represents the soil depth. It should be noted that the discretization of soil depth is smaller in the top soil.

5 Discussion

5.1 Overall effects of modernization

5.1.1 Rice

Our analysis indicates that the irrigation modernization does not have a noticeable effect on the water consumption for rice. The total water consumption in Daqalt and W-10 differs from El Gemeza only within a range of 0-5%, which is within the error boundaries of the SEBAL model (see Appendix E). Typically 80% of the consumed amount is productively consumed for transpiration, and 20% is lost to evaporation. Water consumption is lowest for Daqalt and highest for the non-modernized El Gemeza, although these differences are minor. The same observation counts for average rice yield and water productivity in the three areas, which all lie in the range of a few %.

Absolute values of rice water consumption, crop yield and water productivity are comparable to those that were found for the summer of 2002, and (for crop yield and water productivity) considerably larger than those found for summer 1995. This suggests that the impact of the final, farm-level modernization steps is not yet at the same level as the effects that were obtained during the IIP interventions.

In terms of spatial variability, non-modernized El Gemeza shows the highest variability in terms of biophysical water productivity (and thus, gross return), largely caused by a higher variability in crop yield. This leads to the conclusion that the branch canal and *mesqa* modernizations applied in W-10 and Daqalt have led to an increased equity of water productivity, when compared to conditions in El Gemeza. As exemplified by the head-tail analysis of SEBAL results, higher values of consumptive use and yields are particularly found in upstream areas, with averages generally decreasing along the length of the branch canal.

Since rice is frequently irrigated in all areas and the water consumption is found to be approximately equal for all branch canals and upstream/downstream locations, the amount of drainage water is similar for all branch canals and upstream/downstream locations. These results suggest that the irrigation modernization at the *mesqa* and *marwa* level has not affected the scope for drainage water recycling for rice.

Irrigation modernization up to the *mesqa* level is computed to have a positive impact on salinity levels, which are lower in Daqalt than in El Gemeza. However, no reduction in salinity levels was found for the modernization up to the farm-level (W-10). This is due to the measured irrigation water salinity levels in W-10 in combination with the larger applied irrigation sum. All fields show solute accumulations. Therefore, it is recommended to leach with large amounts of additional water, if this is not already being done by farmers.

5.1.2 Cotton

Non-modernized El Gemeza shows the highest consumptive use of all three areas, indicating that modernization up to the *mesqa* level has resulted in less water consumption (10%) for cotton, which corresponds with one of the purposes of irrigation modernization. However, SEBAL results show that more water is consumed in W-10 compared to Daqalt, which is an indication that altered irrigation behavior of the farmers (reacting to crop stress instead of limited irrigation water availability) not necessarily leads to a reduction in seasonal consumptive use. However, in W-10 the largest portion of this water is put to

productive use (~90%), whereas the beneficially consumed fraction in Daqalt (87%) and El Gemeza (80%) is smaller, meaning that the soil evaporation component is higher in the non-modernized areas. This indicates that both the *marwa* and *mesqa* modernizations have had a desirable effect on the T_a/ET_a partitioning.

The difference in T_a based on SEBAL and SWAP calculations corresponds with the higher reported seed cotton yield in W-10 compared to Daqalt and El Gemeza. W-10 crop yield is also markedly higher (10%) than recorded in 2002, while Daqalt yields have remained at the same level. This indicates that *marwa* level improvements have had a beneficial effect on seed cotton production. On average, W-10 and Daqalt arrive at a similar productivity of water (0.5 kg/m^3) and gross return (LE $9/\text{m}^3$). Crop water productivity in El Gemeza (calculated at 0.41 kg/m^3) is lower, an observation that could be attributed to branch canal and *mesqa* modernizations. From a historical perspective, water productivity values are observed to be increasing steadily when compared to conditions in 2002 and 1995.

Approximately 7-8% of the drainage water from an upstream El Gemeza and Daqalt field is available for reuse further downstream. Since the assumed demand-driven irrigation at the farm-level modernized field results in higher irrigation frequencies with a smaller irrigation depth, water is used more efficiently and subsequently the drainage flux is much smaller (3% of total outflow). Therefore, our simulations indicate that irrigation modernization up to the farm level reduces the amount of drainage water available for recycling. Although this may be seen as more efficient water use at the scale of a single (upstream) field, such an increase in efficiency may reduce water availability to downstream farmers, who previously relied on upstream drainage water. The head-tail analysis of seed cotton yield and water consumption (based on remote sensing and field data, and thus not influenced by canal flow assumptions) suggest that this limiting effect for downstream farmers is currently not occurring in W-10; an indication of continuous irrigation water availability in the downstream part of the canal. Hence, W-10 downstream farmers may have switched from recycling drainage water to using the newly available water at the farm gate.

Lower salinity levels in irrigation water have been measured for the *mesqa* and *marwa* level modernized areas. However, salinity content in the downstream W-10 soil profile are computed to be higher than in downstream Daqalt fields. This is related to the low salinity levels in Daqalt's irrigation water in combination with a large irrigation depth. This results in a substantial drainage flux taking solutes with it. This phenomenon indicates that a change in farmer irrigation behavior due to continuous flow availability may not have a desirable effect on salinity levels. It was shown, however, that cotton does not experience any stress due to high salinity levels. It should be noted that solutes are computed to be accumulating in the soil for all fields, which means that cotton may experience solute stress on the long-term if no additional leaching with large amounts of water is performed. Solute stress will first be experienced in a downstream, non-modernized cotton field.

5.1.3 Maize

Both water consumption as calculated by SEBAL and crop yields as reported by farmers, were noticeably lower in Daqalt than in W-10. As discussed in Chapter 3, this could be an indication that maize farmers in Daqalt are limited by the availability of irrigation water, and are therefore unable to realize the yields that W-10 farmers achieve. It could, however, also have causes unrelated to water availability. In general, it should be noted that the results for maize are reported with a greater degree of uncertainty than rice and cotton results. This is due to the small amount of maize fields present in the areas, their size, the lack of summer fieldwork in El Gemeza, and the subsequent difficulties occurring in the supervised land use classification procedure. This also limits the scope for addressing spatial variability in

terms of the coefficient of variation and the head-tail analysis, which was not performed due to the lack of remaining maize fields when splitting up the branch canal command areas in smaller segments.

From the SWAP analysis, it is concluded that the reported low irrigation frequency in combination with a large irrigation depth results in a substantial amount of drainage water for maize in Daqalt (~19% of total outflow), which is subsequently available for downstream recycling. Irrigation modernization up to the *marwa* level has led to a reduction in drainage water recycling to 6%. In El Gemeza, the drainage flux is also relatively small, but here a large portion of the total outflow is comprised of non-productive soil evaporation (~30%). The large drainage flux in Daqalt, in combination with the lowest solute concentrations in the irrigation water, leads to the lowest solute accumulation in the soil. Therefore, it can be concluded that the irrigation practices in Daqalt have a positive effect on solute accumulations, a similar effect to what is observed for cotton. Maize is computed to experience some salinity stress for all simulated fields, although not substantial. Since solutes accumulate in all fields, it is recommended to leach with large amounts of additional water in order to prevent increased salinity stresses on the long-term. These stresses will first be experienced in downstream, non-modernized fields.

5.1.4 Wheat

For wheat, it was found that water consumption is higher in the fully modernized W-10 command area, when compared to Daqalt and El Gemeza. This corresponds with the summer crop results, indicating that altered irrigation behavior of the farmers (reacting to crop stress instead of limited irrigation water availability) not necessarily leads to a reduction in seasonal consumptive use. Contradictory to the summer results, however, a relatively large portion of the water consumption in W-10 (20%) is due to non-beneficial soil evaporation, compared to 12% in the other two areas. This is due to the lower LAIs in W-10 at the beginning of the growing seasons. The reason for these lower LAIs may not be water related; please see Section 5.2.4 for a discussion of influential factors outside the crop water parameters discussed in this study.

Despite the observed low LAIs for the early part of the season in W-10, seasonal wheat production was found to increase with modernization level. This corresponds with the results of the SWAP analysis, which indicate that the demand-driven irrigation in W-10 results in the smallest water stress throughout the growing season. In terms of wheat water productivity, all canal command areas perform equally, and at a very high level when viewed from a global perspective (approximately 1.7 kg/m³). This is a substantial improvement from 2002/2003 and 1997/1998.

Approximately 14% of the drainage water of an upstream El Gemeza wheat field, and 16% of an upstream Daqalt wheat field is available for reuse by a downstream farmer. The modernization up to the farm-level reduces the available amount of drainage water for reuse to approximately 6%. This is due to the fact that irrigation in the “demand driven” situation is assumed to be only applied whenever a certain amount of stress is experienced. Due to assumed canal seepage losses, downstream canal water levels in El Gemeza are lower when compared to downstream canal water availability in Daqalt and W-10.

Lower salinity levels are generally measured in the irrigation water for the *mesqa* and *marwa* level modernized areas, although downstream salinity levels in W-10 are still higher than in downstream Daqalt fields. It was found that solutes accumulate in the soil profile for all upstream/downstream fields in all three branch canals, with the largest accumulations found for downstream El Gemeza and downstream W-10 fields. This is due to (respectively) the high irrigation water solute concentration and smaller drainage flux. Currently, wheat does not experience any stress due to solutes. It should be noted that wheat may

experience solute stress on the long-term if no additional leaching with large amounts of water is performed. Salinity stress will first be experienced in the downstream non-modernized fields.

5.1.5 Berseem

Berseem water consumption in winter 2011/2012 is highest in W-10, followed by Daqalt, with the least water being consumed in El Gemeza. Irrigation water appears to be abundantly available to the downstream farmer, with the head-tail analysis showing some of the highest ET_a values near the tail end of the command area. This corresponds with the finding that W-10 water stress is lowest throughout the season, with downstream water stress being equal to upstream water stress. Again, similar to the results for cotton and wheat, this indicates that the farmer's reaction to continuous water availability in W-10 in fact leads to an increase in water consumption. However, this water is put to productive use, as only 10% of the consumed water in W-10 is lost to soil evaporation. For Daqalt, the head-tail analysis shows a slightly decreasing trend in water consumption with distance to the inlet point. This corresponds with SWAP computing a higher water stress for downstream fields, due to canal seepage losses. Overall, a positive effect of *marwa* modernizations on productivity and equity of water consumption is found.

Berseem was not distinguished in the previous study, and current findings could therefore not be compared to historical values. Also, for reasons explained in Section 4.1.2, berseem crop yields and water productivity are not quantified in this study.

Roughly 11% of drainage water of an upstream Daqalt field is available for reuse by a downstream farmer. This is more than the amount of drainage water that is available from an upstream non-modernized El Gemeza field (5%). The smallest amount of drainage water is produced in W-10, indicating that the *marwa* modernizations lead to reduced drainage water availability for a downstream user. This is due to the fact that irrigation in the "demand driven" situation is only applied whenever a certain amount of stress is experienced, which results in a relatively smooth drainage pattern throughout the growing season.

Lower salinity levels are generally measured in the irrigation water for the *mesqa* and *marwa* level modernized areas, although downstream salinity levels in W-10 are still higher than in downstream Daqalt fields. It was found that solutes accumulate in the soil profile for all upstream/downstream fields in all three branch canals, with the largest accumulations found for downstream El Gemeza and downstream W-10 fields. Since solutes accumulate for all fields in all three branch canal areas, berseem may experience more stress on the long-term if no additional leaching with large amounts of water is performed. Salinity stress will first be experienced in the downstream non-modernized and downstream *marwa* fields.

5.2 Usefulness and limitations of the integrated approach

The combination of water balance modeling with SWAP and energy balance modeling with SEBAL is an appropriate combination for assessing the spatially distributed soil water flows, including a water quality component. As a result of the applied methodology, all components of the water and solute balance are quantified and results can be intercompared. However, the methodology also knows a number of limitations, related to field data availability and the associated need for assumptions, satellite imagery properties, congruency between the outputs from different tools, and the disregard of factors influencing crop health that are not part of the water and solute balance. These limitations are discussed in this section for the benefit of the World Bank funded FIMP project, that is currently being implemented.

5.2.1 Input data availability

The main limitation in the application of the methodology was found to be the lack of input data that is available on the field scale. With the setup of extensive farm-level measurement campaigns being outside the scope of the current project, existing field monitoring efforts proved to be insufficient to provide information at the *marwa* level. Using the valuable input of several experts currently and previously involved in IIP and IIIMP, it is believed that a full overview of the availability of data related to canal flow, cropping patterns, water supply, water quality, drainage fluxes, soil properties and groundwater levels was achieved and the location of these data was determined. Some of these parameters are indeed being operationally monitored for the studied canal command areas, but only at the branch canal level. Naturally, this is a greatly limiting factor for a study that aims to quantify farm-level effects of irrigation modernization. The problem with data availability turned out to be not a matter of difficulties in obtaining these data from Egyptian authorities, as was expected prior to the study, but the reported total absence of *marwa* level measurements being performed altogether.

The available information was used as input to the SWAP analysis. As salinity of the irrigation water was the only measured parameter for which some differentiation exists beyond the branch canal level, differences between conditions in upstream and downstream fields had to be assumed based on general knowledge on the nature of the completed IIIMP irrigation improvements. The two main assumptions on which the SWAP analysis is based are the continuous supply of water to the farmers in W-10, causing them to be able to base their irrigation behavior on crop stress instead of rotational water availability, and the seepage losses that occur in non-modernized areas with earthen canals as opposed to modernized areas with lined canals. The necessity to make these assumptions follows from the fact that these parameters are currently not being monitored on the field scale. Although these assumptions influence the outcomes of the study in terms of differences between areas, they are required to approach the actual field situation as closely as possible, in the absence of farm-level measurements.

Meteorological data is an important input into both the SEBAL and the SWAP model. The lack of weather stations in the Nile Delta delivering operational data was therefore another limiting factor. The Baltim station is located 32 km from El Gemeza, 35 km from Daqalt and 42 km from W-10. Two measurement stations are known to be located closer to the study areas (Damanhour and Tanta), but unfortunately both stations do not supply data for the period under consideration. The option of including multiple stations and interpolating between them to obtain a gradient in temperature, wind speed and humidity was investigated in the early stages of the project. However, the closest station opposite to the Baltim station that delivers data (Wadi El Natroon) is situated 110 km from the study area. Also, it is located just outside of the Nile Delta at the edges of the desert, resulting in climatic conditions significantly different from those in the study area. Performing meteorological measurements in the study area (or, choosing a study area near a weather station) would improve the quality of the modeling exercises.

Another important source of information in this study are the farmer surveys conducted on location. Although this produces valuable insights in the field situation, the field team (GeoMAP) reports that still some caution should be applied when interpreting this information. In particular, farmers tend to avoid reports of true yield numbers for the sake of tax related inspections by the government on the basis of their performance. This may help to explain the anomalously low crop yields reported for maize and cotton in Daqalt. Also, it turns out that the target group of uneducated farmers is unable to answer questions on applied irrigation depths or pumping durations,

5.2.2 Interpretation and availability of satellite data

With the lack of farm-level measurements, the main tool to determine field scale variations is the remote sensing image interpretation, which provides pixel-by-pixel quantifications of water consumption, crop yield and water productivity. The quality of this analysis is largely dependent on the spatial resolution of the available satellite imagery, which for the summer 2011 study mainly consisted of Landsat 30m images. As typical field sizes in the area around 0.4 - 0.5 ha (Table 5), fields will often consist of no more than a few pixels, increasing the occurrence of 'mixed' pixels. This proved particularly difficult when distinguishing maize fields in the supervised land use classification for summer 2011. The winter 2011/2012 analysis relied on a more regular temporal coverage of 15m ASTER satellite images, providing a better view of farm-level spatial variation in crop water conditions. Therefore, the limitation in this study mainly concerns the temporal coverage of high-resolution imagery rather than the pixel sizes themselves, as the resolution of the available optical bands is sufficient for determining field-level conditions (Table 5). For a future study, it would be essential to allow for the programming of high-resolution satellites prior to the growing season, to ensure a regular coverage of the study area. Thermal "bleeding" effects from the courser, thermal bands can currently not be avoided unfortunately, as no current satellite provides operational thermal information with pixel sizes smaller than the average Nile Delta field.

Another factor related to the spatial aspect is the size of the canal command areas that were selected for evaluation. With the 'reference' area El Gemeza having only a size of approximately 5.6 km², and a number of 35 separate fields being located along the length of the branch canal, a meaningful head-tail analysis of consumptive use and crop yields did not prove feasible for this area.

5.2.3 Congruency between methodologies

The integrated approach consists of three main components: fieldwork, remote sensing interpretation with the SEBAL algorithm and SWAP simulation modeling of the soil water balance. In the current study it was chosen to calibrate the SWAP hydrological model based on SEBAL results, using the applied irrigation depth as the main calibration parameter, similar to the approach presented by Droogers and Bastiaanssen (2002). The SEBAL model is widely documented and, based on a review of existing literature of studies conducted around the world, provides a reliable way of assessing water consumption and crop yields (average deviation of 5% over a growing season, see Appendix E). Similar to SEBAL, the SWAP model has been abundantly applied and described in scientific literature, including application and validation in the Nile Delta (Bastiaanssen et al., 1996). The error introduced by this methodology is assessed in Table 19 and Table 20 of this report (ranging from 1 to 5%).

Consistency between the two models is achieved by using ET_{ref} , ET_a and K_c from SEBAL as an output in SWAP. Also, temporal profiles of remotely sensed LAI are used for the partitioning of E and T in SWAP. Still, for certain combinations of crop type and location, the different information sources produce results that do not seem fully congruent. As mentioned in Section 5.2.1, a number of assumptions were made in the procedures of the SWAP model application based on the known differences in modernization conditions. However, field reports and remote sensing observations that became available during the execution of the study are not always in line with the expected changes in the system. Hence, different data sources need to be integrated that are not always mutually consistent. Integration of these data sources can, for example, lead to a high crop yield based on field surveys in an area where water stress would be expected to lead to a seasonal reduction in biomass production (see the analysis for rice in Daqalt). Where the error lies is difficult to verify in such a case. Flow measurements are only available at the branch canal level, and can therefore not be used for validation of assumptions on farm-gate water

availability, but they can also not be ignored because they provide valuable information on the supply conditions. On the other hand, reported field yields also come with an uncertainty (Section 5.2.1).

5.2.4 Other factors influencing crop health

It should be noted that the crop water parameters analyzed in this report are not the only factors contributing to crop health and a well-performing irrigation system. In the farmer surveys, local farmers report important factors such as seed type, with a substantial difference being reported between the seeds sold by the Ministry of Agriculture, and the seeds that were left over by the farmers from the previous year. In addition, the farmers mention that a major factor in obtaining high crop yields is farmer skill and experience. Next to these results from the farmer surveys, one can also think of factors such as nutrient deficiencies or crop diseases. All these factors may influence crop growth and eventually fresh yield, and are thus incorporated in the remote sensing observations and locally reported yields. However, they are discounted for in the presented stresses in this report, as these are solely related to moisture and solute conditions.

To assess the effect of irrigation modernization on crop production with more certainty, it is recommended that an extensive farmer survey campaign will be conducted in the framework of the FIMP. In particular, questions concerning used seed type, farmer experience and fertilizer application would be relevant, according to the outcome of the survey conducted under the local farmers. Spatial information on these parameters would allow for a more thorough analysis of the data that is produced in the current study.

6 Conclusions and recommendations

The integrated approach of fieldwork, remote sensing interpretation and hydrological modeling that was applied in this study is a useful way to obtain a picture of the entire water balance for the selected irrigated areas in the Nile Delta. With SEBAL as the selected tool to quantify actual evapotranspiration and the use of SWAP to separate evaporation and transpiration, and to assess mass balance parameters such as drainage, seepage and salinity content, a full picture of both the water and solute balance could be obtained. Based on the biomass production component of SEBAL, performance indicators such as crop yield, crop water productivity and gross return could also be evaluated and intercompared.

Several crop water parameters were assessed to evaluate farm-level effects of irrigation modernizations. These include water consumption, crop yields, water productivity, equity of water availability, reliability of irrigation water supply, drainage, canal seepage, and water quality. When looking at the findings of this study regarding these parameters, it cannot be concluded that the farm-level modernizations have led to substantial improvements. For most of these parameters, similar results were obtained for the area modernized up to *marwa* level (W-10) and the area modernized up to *mesqa* level (Daqalt), both in terms of absolute values, spatial variability, and temporal variability.

A consistent pattern for all summer and winter crops is the occurring of higher average water consumption values in W-10 compared to Daqalt. Whether this additional consumed water is put to productive use (transpiration) is crop type dependent. For berseem and cotton, results indicate a beneficial effect of *marwa* improvements, whereas for wheat non-productive soil evaporation is computed to be highest in W-10. It is recommended to dedicate further research to examine the farmer's behavior in the new situation of water delivery, and possibly provide capacity building in order to reduce non-beneficial water consumption.

The performance of W-10 and Daqalt irrigation systems was also evaluated at a lower level of spatial detail, in order to assess the effects of branch canal and *mesqa* scale irrigation improvements. This was done by comparing the results to those for a reference area without modernization (El Gemeza), and by comparing summer 2011 results with the outcomes of a previous study for summer periods 1995 and 2002. Beneficial effects were observed in several analyses at this spatial level, with water consumption being lower and yields being higher for all crops in 2011/2012 and 2002/2003 compared to 1995/1998, with the exception of wheat yields. Looking at water productivity of both summer and winter crops, and thus gross return, the efficiency of water use has been steadily increasing over these years for all combinations of crop type and command area for which historical data are available.

Drainage flows are computed to be smaller in case of an irrigation practice of more frequent applications of smaller irrigation depths. Combined with reduced upstream canal seepage losses, one may expect that the more efficient use of water at the upstream field could reduce water availability for the downstream farmer. In general, the W-10 head-tail analyses of water consumption indicate that this is not the case, which suggests that downstream farmers are switching from using drainage water to using water that is now continuously available at the farm gate.

For all combinations of crop, branch canal and upstream/downstream location (except for maize in an upstream Daqalt field), solutes are computed to be accumulating in the soil for all fields, which means that the crops may experience solute stress on the long-term if no leaching with large amounts of water

occurs. This study indicates that this issue is particularly relevant with respect to the switch to continuous water supply in W-10, where individual irrigation depths are smaller and the flushing out of solutes from the soil profile is decreased.

The main limitation that was encountered in this study is the absence of available data measured on-site at the farm level, specifically canal flows, groundwater levels, and water quality measurements. This turned out to be not a matter of difficulties in obtaining these data, but the reported total absence of *marwa* level measurements being performed altogether. For this reason, observed spatial variations at a higher level than the branch canal are mainly a result of the available satellite data and assumptions made based on knowledge on the general state of the irrigation systems (see Section 4.3).

One recommendation that would improve the quality of a future similar study is therefore to initiate the operational, farm-level monitoring of some key parameters concerning water quantity and quality, including *mesqa* and *marwa* canal flows, groundwater levels, drainage fluxes, and irrigation applications. Also, a field campaign should be undertaken to assess other factors influencing crop growth (next to water availability), that were identified in the farmer surveys of this study. Finally, the remote sensing analysis for summer 2011 had to rely on archived satellite data, due to the lack of time to program a high-resolution sensor to ensure regular coverage of the study areas. Especially as long as *marwa* level field measurements are non-existent, a small pixel size and frequent revisit time of the raw satellite data is vital to produce reliable farm level estimations. The accuracy of future remote sensing studies can be improved by allowing enough time for the programming of regular, high-resolution satellite imagery of the study area, comparable to what was achieved for the winter season 2011/2012. For example, multiple high-resolution images during the rice preparation phase would provide a better representation of the temporal variety in land management practices.

A more general recommendation with respect to future irrigation improvement projects would be to set clear goals in terms of the **productive** use of water (T for transpiration). Over the course of this project, a number of written and spoken statements were encountered in the context of the IIIMP project, concerning general ambitions related to 'water use' and 'water consumption'. The current study demonstrates that it is possible to distinguish the fraction of consumed water that is used beneficially for crop growth, and this is the parameter that should be maximized in a well-functioning irrigation system.

References

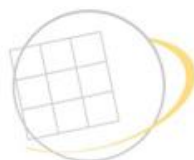
- Allen, R.G., M. Tasumi and R. Trezza. 2007. Satellite-based energy balance for mapping evapotranspiration with internalized calibration (METRIC) - Model. *ASCE J. Irrigation and Drainage Engineering* 133(4):380-394.
- Allen, Richard, Ayse Irmak, Ricardo Trezza, Jan M. H. Hendrickx, Wim Bastiaanssen, Jeppe Kjaersgaard, 2011. Satellite-based ET estimation in agriculture using SEBAL and METRIC, *Hydrological Processes*, 25 (26), 4011-4027
- Allen, R.G., L.S. Pereira, D. Raes and M. Smith. 1998. Crop evapotranspiration. Guidelines for computing crop water requirements. FAO Irrigation and drainage paper. 56.
- Amer, M. and N. de Ridder. 1989. Land Drainage in Egypt. Drainage Research Institute, Cairo, Egypt.
- Badawi, A. Tantawi, 1995. Rice agronomic research in Egypt, *Cahiers Options Mediteraneennes*, vol. 15(1): 71-76
- Baskin, C.C. Hopper, N.W., Tupper, G.R., Kunze, O.R., Techniques to evaluate planting seed quality, Chapter 33, retrieved from the website of The Cotton Foundation: www.cotton.org
- Bastiaanssen, W.G.M., M. Menenti, R.A. Feddes and A.A.M. Holtslag, 1998. The Surface Energy Balance Algorithm for Land (SEBAL): Part 1 formulation, *J. of Hydr.* 212-213: 198-212
- Bastiaanssen, W.G.M., 2000. Sensible and latent heat fluxes in the irrigated Gediz Basin, Western Turkey, *J. of Hydr.* 229: 87-100
- Bastiaanssen, W.G.M. and S. Ali, 2003. A new crop yield forecasting model based on satellite measurements applied across the Indus Basin, Pakistan, *Agriculture, Ecology and Environment* 94 (3): 321-340
- Bastiaanssen, W.G.M. and K.M.P.S. Bandara, 2001. Evaporative depletion assessments for irrigated watersheds in Sri Lanka, *Irrigation Science* 21 (1): 1-15
- Bastiaanssen, W.G.M., E.J.M. Noordman, H. Pelgrum, G. Davids and R.G. Allen, 2005. SEBAL for spatially distributed ET under actual management and growing conditions, *ASCE J. of Irrigation and Drainage Engineering* 131(1): 85-93
- Bastiaanssen, W., K.E.D.M. Soliman, C. Mirabile, M. Korani and S.A. Gawad, 1996. Data management related to the application of two-crop-water-environment-models in Argentina and Egypt. Sustainability of Irrigated Agriculture. Workshop on crop-water-environment-models. ICID CIID. Cairo International Conference Center.
- Bouman, B.A.M., Kropff, M.J., Tuong, T.P., Wopereis, M.C.S., Ten Berge, H.F.M., & Van Laar, H.H. (2001). ORYZA2000: modeling lowland rice. International Rice Research Institute, Los Baños, Philippines, and Wageningen University and Research Centre, Wageningen, Netherlands, 235 pp.

- Doorenbos, J. and A.H. Kassam, 1979. Yield response to water, FAO Irrigation and Drainage Paper no. 33, Rome, Italy: 170 pp. + appendices
- Droogers, P. and W.G.M. Bastiaanssen, 2002. Evaporation in irrigation performance and water accounting frameworks: an assessment from combined hydrological and remote sensing modeling, *ASCE Irrigation and Drainage Engineering* 128 (1): 11-18
- Droogers, P., and G. Kite. 2001. Simulation modeling at different scales to evaluate the productivity of water. *Physics and Chemistry of the Earth* 26: 877-880.
- Ernst, L.F., 1956. Calculation of the steady flow of groundwater in vertical cross-sections. *Netherlands Journal of Agricultural Science* 4, 126-131.
- Feddes, R.A., P.J. Kowalik and H. Zaradny, 1978. Simulation of field water use and crop yield. *Simulation Monographs*. Pudoc. Wageningen. 189 pp.
- Hellegers, Petra J.G.J., Richard Soppe, Chris J. Perry, and Wim G.M. Bastiaanssen, 2009. Remote Sensing and Economic Indicators for Supporting Water Resources Management Decisions. *Water Resource Management*, 24 December 2009.
- Hooghoudt, S.B., 1940. Algemene beschouwing van het probleem van de detailontwatering en de infiltratie door middel van parallel lopende drains, greppels, sloten en kanalen. *Verslag Landbouwkundig Onderzoek*. 46, B, 193 pp.
- IWMI, 1999, Alexandridis, Th., Asif, S., Ali, S. Water performance indicators using satellite imagery for the Fordwah Eastern Sadiqia (South) irrigation and drainage project. Report No. R-87, Pakistan Program, IWMI
- Kotb, T.H.S., Watanabe, T., Ogino, Y., Tanji, K., 2000. Soil salinization in the Nile Delta and related policy issues in Egypt, *Agricultural Water Management* 43, pp. 239-261
- Kroes, J.G., J.C. Van Dam, P. Groenendijk, R.F.A. Hendriks, C.M.J. Jacobs, 2008. SWAP version 3.2. Theory description and user manual. Wageningen, Alterra, Alterra Report1649(02) - Swap32 Theory description and user manual.doc. 262 pp.
- Mohamed, M.N.E.D., 2008. Technical Support for on-Farm Improvements in the W-10 Pilot Area. Final Report.
- Molden, D. 1997. Accounting for water use and productivity. SWIM Paper 1. International Irrigation Management Institute, Colombo, Sri Lanka.
- Monteith, J.L., 1965. Evaporation and the environment. In the state and movement of water in living organisms, XIXth Symposium. Soc. for Exp. Biol. Swansea, Cambridge University Press. 205-234.
- Mualem, Y., 1976. A new model for predicting the hydraulic conductivity of unsaturated porous media. *Water Resources Research*. 12. 513-522.



- Salem, M.H., K.E.D.M. Soliman, M.A.E.A. Elmhssen, M. Korani and M. Hussein, 1996. Intercomparison of simulation models in Argentina and Egypt: on farm BIWASA model. Development Research and Technological Planning Center, Cairo University.
- Teixeira, A.H. de C., W.G.M. Bastiaanssen, M.D. Ahmad, and M.G. Bos, 2008. Reviewing SEBAL input parameters for assessing evapotranspiration and water productivity for the Low-Middle Sao Francisco River basin, Brazil. *Agricultural and Forest Meteorology*, 149, 462-476.
- Terink, W., P. Droogers, J. van Dam, G.W.H. Simons, M. Voogt.. 2012. The added value of high-resolution above coarse-resolution remote sensing in crop yield forecasting. A case study in the Egyptian Nile Delta. FutureWater report 116.
- Terink, W., P. Droogers, J. van Dam, G.W.H. Simons, M. Voogt. 2012a. The added value of high-resolution above coarse-resolution remote sensing in crop yield forecasting. In preparation to be submitted to *Remote Sensing of Environment*.
- Van Dam, J.C, 2000. Field scale water flow and solute transport. SWAP model concepts, parameter estimation and case studies. PhD thesis, Wageningen University, 167 pp.
- Gastel, A.J.G. van, Bishaw, Z., Gregg, B.R., 2002. Bread wheat: improvement and production. FAO Plant Production and Protection Series.
- Van Genuchten, M.Th., 1980. A closed form equation for predicting the hydraulic conductivity of unsaturated soils. *Soil Science Society of America Journal*. 44. 892-898.
- Wachyan, E., K.R. Rushton. 1987. Water losses from irrigation canals. *Journal of Hydrology*. 92: 275-288.
- Willcutt, M.H., 2010. Harvesting, Drying and Storing Corn. Mississippi State University Extension Service, Volume 2285.
- Zwart, S.J., 2010. Benchmarking water productivity in agriculture and the scope for improvement. PhD thesis, TU Delft, 102 pp.

Appendix

Appendix A: Fieldwork sheet



GEOMAP CONSULTANTS
المجموعة الاستشارية للخرائط والمعلومات الأرضية

Area Name: W-10 Command Area	Date of Fieldwork: 19/10/2011	
Field No.: 11	Type of Crop: Rice	
Photo Number: 715	GIS File: Area2.mxd	
		
GPS Measurements:		
UTM Corner Coordinates		
Position	X (m)	Y (m)
Upper Left	291539	3461174
Upper Right	291578	3461166
Lower Right	291546	3461044
Lower Left	291509	3461053
Remarks:		
		

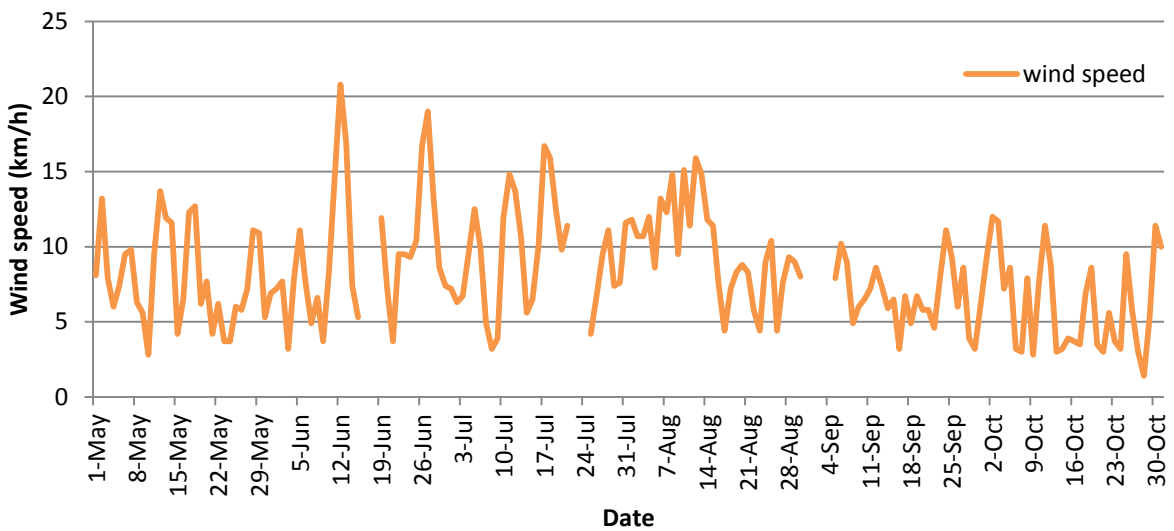
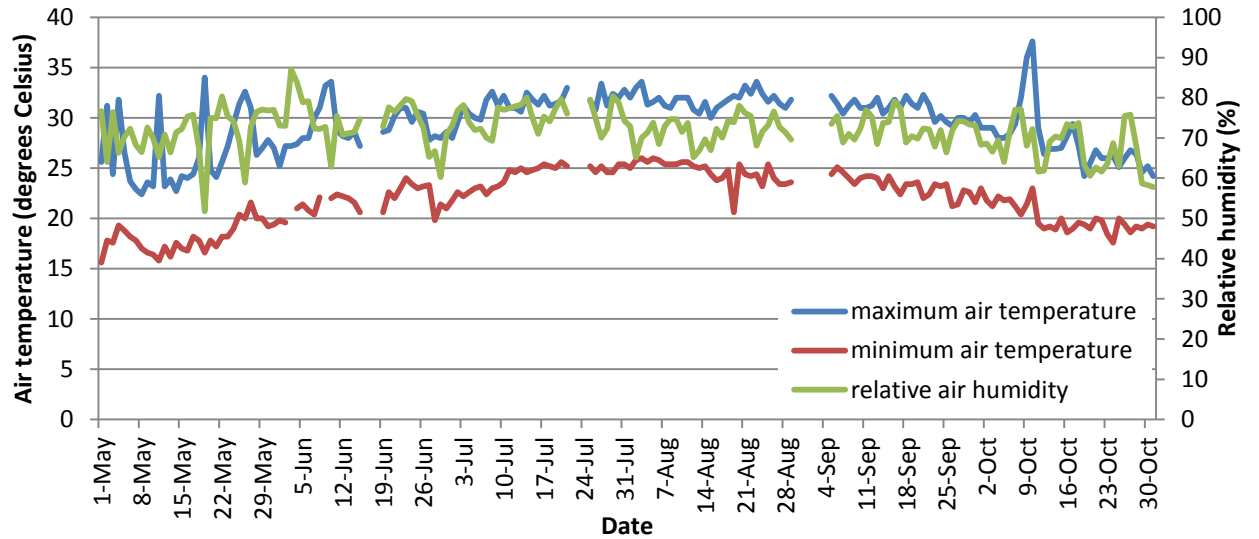
Appendix B: Daily meteorological data

Station: Baltim, Egypt

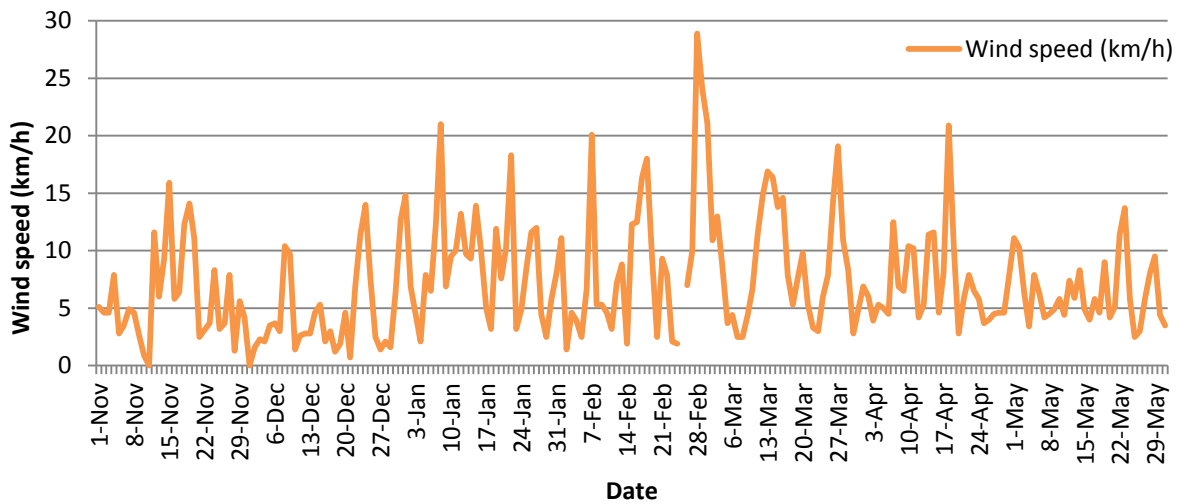
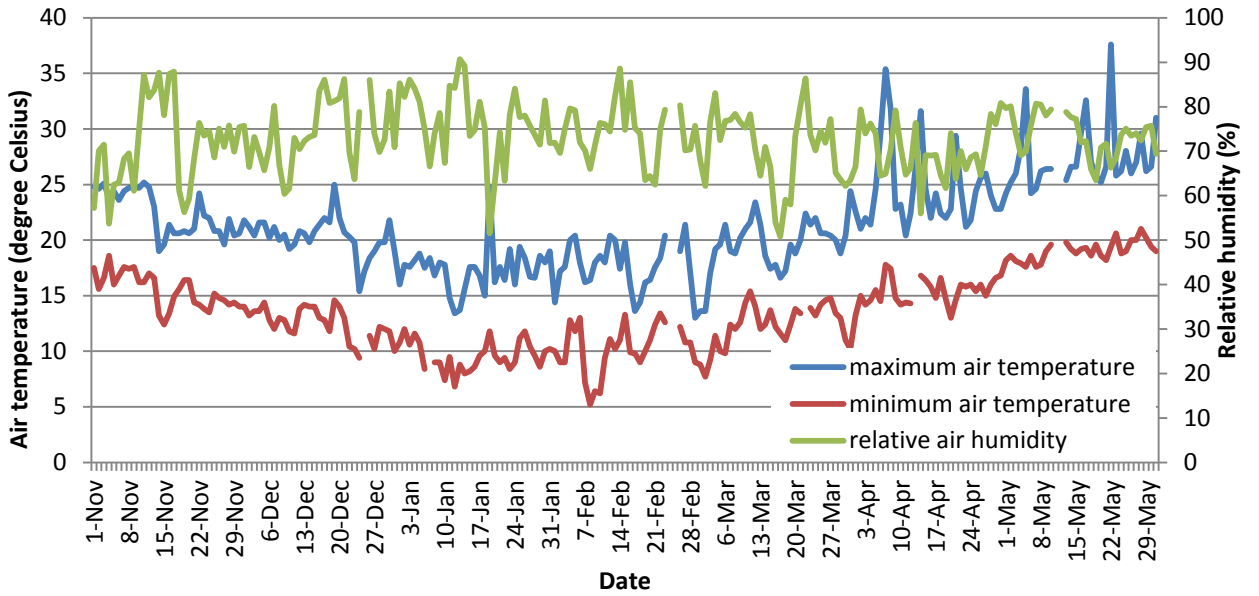
Latitude 31-33N, Longitude 06-31E, Altitude 1m

WMO Code: 62325

Summer season



Winter season



Appendix C: Uncertainty assessment in SWAP

The table below shows the 1-year water balance for Daqalt for the period 1-Nov-2010 through 31-Oct-2011. During this period, maize is the crop in the sample location taken below. The change in storage (dS) is exactly zero during this period. The coefficients of variation (CV) per parameter (%) in this table represent the variability in model output per parameter. These CV values are based on a Nile Delta study by Terink et al. (2012; 2012a), where 256 SWAP simulations were performed for individual high-resolution pixels located in the same 240x240m square. For each of the SWAP water balance terms, the CV (%) was calculated using the outputs of these 256 model runs. Rainfall and the bottom flux are measured values and go directly as input into the model, and are not spatially variable within the 240x240m square: 0% CV.

The table shows that the total uncertainty in dS is +/- 67 mm. This uncertainty is calculated as the square root of the quadratic sums of the other balance terms. The uncertainty in drainage is with +/- 9 mm relatively small.

	mm	CV %	mm (+/-)
Rainfall	121	0	0
Irrigation	560	11	62
Transpiration	395	6	24
Evaporation	166	1	2
Q _{bottom}	66	0	0
Drainage	186	5	9
dS	0		67

One-year water balance for the period 1-Nov-2010 through 31-Oct-2011 for Maize in Daqalt. Uncertainties (CV %) are model uncertainties and are based on a study by Terink et al. (2012; 2012a).

Appendix D: Attendance list kickoff workshop

Kickoff Workshop, 26-27 October, 2011

Gijs Simons, WaterWatch BV

Location: Executive Authority for Land Improvement Projects (EALIP), Ministry of Agriculture and Land Reclamation, Cairo

name	affiliation
1 Mohamed Hafez	SWERI
2 Abd El-Hamid El-Ghadpan Abd El-Latif	SWERI
3 Shreen Samy Ahmed	SWERI
4 Dr. Nader Ramzy Habashy	SWERI
5 Mahmoud Mohamed Abdalla Mahmoud	SWERI
6 Azza Rashad Ahmed	SWERI
7 Salwa Abd El-Rahman Eisa	SWERI
8 Samiha Ouda	SWERI
9 Khaled Mahmoud Abdellatif	SWERI
10 Mohamed Ahmed El Shazly	SWERI
11 Abdalla Ahmed Mohamedin	SWERI
12 Dr. Mohamed Saied Awad	SWERI
13 Dr. Mohamed Abdelaziz Bayoami	SWERI
14 Dr. Sayed Ahmed El Tohamy	SWERI
15 Prof. Dr. Mohamed Reda Mahmoud Ahmed	SWERI
16 Dr. Khaled Abdou Shaban	SWERI
17 Dr. Nadia Abd El Azeem Mohamed	SWERI
18 Neiveen Hassan Sayed Seleem	EALIP
19 Mohamed Arafa Arafa Ali	EALIP
20 Ibrahim Mohamed Ahmed El Roby	IIIMP
21 Mohamed Fahmy Weshahy	IIIMP
22 Aya Mahmoud Sayed	EALIP
23 Hesham Mahmoud Abo El Saud	ARC
24 El Sayed Mohamed Ali	SWERI
25 Dr. Mohamed El Shahawy	SWERI
26 Mahmoud Mohamed Shabana	SWERI
27 Mostafa Abdel El Damouch	SWERI
28 Ahmed Khalil Solaiman Amer	SWERI
29 Kadria Moustafa El Azab	SWERI
30 Ayaa Khalil Moustafa Khalil	EALIP
31 Gabriella Izzi	World Bank

Appendix E: SEBAL Validation

Source: Bastiaanssen et al., 2010.

Field instrument	Country	Location and year	Irrigated crop	Number of images	Source	Deviation instantaneous (%)	Deviation (%)
Drainage lysimeter	U.S.	Montpellier, Idaho, 1985	Native sedge forage	4	Allen et al. (2007b)	NA	4
Weighing lysimeter	U.S.	Kimberly, Idaho, 1989	Sugar beet	12	Allen et al. (2007b)	NA	1
Weighing lysimeter	U.S.	Parlier, California, 2002	Peaches	7	Cassel and Robertson (2006)	NA	7
Weighing lysimeter	U.S.	Parlier, California, 2002	Alfalfa	7	Cassel and Robertson (2006)	NA	2
Soil water balance	U.S.	Central Valley, California, 2002	Almonds	7	Sanden (2005)	NA	1
Soil water balance	U.S.	Imperial Valley, 1997-1998	Several	12	Thoreson et al. (2009)	NA	1
Soil water balance	South Africa	Western Cape, 2004-2006	Grapes	12	Jarmain, et al. (2007)	NA	12
Soil water balance	Philippines	Central Luzon, 2001	Rice	3	Hafeez et al. (2002)	NA	8
Bowen ratio	France	Alpilles, 1996	Alfalfa, wheat, sunflower	55	Jacob et al. (2002)	3*	NA
Bowen ratio	Brazil	Petrolina, 2002-2003	Grapes	2	Teixeira et al. (2007)	3	NA
Eddy correlation	Spain	Barrax, 1991	Maize	2	Bastiaanssen et al., (1997)	6	NA
Eddy correlation	China	Zhangye, 1991	Maize	2	Wang et al. (1995)	9	NA
Eddy correlation	Brazil	Petrolina, 2001-2007	Mango, grapes	9	Teixeira et al. (2008)	10	1
Eddy correlation	U.S.	Middle Rio Grande,	Pecan, alfalfa	7	Wang et al. (2005)	NA	3

Eddy correlation	Brazil	Petrolina, 2001-2007	Mango, grapes	9	Teixeira et al. (2008)	10	1
Eddy correlation	U.S.	Middle Rio Grande, 2002-2003	Pecan, alfalfa	7	Wang et al. (2005)	NA	3
Surface renewal	U.S.	Sacramento Valley, 2001	Rice	8	SNA, unpublished	NA	1
Scintillometer	Turkey	Gediz basin, 1998	Grapes, cotton	4	Kite and Droogers (2000)	NA	16
Scintillometer	Sri Lanka	Horana, 1999	Palm trees and rice	10	Hemakumara et al. (2003)	NA	3
Scintillometer	France	Alpilles, 1997	Sunflower, wheat	17	Lagouarde et al. (2002)	1*	NA
Scintillometer	Morocco	Marrakech, 2003	Olives	17	Van den Kroonenberg (2003)	16 *	NA
Mathematical average						7%	5%

Note: NA = not applicable.

*Validation on sensible heat flux, not on ET flux.

SEBAL validation over irrigated areas

